



QEX

\$5

July/August 2010

www.arrl.org

A Forum for Communications Experimenters

Issue No. 261



KD1K explains heat pipe cooling technology and suggests that Amateur Radio operators may be able to use heat pipe coolers that were designed for computer applications to advantage in amplifier projects.

KENWOOD

Listen to the Future

Kenwood & AvMap The Ultimate APRS[®] Combination

TM-D710A



AvMap G5



Two Great Companies...Providing One Outstanding Solution!

KENWOOD U.S.A. CORPORATION
Communications Sector Headquarters
3970 Johns Creek Court, Suite 100, Suwanee, GA 30024
Customer Support/Distribution
P.O. Box 22745, 2201 East Dominguez St., Long Beach, CA 90801-5745
Customer Support: (310) 639-4200 Fax: (310) 537-8235



www.kenwoodusa.com
ADS#01308



JQA-1205
091-A
ISO9001 Registered
Communications Equipment Division
Kenwood Corporation
ISO9001 certification



AVMAP
SATELLITE NAVIGATION



www.avmap.us • e-mail: info@avmap.us
1.800.363.2627



QEX (ISSN: 0886-8093) is published bimonthly in January, March, May, July, September, and November by the American Radio Relay League, 225 Main Street, Newington, CT 06111-1494. Periodicals postage paid at Hartford, CT and at additional mailing offices.

POSTMASTER: Send address changes to: QEX, 225 Main St, Newington, CT 06111-1494 Issue No 261

Harold Kramer, WJ1B
Publisher

Larry Wolfgang, WR1B
Editor

Lori Weinberg, KB1EIB
Assistant Editor

Zack Lau, W1VT
Ray Mack, W5IFS
Contributing Editors

Production Department

Steve Ford, WB8IMY
Publications Manager

Michelle Bloom, WB1ENT
Production Supervisor

Sue Fagan, KB1OKW
Graphic Design Supervisor

David Pingree, N1NAS
Senior Technical Illustrator

Advertising Information Contact:

Janet L. Rocco, W1JLR
Business Services
860-594-0203 – Direct
800-243-7768 – ARRL
860-594-4285 – Fax

Circulation Department

Cathy Stepina, *QEX Circulation*

Offices

225 Main St, Newington, CT 06111-1494 USA
Telephone: 860-594-0200
Fax: 860-594-0259 (24 hour direct line)
e-mail: qex@arrl.org

Subscription rate for 6 issues:

In the US: ARRL Member \$24, nonmember \$36;

US by First Class Mail: ARRL member \$37, nonmember \$49;

International and Canada by Airmail: ARRL member \$31, nonmember \$43;

Members are asked to include their membership control number or a label from their QST when applying.

In order to ensure prompt delivery, we ask that you periodically check the address information on your mailing label. If you find any inaccuracies, please contact the Circulation Department immediately. Thank you for your assistance.



Copyright © 2010 by the American Radio Relay League Inc. For permission to quote or reprint material from QEX or any ARRL publication, send a written request including the issue date (or book title), article, page numbers and a description of where you intend to use the reprinted material. Send the request to the office of the Publications Manager (permission@arrl.org).

July/August 2010

About the Cover

Dick Jansson, KD1K, explains heat pipe cooling technology, especially as he used it to solve a cooling problem with the AMSAT Phase 3D (AMSAT OSCAR 40) satellite. Dick suggests that we may be able to mount heat pipe coolers that were designed for computer applications to the power transistors in amplifier projects. Photos courtesy of AeroCool and SilverStone Tek.



In This Issue

Features

3 Heat Pipes
By Dick Jansson, KD1K

10 The “True” TLT H-mode Mixer
By Oleg Skydan, UR3IQO

16 The Shunt Method for Crystal Parameter Measurement
By Jim Koehler, VE5FP

26 Using QuickSmith—Part 1
By Harold Kinley, WA4GIB

35 A 20 Meter Sleeve Dipole Without the Sleeve
By Robert Zimmerman, VE3RKZ

39 Amateur Radio Astronomy Projects — Total Power Radio Telescope
By Jon Wallace

44 Book Review: Noise Temperature Theory and Applications for Deep Space Communications Antenna Systems
By Dick Kolby, K6HIJ

Columns

45 Upcoming Conferences **48 Letters**

47 Reader’s Page **48 In the Next Issue of QEX**

Index of Advertisers

American Radio Relay League:.....	Cover III	National RF, Inc:	15
Down East Microwave Inc:.....	15	Nemal Electronics International, Inc:	15
Harpo Electronics	Cover IV	RF Parts	43, 45
Kenwood Communications:	Cover II	Tucson Amateur Packet Radio:	46

The American Radio Relay League

The American Radio Relay League, Inc. is a noncommercial association of radio amateurs, organized for the promotion of interest in Amateur Radio communication and experimentation, for the establishment of networks to provide communications in the event of disasters or other emergencies, for the advancement of the radio art and of the public welfare, for the representation of the radio amateur in legislative matters, and for the maintenance of fraternalism and a high standard of conduct.



ARRL is an incorporated association without capital stock chartered under the laws of the state of Connecticut, and is an exempt organization under Section 501(c)(3) of the Internal Revenue Code of 1986. Its affairs are governed by a Board of Directors, whose voting members are elected every three years by the general membership. The officers are elected or appointed by the Directors. The League is noncommercial, and no one who could gain financially from the shaping of its affairs is eligible for membership on its Board.

"Of, by, and for the radio amateur," ARRL numbers within its ranks the vast majority of active amateurs in the nation and has a proud history of achievement as the standard-bearer in amateur affairs.

A *bona fide* interest in Amateur Radio is the only essential qualification of membership; an Amateur Radio license is not a prerequisite, although full voting membership is granted only to licensed amateurs in the US.

Membership inquiries and general correspondence should be addressed to the administrative headquarters:

ARRL
225 Main Street
Newington, CT 06111 USA
Telephone: 860-594-0200
FAX: 860-594-0259 (24-hour direct line)

Officers

President: KAY C. CRAIGIE, N3KN
570 Brush Mountain Rd, Blacksburg, VA 24060

Chief Executive Officer: DAVID SUMNER, K1ZZ

The purpose of QEX is to:

- 1) provide a medium for the exchange of ideas and information among Amateur Radio experimenters,
- 2) document advanced technical work in the Amateur Radio field, and
- 3) support efforts to advance the state of the Amateur Radio art.

All correspondence concerning QEX should be addressed to the American Radio Relay League, 225 Main Street, Newington, CT 06111 USA. Envelopes containing manuscripts and letters for publication in QEX should be marked Editor, QEX.

Both theoretical and practical technical articles are welcomed. Manuscripts should be submitted in word-processor format, if possible. We can redraw any figures as long as their content is clear. Photos should be glossy, color or black-and-white prints of at least the size they are to appear in QEX or high-resolution digital images (300 dots per inch or higher at the printed size). Further information for authors can be found on the Web at www.arrl.org/qex/ or by e-mail to qex@arrl.org.

Any opinions expressed in QEX are those of the authors, not necessarily those of the Editor or the League. While we strive to ensure all material is technically correct, authors are expected to defend their own assertions. Products mentioned are included for your information only; no endorsement is implied. Readers are cautioned to verify the availability of products before sending money to vendors.

Larry Wolfgang, WR1B

lwolfgang@arrl.org

Empirical Outlook

Sharing Our Enthusiasm for Technology

Most QEX readers have a few things in common. We all enjoy learning about new technology, and sharing that knowledge with others. Some of us are just beginning to learn about technology and techniques that have been around for years, while others are truly exploring and pushing the limits to develop new communications methods. Those of us who are just beginning to learn something that others have been doing, stand in awe of the real innovators. We all share a desire to learn more, and also to help others learn about our "discoveries."

QEX authors have found a great way to share their interests and discoveries, and I believe our readers enthusiastically devour their offerings. We don't necessarily have to be on the "cutting edge" of technology, though, to share our joy of Amateur Radio.

While driving to Dayton this year, I had my APRS station running in my car. My friend Mark, who had not "played" with APRS yet, was very interested to learn how it works and what we could do with it. We saw a few other cars pop up on the GPS map, and it was fun to try calling them. When I heard the packets from one station and saw his icon pop up on the screen, I switched "sides" on the radio and said "Give him a call." We had a brief simplex chat on the APRS frequency, then moved to another simplex frequency. Just about the time we arrived at our hotel, the radio beeped to indicate that I had received a text message. When I hit the MSG button, a note from W1GTT, back home in Connecticut popped up on the radio display. It's all technology that has been around for years, but it is still fun to show it off, and Mark was amazed.

I recently spent a weekend at a gathering of about 7000 Cub Scouts, Boy Scouts and Venture Scouts in Connecticut. My purpose was to show off some Amateur Radio technology, and give the Scouts an opportunity to operate a radio and to talk to hams who knows where. The display was relatively modest, but the several other operators who helped with the demonstration were enthusiastic, and everyone had fun.

The first question I often hear from someone who has never seen an Amateur Radio station is "What is the farthest you have ever talked to someone?" Their eyes light up when I say "Halfway around the world!" It doesn't seem so amazing to me, but it can be fascinating to someone who has never thought about talking on a radio. When I mentioned that I had once been visiting a friend and watched while he contacted another ham by bouncing his signals off the moon, the Scout's eyes lit up! "Wow! That sounds neat!"

In just a few weeks I will be heading to Fort A. P. Hill, just outside Fredericksburg, Virginia, for the Boy Scout National Jamboree. That gathering will be a bit larger than my recent event in Connecticut! Somewhere in the neighborhood of 35,000 Scouts will gather as part of the celebration of the 100th birthday of the Boy Scouts of America. The demonstration station there will be a bit more elaborate, the technology a bit more advanced and the enthusiasm boundless. We will be showing off digital modes, satellite communications and hope to talk with astronauts aboard the International Space Station! Many Scouts will have their first taste of Amateur Radio, and they will be amazed by what they see!

There will be so many events and activities available for the Scouts that ten days will not be nearly enough time to see and do it all. Yet we can expect hundreds of them to earn their Radio Merit Badge and hundreds more to take classes and study for their Technician licenses. If past Jamborees have been any indication, VE test sessions will be packed, and many of those who pass will even learn their new call signs (and make their first contacts) before they leave for home. Can you imagine the excitement of coming to the Jamboree with no knowledge of Amateur Radio, and going home with a license? Oh, the stories they will have to tell mom and dad!

If you would like to be part of that excitement, look for K2BSA on the air from July 26 through August 3. Listen for us around the "Scout Frequencies" as listed on the ARRL Web site (www.arrl.org/jamboree-on-the-air-jota) with the information about the annual Jamboree on the Air (JOTA). Take a few minutes to talk with some Scouts at the Jamboree if you have the opportunity. I'll bet your smile will be almost as big as theirs.

I hope you will also seek out other ways to share your enthusiasm for Amateur Radio with someone who is just learning about this hobby of ours. Whether you are showing off the latest high-tech communications technology, age-old Morse code or "just plain voice," you will have fun, and so will the person or people you are showing it to. Enjoy!

Heat Pipes

*Your computer may be using this technology to cool the CPU.
Learn how you can use heat pipes in your Amateur Radio station.*

Many hams will think of heat pipes as new devices, but in reality they have been around for more than 30 years. It is just that it is only relatively recently that these devices have been perfected and placed into the commercial consumer marketplace. More than 20 years ago I studied the application of heat pipes to solve a difficult thermal problem in the AMSAT Phase 4 satellite (geostationary ham radio communications platform).¹ At that time I found a (then) 10+

year old reference and description of heat pipes.²

Study Figure 1 and the following description and you will get the idea: “The heat pipe is a thermal linkage of very high thermal conductivity. It is a closed, evacuated chamber lined with a wick. Heat is transported by evaporation of a volatile fluid, which is condensed at the cold end of the pipe and returned by capillary action to the hot end. The vapor passes through the cavity. Heat pipes consist of three zones or sections: the evaporator, the condenser and an adiabatic section connecting the two. In some designs

the adiabatic section may be very short. This device offers a number of important properties useful in electronic equipment cooling systems. It has many times the heat transfer capacity of the best heat-conducting materials, while maintaining an essentially uniform temperature and transporting heat over distances of several feet. It requires no power and operates satisfactorily in a zero gravity environment.”

[For readers unfamiliar with the physics of heat transfer, it may be helpful to turn to a definition of an adiabatic process, such as can be found on Wikipedia (<http://en.wikipedia>).

¹Notes appear on page 9.

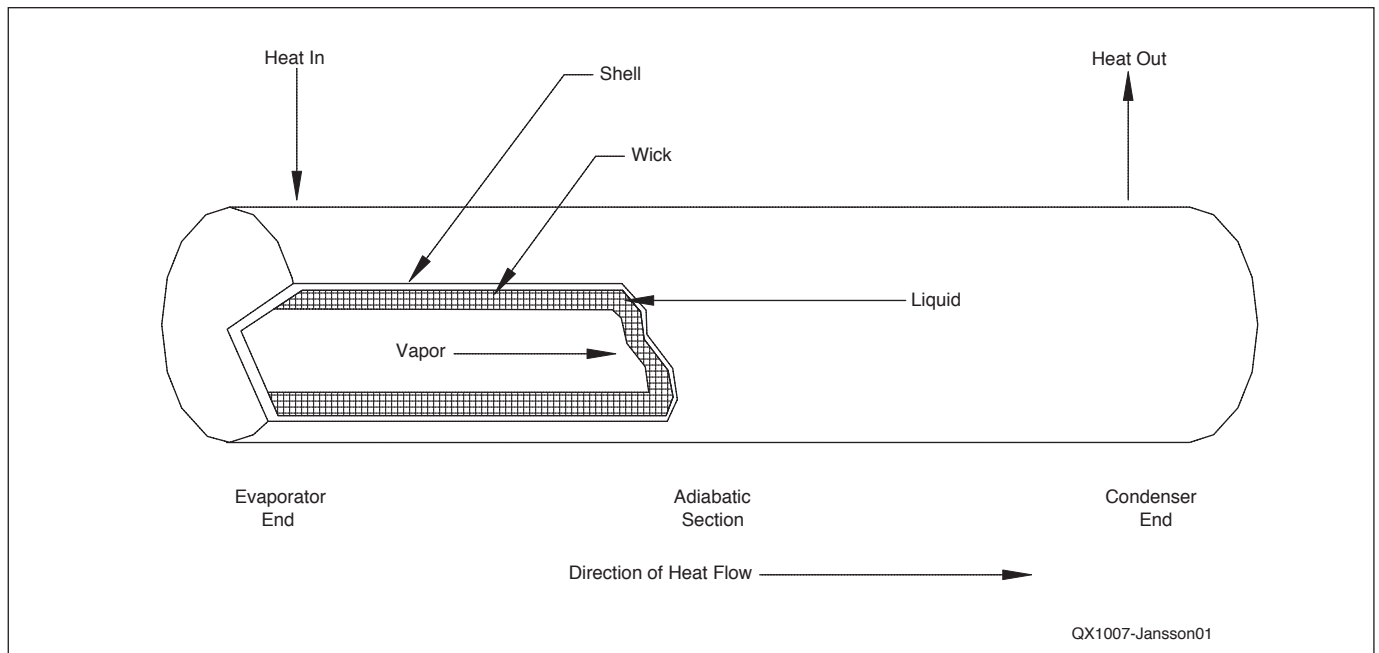


Figure 1 — Heat pipe basics. KD1K drawing

org/wiki/Adiabatic_process). The short definition, taken from the Wikipedia source, is that an adiabatic process is a thermodynamic process in which no heat is transferred to or from the working fluid. For example, adiabatic heating occurs when the pressure of a gas is increased from work done on it by its surroundings, such as by a piston. Diesel engines rely on adiabatic heating during their compression stroke to elevate the temperature sufficiently to ignite the fuel. Adiabatic cooling occurs when the pressure of a substance is decreased as it does work on its surroundings. — Ed.]

Putting this description into other terms,

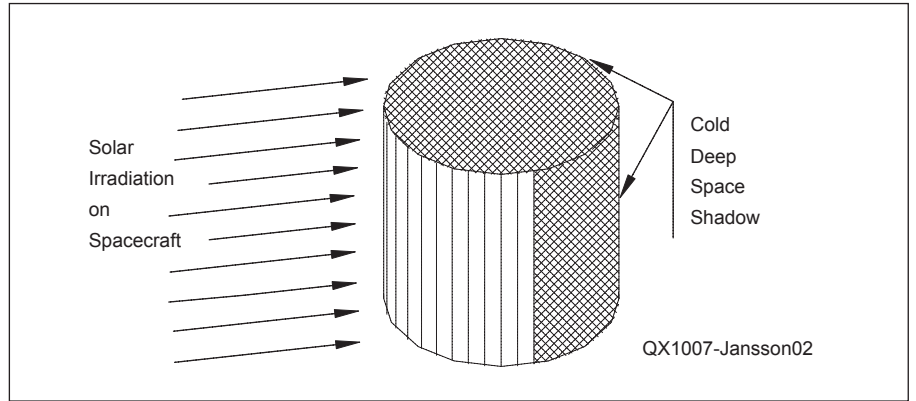


Figure 2 — Solar heating problem for stabilized, pointing satellites. KD1K drawing

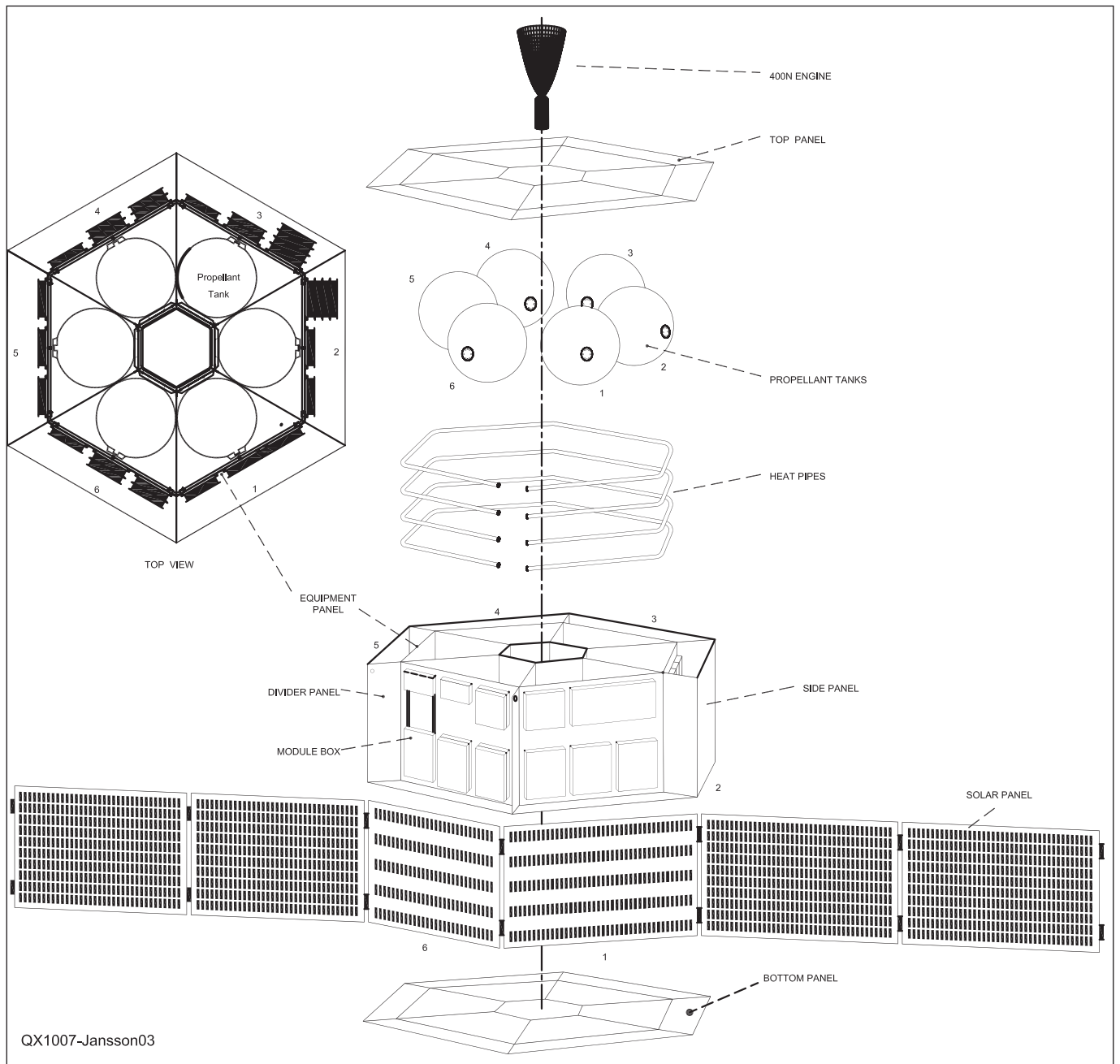


Figure 3 — Exploded view of AO-40 spacecraft, showing major components and heat pipes. Wilfred Gladisch, AMSAT-DL, drawing

a heat pipe is a linear thermal conductor that is hundreds to thousands of times better than the purest of copper or silver bars — they just don't get any better than that.

The applications and materials of heat pipes have been perfected over the years into some truly meaningful devices. Spacecraft heat pipes are considerably more demanding than those used in the commercial applications, such as the cooling of modern-day computer CPUs. I shall try to illustrate these differences and also to show how you can use heat pipes.

Space Application

One space application that has been experienced is that of the AMSAT AO-40 (formerly the Phase 3 D (P3D) Program before being launched and placed into service). Recalling the AO-40 effort will illustrate the evolution of its thermal design. Because of the spacecraft size, the thermal activities happening on one side of the spacecraft would not significantly affect another side. In a stabilized, "pointing mode" orientation, one side would continuously face the Sun, while the opposite side would never see any sunshine. See Figure 2. As a result, the sun side would become quite warm while the back side would get dreadfully cold, all of this even though the structure is made of aluminum, which is thought of as a pretty good heat conductor. In these dimensions, sheet aluminum structures of the size of AO-40 are incapable of moving enough thermal energy to make a difference in this matter.

In addition to solar heating, the RF transmitters installed in AO-40 had outputs up to 300 W PEP, with average power dissipation levels in the 25 to 75 W categories. This meant that there were power transistors (MOSFET devices, actually) with quite small mounting surfaces trying to get rid of tens-of-watts of power. Numerically, heat fluxes of 30 W/cm² could be expected at the mounting face of any single transistor. To give you a feeling for this type of heat flux, the sunshine that you get at the beach on a clear summer day is in the order of 60 mW/cm² or 1/500th of the flux at the mounting surface of each of these transistors! To further heighten this problem of cooling of high-powered solid-state electronics, the semiconductor junction inside these devices should not be allowed to become any warmer than about 125°C for reliability reasons. These devices cannot be allowed to glow red like the handy radiant heater in your house!

The solution to all of these basic thermal problems on AO-40 was to employ the use of heat pipes inside the spacecraft. This arrangement is shown in Figure 3, which illustrates the basic six-sided prismatic structure of this spacecraft. The six Equipment Panels

were mounted about 220 mm (≈8.7 inches) below the exterior side panels. The key to this design is that the equipment panels were in contact, actually bonded, with the four heat pipes and that the heat pipes were not connected directly to any external panel. The basic tenet here is that the "waste" heat removed from one part of the spacecraft was used to keep the cooler parts suitably warm, a thermal redistribution system, if you will. This thermal design concept provided for heat rejection from the spacecraft by radiant exchange between the equipment panels and the side panels, which can get very cold, as intended. As you can also see in Figure 3, all of the basic electronic modules were mounted to those same equipment panels. I do not know of other satellite designs that have used this principle.

The heat pipes used in AO-40 were a very sophisticated aluminum extrusion. These were available in a maximum length of 16 feet, just long enough to be formed into a nearly complete hexagon on the inside of the equipment panels. Working with this particular heat pipe extrusion was a continuation of efforts started with the earlier Phase 4 program. That experience was usefully assimilated into the AO-40 spacecraft. An enlarged view of this extrusion is shown in Figure 4. As you can see, the liquid "wick" is really a group of 27 closely spaced channels in the wall of the extrusion. The geometry of these channels allowed a very substantial flow of liquid returning from the "condenser section" to the "evaporator section," thus providing for an equally substantial thermal transfer rating for the heat pipe. In AO-40 use, there was no clear geometric definition for these evaporator and condenser sections, as the pipes were exchanging thermal energy with

the spacecraft in many locations, but this was what was intended for this design.

While the bonding of the heat pipes to the equipment panels was sufficient for the heat exchange with the panels, such methods were insufficient for the high-powered transmitter modules. Coupling high power transistors to this heat pipe system therefore required some additional measures to be taken. Figure 5 shows a cross-sectional view of this arrangement. At the high heat fluxes presented by these transmitters, coupling to just one side of the heat pipe was not adequate. Therefore a specially machined aluminum "Heat Pipe Clamp" was made of high purity aluminum (for maximum thermal properties) and carefully bonded to each side of the heat pipe using a special fixture. Such a design step was intended to bring at least two other sides of a heat pipe into thermal contact with the module heat sink. These heat pipe clamps were, in turn, bonded to the equipment panels at the same time as the heat pipes. On the other side of this thermal path, the transmitter modules were equipped with two high-purity aluminum heat sink plates for the mounting of the power transistors. These modules were also closely mounted to the equipment panels as well as being bolted through to their respective heat pipe clamp. The final step, shown in Figure 5, was to mount the power transistor to the heat sink, using space-rated silicone grease. All of these bonding and bolting steps are necessary to insure a very high quality thermal path from the transistor to the heat pipe fluid (anhydrous ammonia, NH₃). Figures 6 and 7 are photo illustrations of these heat pipe clamps as a separate assembly and as installed in the spacecraft.

The thermal performance of this complete high-power coupling of transmitter transis-

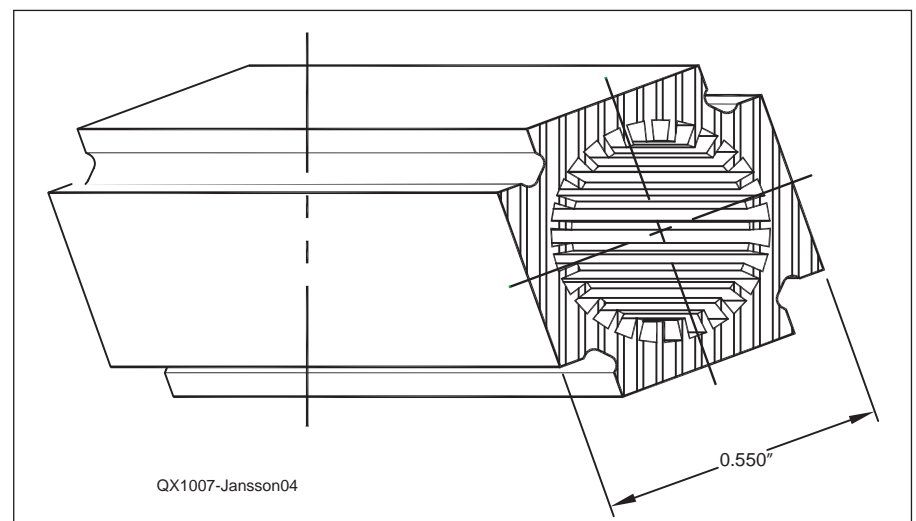


Figure 4 — AO-40 heat pipe extrusion cross section. KD1K drawing

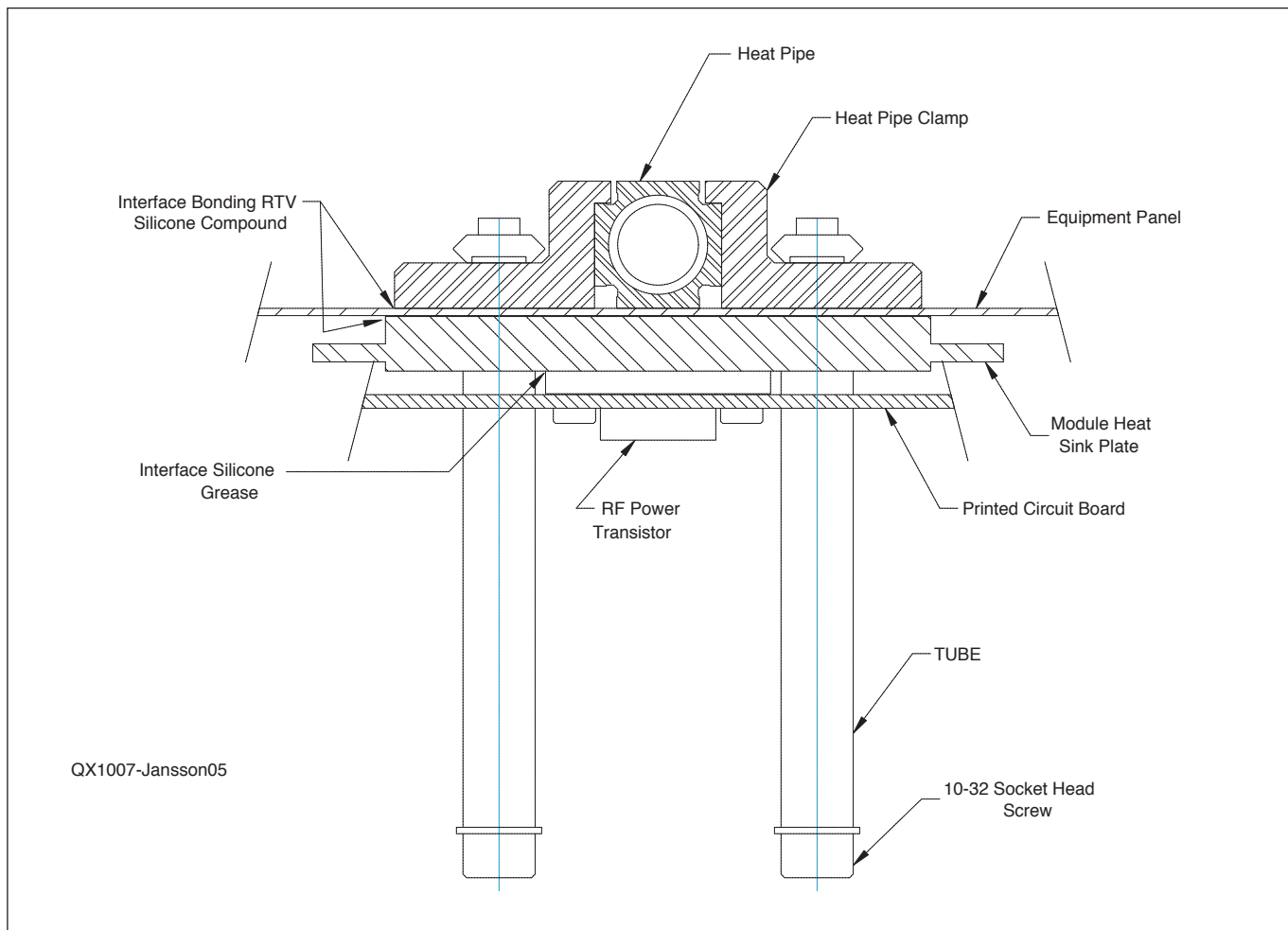


Figure 5 — AO-40 module mounting to heat pipe cross section view. KD1K drawing

tors to the heat pipe system was the subject of a fairly extensive thermal analysis as well as a specially constructed physical thermal model, including a short section of active heat pipe. Building such a thermal model was one of the extra-special fun things that I did for the AO-40 program (thermal designers are strange people, after all). The need for such elaborate evaluation is that in the vacuum of space, the satellite does not have thermally conductive air between parts, and nearly none of the parts will be in perfect contact. These “interstitial” spaces needed to be filled with a compliant material to permit the thermally conductive joining of the parts. The analyses and testing checked out the use of these various materials and I made trade-off evaluations as a result. The “bottom line” of this effort was a transistor thermal mounting with an effective thermal resistance (between the transistor case and the heat pipe fluid) of $\theta_{sf} = 0.27^{\circ}\text{C}/\text{W}$; that is quite low, even lower than that of the transistor junction to its case. The results of this effort were

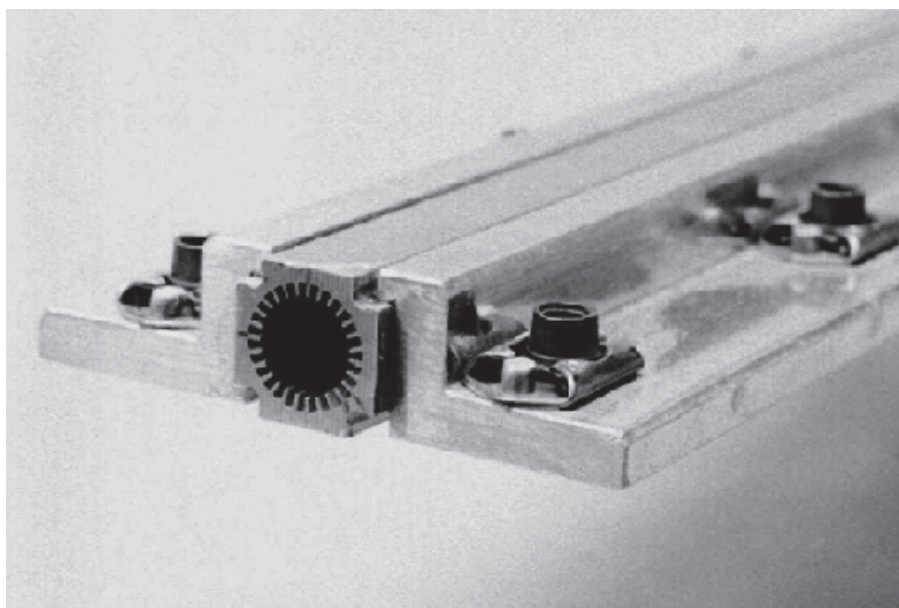


Figure 6 — AO-40 heat pipe and clamp. KD1K photo

very gratifying, as the initial concerns that it wouldn't work well had been great.

I have emphasized the use of heat pipes in space, so far — and for good reason. Heat pipes are sensitive — very sensitive — to environmental accelerations, a fancy description of the Earth's gravity. On Earth, if the evaporator section of an ammonia heat pipe is higher than the condenser section by much more than 0.1 inch in a foot of length, then the capillary forces of the liquid wick may not be strong enough to draw the liquid "up hill" and overcome these gravitational effects. If, however, the evaporator section is lower than the condenser section, then gravity will help the flow of liquid back to the evaporator section — which is how heat pipes work for computer users here on Earth. In the "gravity freedom" of space, this is not very much of a problem, as spaceflight is thought of as being in zero gravity. This is not an absolute condition, however, as spacecraft motions can cause local accelerations that can pose problems. Let me describe just such a case.

AO-40 was designed as a cylindrical spaceframe, albeit a hexagonal cylinder. It was also designed to initially spin about its principal axis until the mission was ready to stop the spin, deploy the solar panels and operate as a three-axis stabilized satellite. For reasons not germane to this discussion, the stable mode of operation was never achieved for AO-40. Spin-stabilized operation is useful for times when the orbit-adjusting propellant motor was operated, because such a spin will average out any small errors in propellant motor alignment. As a result, for motor operation, AO-40 was spun up to more than 10 rpm. Since the heat pipes were placed on the walls of a cylindrical satellite, they were nominally equidistant from the spin axis and thus saw a uniformly distributed centrifugal acceleration...except. That exception was that the heat pipes were part of a hexagonal cylindrical form, not a circular cylinder. That meant that the corners of the hexagon were farther from the spin axis than the "flats" of the hexagon. As a result these corners had a higher centrifugal acceleration (caused by the spin motion) than for the flat sides. At the low spin rate of AO-40 in normal operation, these acceleration differences were not so large as to overcome the capillary forces inside of the heat pipes, and all operated just fine.

During one of the motor-burn phases of the early AO-40 operation, the heat pipes stopped operating. There was some considerable concern by those controlling AO-40, and I was consulted on the matter. As the heat pipe operation had been very well characterized, the problem was confirmed and a projection was made of just what spin rate

would again achieve operation and that computation was confirmed by the controllers as the spin rate was slowed, much to their relief — so much for zero gravity in space. There are always caveats to be addressed.

Terrestrial Applications

All successful heat pipe operations depend upon some fairly tight technical details, regardless of where a heat pipe is used. In addition to the challenging design of the fluid wick on the walls of the heat pipe,

the purity of the working fluid is paramount. The fluid in the AO-40 heat pipes was anhydrous ammonia, NH_3 , owing to the need for the heat pipe to operate at temperatures below 0°C and up to 40°C . The steps used to make sure that the inside of the heat pipe was truly clean was enough to make one wonder just what does "clean" really mean. Any impurity can seriously reduce the operating capability of a heat pipe, because it will result in a non-condensable gas that impairs the working fluid from getting to where it is needed.

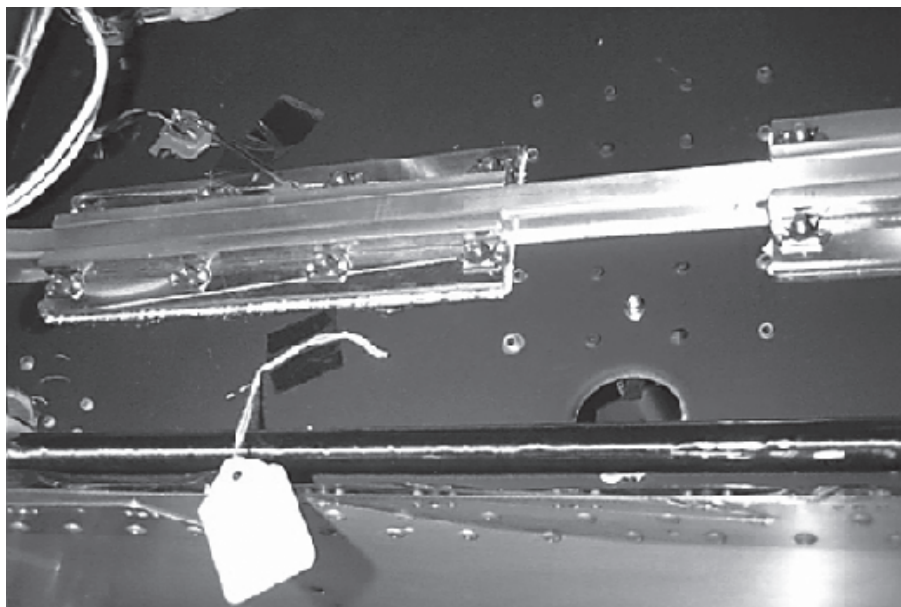


Figure 7 — Heat pipe assembly with clamp mounted inside of AO-40. KD1K photo



Figure 8 — SilverStone CPU cooling heat pipe. SilverStone Tek photo

Using a powerful and hazardous reagent like ammonia for a consumer-market device would be out of the question — but there is no need for such a heat pipe to operate at low temperatures. So the ground rules are changed. Computer heat pipes need only to operate from room temperature, $\approx 20^{\circ}\text{C}$ up to perhaps 70°C . This opens the opportunity to use one of the very best heat transfer fluids that is available for us — water, just plain (but very pure) water, H_2O . The pressure inside of water heat pipes is less than 1 atmosphere (14.7 psia). For example, at 20°C the pressure would be 2.34 kPa (0.34 psia) and at 50°C a pressure of 12.3 kPa (1.8 psia) would be observed. Operating at lowered pressures, such as noted, is not a great concern because a heat pipe must be truly sealed, and water does not care until the temperatures would get nearly to freezing, 0°C .

Heat pipe wick operation will be quite good with water because the surface tension of water is relatively high, meaning that a water heat pipe wicking operation will be somewhat better in the anti-gravity situation than many other fluids can support, including ammonia. Nevertheless, the water heat pipes that I have found all are positioned in the gravity-assist position — the condenser section is located above the evaporator section.

Consumer application heat pipes come in two basic varieties, based on the materials used for the heat pipe and the CPU heat sink. You will find these heat pipes in aluminum and copper and these differences will drive other factors such as in the details of the internal fluid wick design and fabrication.

Figures 8 and 9 illustrate heat pipes that are manufactured for computer CPU cooling. This is a relatively recent application for heat pipes, driven by the ever-increasing complexity and power density of today's CPU devices. Traditionally, as electronic circuits have been miniaturized, made more complex, and made to operate with faster clock speeds, their power dissipation has also dramatically increased. The days of truly low-power CMOS devices are long gone. Consequently the computer designers have had to become much more inventive in their schemes to cool these devices — the opening for useful heat pipe applications.

Using copper in the design of a CPU heat pipe is promoted as an advantage over using aluminum, because copper has a thermal conductivity that is more than twice as high as aluminum. A disadvantage of copper heat pipes is the weight of copper assemblies, which all bear more heavily on the printed circuit board. This issue becomes a concern of PCB designers, as it is a hazard for the electrical trace integrity of the PCB itself.

Another concern in these CPU applications is that of the thermal coupling between

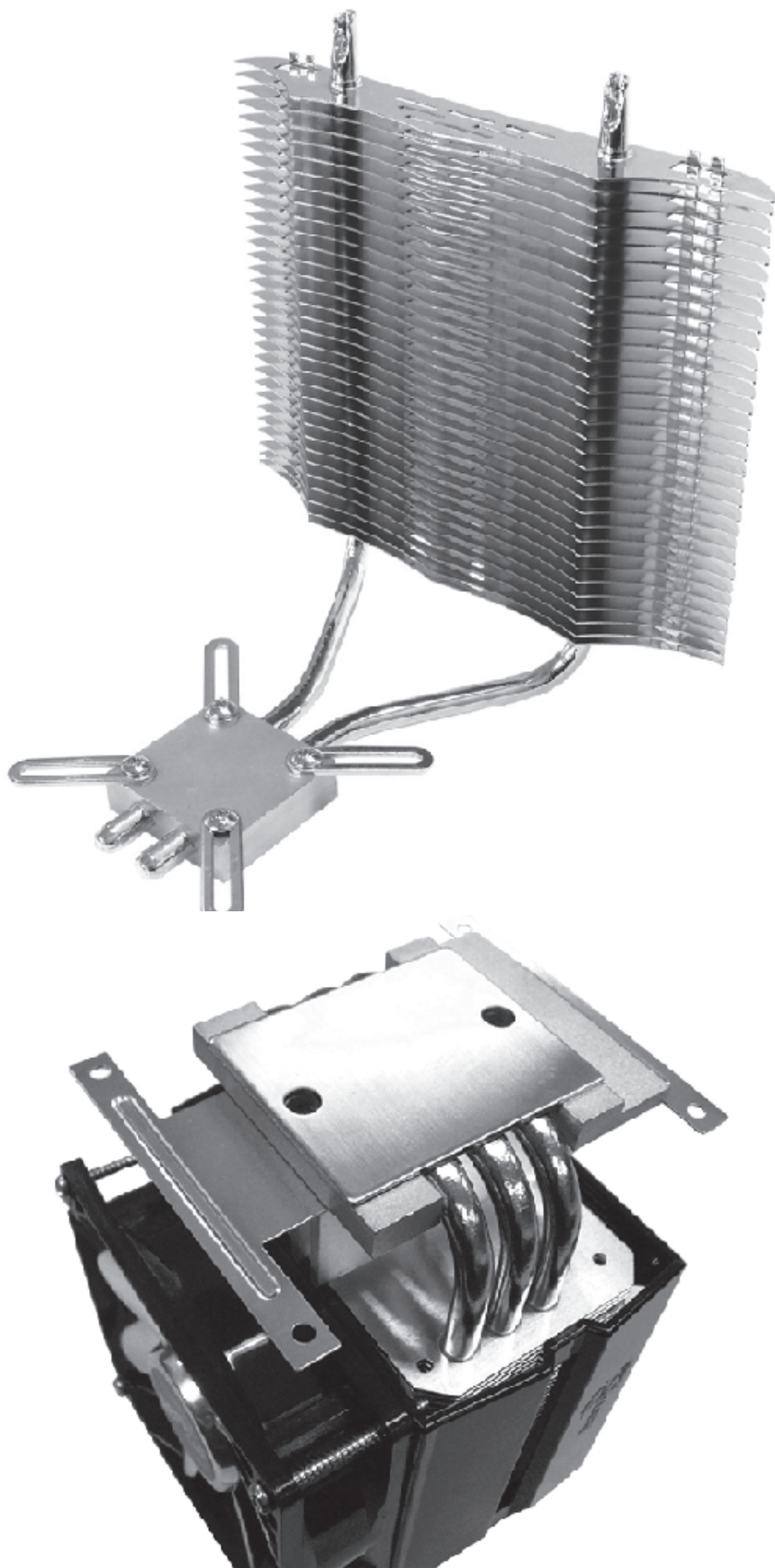


Figure 9 — AeroCool CPU cooling heat pipe devices. Note that the unit at the bottom is shown upside down to show the CPU mounting surface and the heat pipes. This unit includes a fan for extra cooling. AeroCool photos.



Figure 10 — W1TKZ 1976 Field Day 6m station; L-R unknown youth; Ed Jansson, WD4DTC (then WA1UTJ); (the somewhat younger) KD1K (then WA1QLI); with the liquid cooled 6m amplifier and the author's Yaesu FT620B transceiver. Chris Wiles, WA1RGA, photo

the CPU device and the heat pipe. CPU designers are faced with a nearly impossible nightmare task of moving the device heat out to the surface of the package to a point where a cooling device can be attached. The heat pipe designer also has the challenging problem of getting this CPU heat to the heat pipe fluid, which is the area that involves a thick copper plate (and its attendant weight) or an aluminum plate (with its lowered thermal properties). These coupling plates can be seen in Figures 8 and 9. There was a review of several of these CPU coolers in a special issue of *Computer Power User* magazine in 2005. This review gives considerable insight into the thermal issues involved with these coolers.³ (You can also do a Google search on “heat pipe” to find this article and much more information.)

An Amateur Radio Application?

I am going to get inventive now and hypothesize how these CPU heat pipes can be used in an Amateur RF application. Suppose you have a transmitter that employs ceramic-cased high-power transistors in the output stage. Normally these devices are screw-mounted through openings in a PCB to a heat sink. This device mounting could be done instead to the underside — the CPU

side — of a water heat pipe cooler, along with its PCB. The transistors would be hanging upside down, but they do not really care at all about that position. Such transistor mounting would have to be very carefully done so that any screw hardware does not penetrate the several heat pipes. Alternatively, an intermediary aluminum or copper plate could be used between the transistors and the cooler.

This conjecture reminded me that about 35 years ago I constructed a somewhat similar transmitter cooler for the home-brew compact 100 W amplifier of my 6 meter station at that time. While this cooler did not use any wicking agent inside the cooler, it had all of the other elements: a copper evaporator section in a portable cabinet, with an air-finned condenser section above the cabinet. This was operated at atmospheric pressure and employed one of the suitable (now banned) Freon liquid cleaning agents available at the time. This transistor cooler worked very well, bringing quite ample cooling into the tight space typically seen in a high power solid-state amplifier. Figure 10 shows this amplifier in action during the Field Day 1976 operations by the Wellesley Amateur Radio Society, W1TKZ. (I also very well remember that right after the opening bell, my first contact was YV5ZZ. That

opened up the eyes of the HF operators.) As this was a liquid cooler operated at atmospheric pressure, it depended upon having liquid flooding the evaporator section and the necessity of a sight glass to insure that sufficient liquid was available. In a heat pipe, the sidewall wick makes that assurance.

So you can see that I have had off and on experiences with liquid cooling of power electronics, some of it considerably before becoming involved in the AO-40 experience starting in 1990. I do not currently employ any liquid coolers in my current computer and station installation, as air-cooled heat exchangers have sufficed for these applications, but I have not abandoned the concept.

Let your imagination be your guide.

Notes

¹Dick Jansson, WD4FAB, “Spaceframe Design Considerations for the Phase IV Satellite,” *AMSAT-NA Technical Journal*, Vol 1, No. 2, Winter 1987-88.

²*Military Handbook Reliability/Design Thermal Applications*, MIL-HDBK-251, 19 January 1978, Chap.12, p 405.

³This *Computer Power User* review article about some CPU heat pipe coolers is available on the Internet at: www.computerpoweruser.com/Editorial/article.asp?article=articles/archive/u0904/52r04/52r04.asp&guid=



The “True” TLT H-mode Mixer

Transformers are important components in H-mode mixers, but conventional transformers introduce limitations. Here is a novel H-mode mixer configuration that uses transmission line transformers (TLTs) for improved performance.

In 2003 I built the first version of my transceiver with DSP IF processing.¹ I've used it since then and I have made many improvements (both in hardware and software). In 2008 I realized that I had to design a different hardware platform to implement all my new ideas. I wanted flatter IP3 values across the bands and better NF. The goal was IP3 at or above +40 dBm on all HF bands with the lowest possible NF (without compromising IP3 performance). So I started a new project and needed a new mixer to go along with it.

The H-mode mixer^{2,3} has become a standard in high performance HF front ends⁴ in recent years. It is simple, inexpensive and performs exceptionally well. I've enjoyed good results using a single balanced H-mode mixer variant in my T03DSP transceiver and that was my inspiration to pursue the enhanced H-mode mixer described here.

Martin Bakker, PA3AKE,⁵ did excellent research on high-performance H-mode mixers. His research demonstrated that the performance of an H-mode mixer greatly depended on two key components: switches and transformers.

I was limited to FST3125 switches, T4-1 and homemade transformers in my experiments. I had made two test H mode mixers (one using T4-1 transformers and another one with homemade conventional transformers) and measured their IP3 performance. Both mixers showed substantial IP3 drops with increasing operating frequency (+35 to +40 dBm on 160 meters, dropping to +25 to +30 dBm at 10 meters). I was disappointed with such results, so I started to look for improvements.

¹Notes appear on page 15.

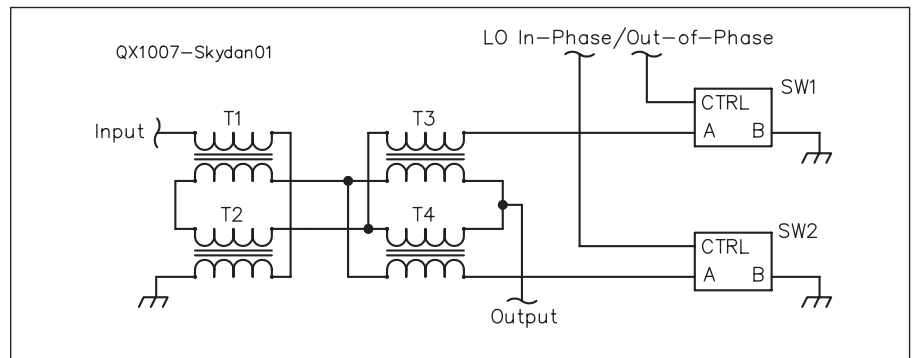


Figure 1 — RZ4HK's TLT H-mode mixer.

RZ4HK's TLT H-mode Mixer

During the Radio Communication 2007 design contest in Moscow (sponsored by the Suntlet Corporation), Gennady Bragin, RZ4HK, demonstrated his transmission line transformer (TLT) H-mode mixer. See Figure 1.

He claimed that it was better than H-mode mixers that relied on conventional transformers, particularly in terms of broadband and intermodulation performance. But my tests seemed to show that RZ4HK's approach was really no better than designs that used conventional transformers. (Actually, I was able to obtain good numbers on one band, but not over the entire HF spectrum.)

After further analysis of RZ4HK's TLT H-mode mixer I realized that there was a flaw. Look again at Figure 1. During each half of the LO cycle we have an open line (T3 or T4), which is connected in parallel

to the input transformers. This introduces additional parasitic capacitance and hampers wideband performance.

To craft a real high-performance TLT H-mode mixer, we must avoid configurations that create open lines in this fashion. The TLTs should operate without useless windings/lines that introduce parasitic, reactive loading. Otherwise we compromise the TLT's main advantage — its broadband performance.

Designing the “True” TLT H-mode Mixer

I started to think about a TLT H-mode mixer design that could maximize its performance while reducing the number and types of transmission lines.

A single balanced “true” TLT mixer is shown in Figure 2. It consists of the Guanella 1:1 TLT (T1) and the Ruthroff 4:1 TLT (T2).⁶

The principle of operation is shown in

Figure 3. When switch S1 is closed and S2 is open, transformer T1 will introduce an additional 180° phase shift (Figure 3A), compared to when S1 is open and S2 is closed (Figure 3B). In the latter case T1 will act as just a piece of matched TL. As we can see, alternating between the two switching configurations effectively results in 180° signal phase rotation. There are no open lines and all transformers work in their usual modes during the both phases of the LO signal. Such

a TLT configuration provides a 4:1 impedance transformation, so we will have a 12.5 Ω output impedance for the 50 Ω input, 25 Ω output for the 100 Ω input and so on.

Now, let's move to the double-balanced variant. We need two mixers fed with out-of-phase signals and a balanced-unbalanced transformer at the output.

The out-of-phase input signals can be easily obtained at no cost; we can just connect two identical mixers (Figure 2) in parallel

and twist the input lines on the one of them (Figure 4). The usual Guanella 1:1 balun transformer is used to combine the output of the two mixers and convert the balanced output to an unbalanced one. As we can see, only five simple TLTs were needed for a double balanced “true” TLT H-mode mixer and only 100 and 50 Ω TLTs were used.

The principle of operation is shown in Figure 5 (A and B). The double balanced configuration retains all the advantages of the single balanced variant (no open TLTs) and introduces even more. The mixer now has the same input and output impedances. It is possible to compensate for minor imbalances in the T1/T3 transformers by using units with closely matched characteristics.

The Prototype

An idea can certainly look good on paper, but the real proof is when you actually build the hardware and take measurements.

The first things I needed to make were the TLTs. To do this I needed 100 Ω and 50 Ω TLTs. I decided to use twisted wire lines, but the available reference data needed to make the line with the required impedance was not consistent.^{7,8} I wanted to be sure the TLTs had the required impedance, so, I used my RLC meter (it is able to measure inductance down to 1 nH and capacitance down to 0.01 pF) to measure the inductance and the capacitance of the lines and calculated line impedance using the following formula:

$$Z = \sqrt{\frac{L}{C}}$$

After spending some time twisting different wires, I finally made TLTs with the necessary impedances and then subsequently wound the transformers. Two test configurations (I just assembled the transformers in configurations shown in Figure 5) were assembled and tested with the network analyzer before soldering the transformers on the mixer board. I was satisfied with the results; the combined insertion loss of the five-TLT system was less than 0.3 dB at 30 MHz and approximately 0.5 dB at 100 MHz. I was unable to find any imbalances between the two configurations. It was time to assemble the mixer and test it.

The mixer schematic is shown in Figure 6. I used FST3125 switches with a 6 V power supply. The assembled RF unit, which uses the “true” TLT H-mode mixer, is shown in Figures 7 and 8.⁹

The transformers were wound on K10x6x5 400HH ferrite cores (10 mm outer diameter, 6 mm inner diameter, 5 mm height, 400 permeability). The T1 and T5 transformers contain 14 turns of 0.25 mm diameter twisted silk-lacquer-insulated wire (TL Z = 100 Ω). T2, T3 and T6 were made with

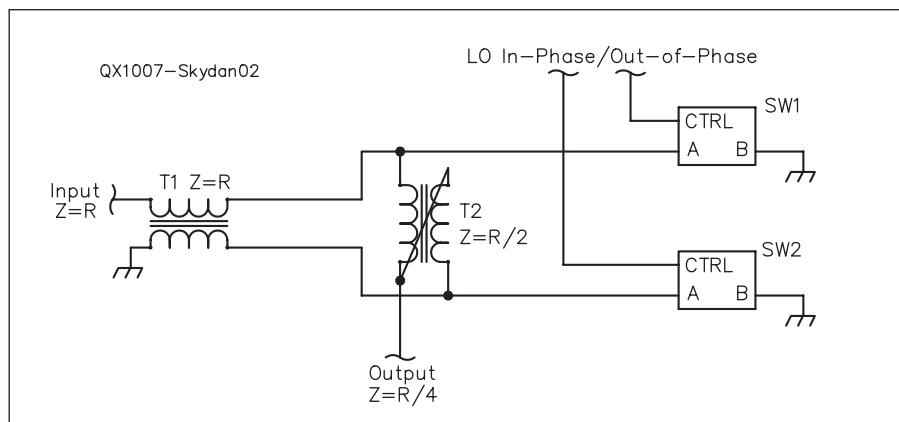


Figure 2 — The single-balanced “true” TLT H-mode mixer.

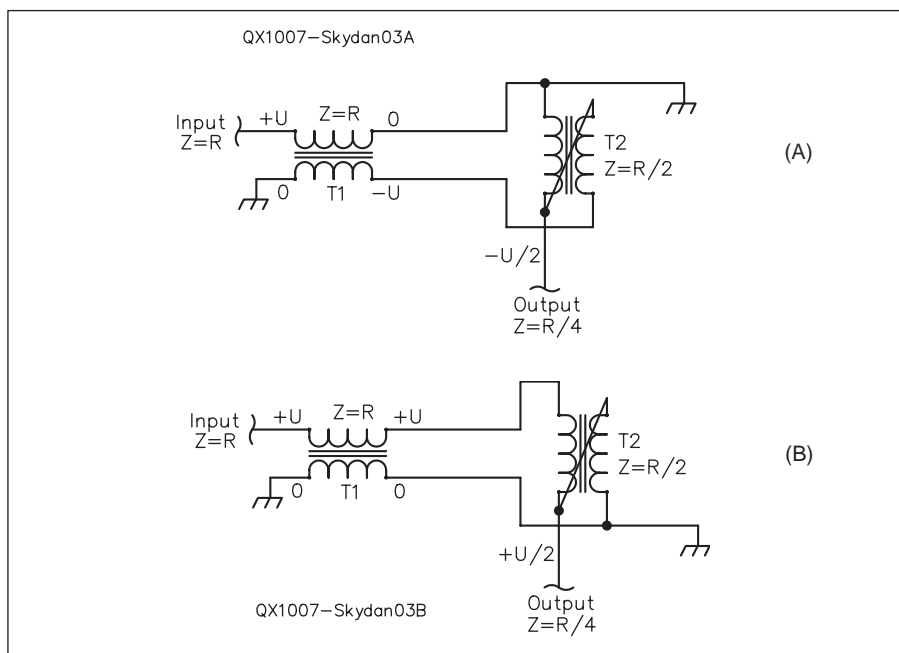


Figure 3 — The operating principal of the single-balanced “true” TLT H-mode mixer.

Table 1

“True” TLT Mixer Conversion Loss (CL, dB)

Band (meters)	160	80	40	20	15	10	6
	4.7	4.8	4.8	4.8	4.9	5.0	5.3

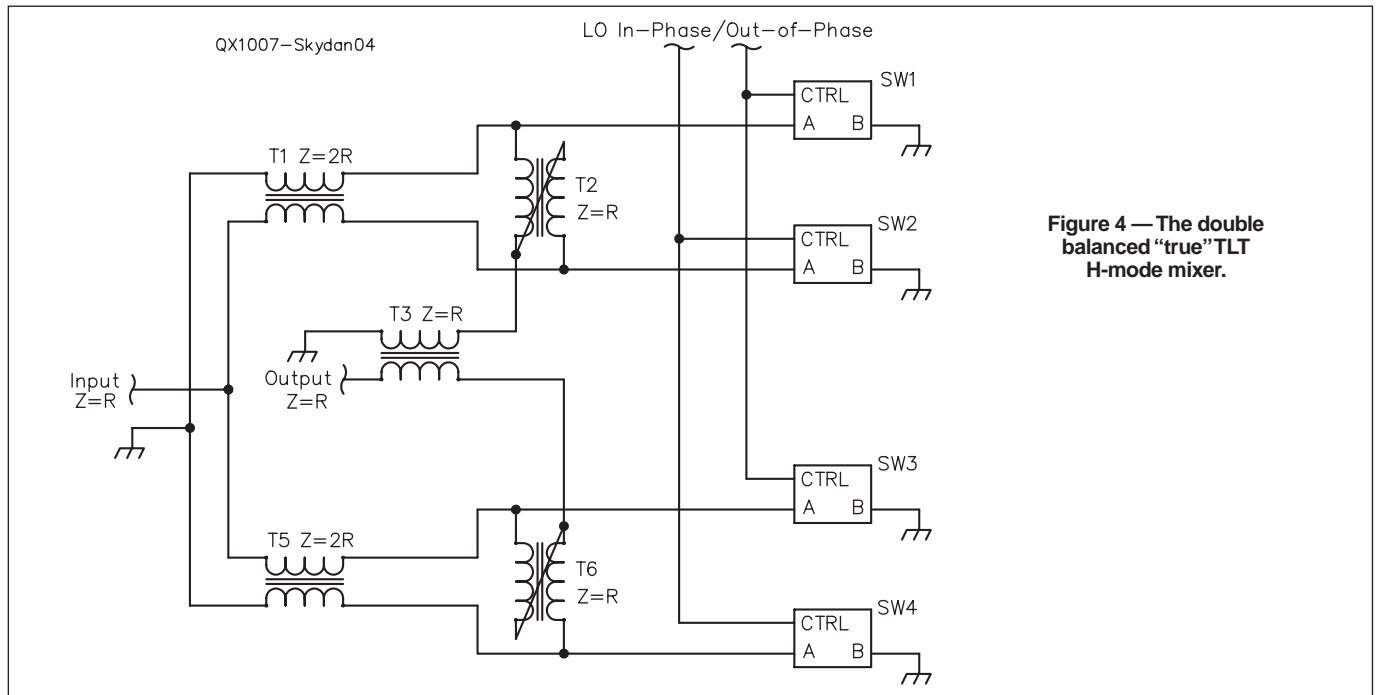


Figure 4 — The double balanced “true”TLT H-mode mixer.

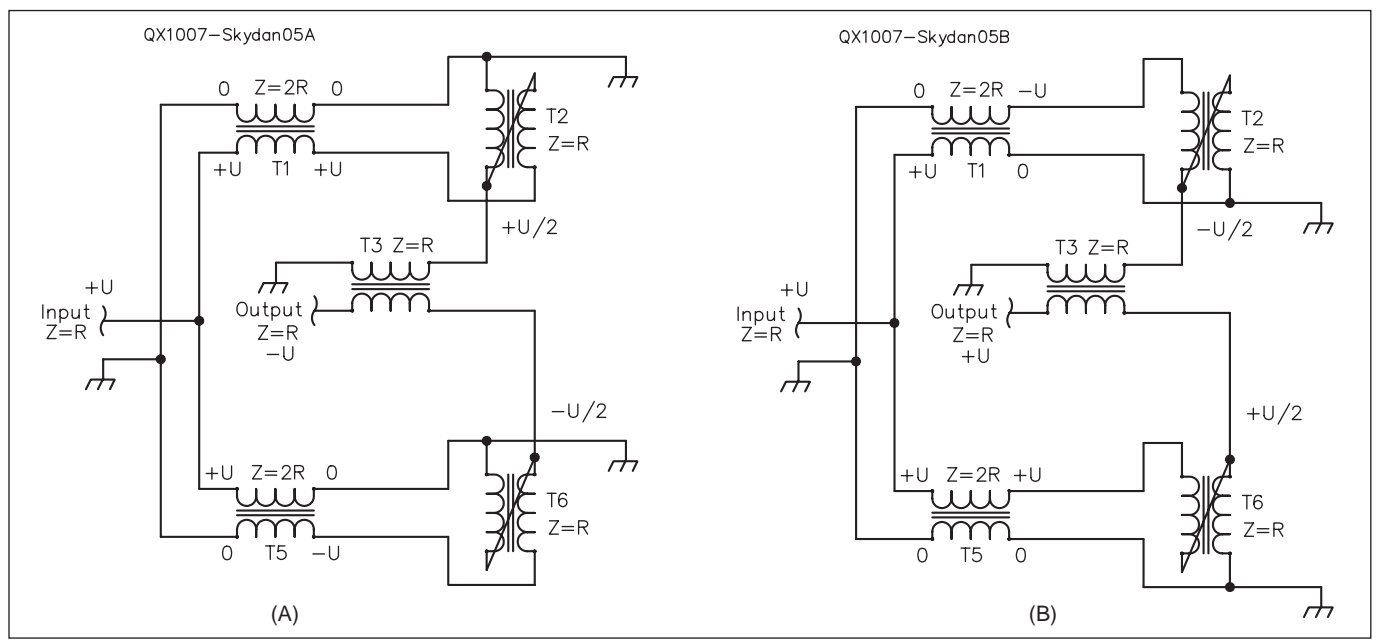


Figure 5 — The operating principal of the double balanced “true”TLT H-mode mixer.

Table 2
“True”TLT Mixer IP3 by Band (meters)

	160	80	40	20	15	10
IP3 (two test signals $F_{in} - 20$ kHz & $F_{in} - 40$ kHz, 0 dBm), dBm	46.9	43.2	41.6	39.4	37.2	37.6
IP3 (two test signals $F_{in} - 20$ kHz & $F_{in} - 40$ kHz, -5 dBm), dBm	45.1*	43.3	41.4	39.2	37.0	37.2
IP3 (two test signals $F_{in} + 20$ kHz & $F_{in} + 40$ kHz, 0 dBm), dBm	45.2	43.4	42.0	39.3	37.8	38.1
IP3 (two test signals $F_{in} + 20$ kHz & $F_{in} + 40$ kHz, -5 dBm), dBm	47.1*	43.4	41.9	39.0	37.6	37.6
IP3 (minimal), dBm	45.1	43.2	41.4	39.0	37.0	37.2

* - measurements were noise limited

10 turns of 0.35 mm diameter twisted lacquer-insulated wire (TL Z = 50 Ω).

Results

I measured the conversion loss (CL), IP3 and isolation of the mixer. The CL and IP3 results are shown in Tables 1 and 2. The RF-IF isolation was better than 46 dB (the worst case result on 10 meters; there is no balance adjustment). The residual LO voltage at the RF mixer port was -53 dBV on 10 meters (35 MHz LO frequency), improving with an LO frequency reduction to -68 dBV on 160 meters (7 MHz LO frequency).

The mixer showed its best IP3 performance (among the alternatives measured in my lab) over the whole HF range. The FST3125/T4-1 mixer showed substantial IP3 drop to +25-30 dBm on 10 meters.

Another important feature of this mixer is that it is much less sensitive to the switch biasing voltage. (After a test of the biasing voltage influence I just set the biasing point to $1/3 V_{cc}$, the center of the linear portion of the FST3125 switch transfer function). The T4-1 variant needed biasing adjustment on a per-band basis. Also, the “true” TLT H-mode mixer has much better IP3 amplitude law behavior and is less sensitive to termination quality. (I used the simple diplexer shown in Figure 9 between the 4-pole crystal filter and mixer, and managed to achieve front end IP3 performance at or above +40 dBm.)

Conclusions

I have presented a novel configuration of the H-mode mixer that makes use of TL transformers. This mixer has definite advantages over those designed with traditional transformers. It provides better broadband (both IP3 and insertion loss) performance. It has the potential to obtain better linearity and less conversion loss since the flux is effectively cancelled out in the transformer

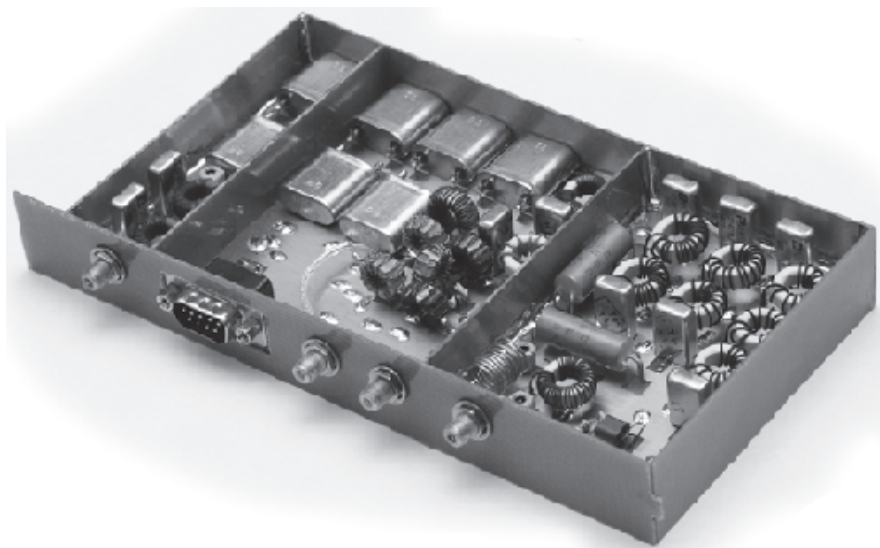


Figure 7 — The top side of the RF block.

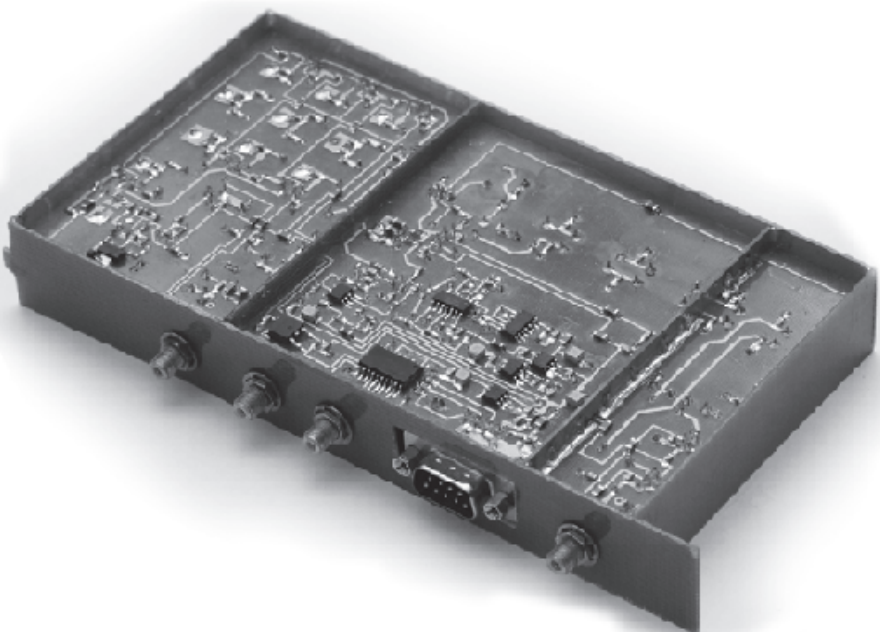


Figure 8 — A bottom-side view of the RF block.

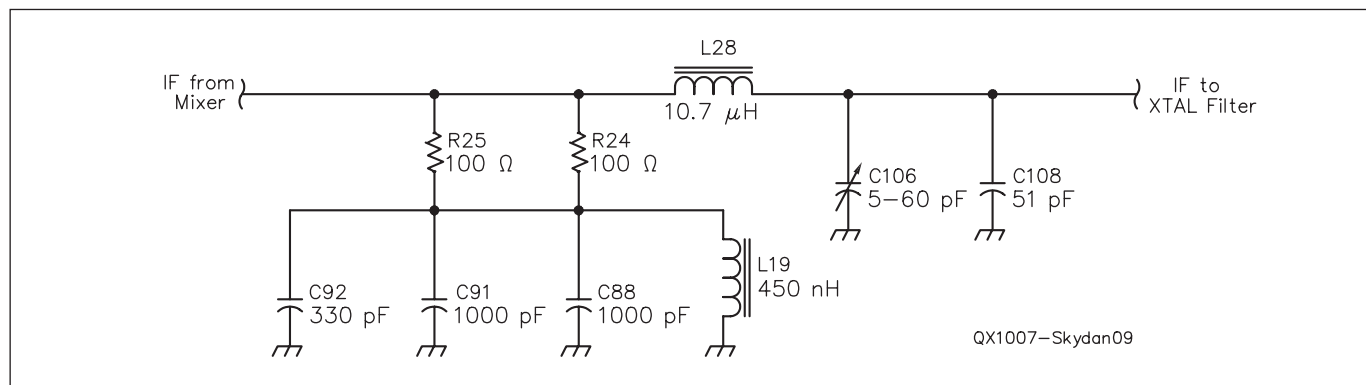


Figure 9 — The crystal filter matching network.

cores; the linearity of the "true" TLT H-mode mixer is determined by the switches alone. It is much cheaper and easier to obtain good results when using homemade transformers. TLTs are usually much less sensitive to the core material and provide more stable results when they are homemade with "primitive" technology compared to the conventional transformers.

The mixer performance numbers might be better if the proper termination is used (two hybridized crystal filters with a diplexer should do the job), but even with the simple termination I used, the results satisfy my requirements.

I think the mixer can be successfully used on VHF as well. The transformers are not the factors that limit broadband performance. Of course, we will need to solve the fast-switch-

ing problem at VHF; fast GaAs transistors might be the right choice.

Oleg Skydan, UR3IQO, was born in Kramatorsk, Ukraine in 1978 and graduated with a Masters degree in Computer Science from the Donetsk Artificial Intelligence Institute. He obtained his Amateur Radio license in 1994 and began experimenting in transceiver and antenna design. In addition to his innovative T03DSP transceiver that debuted in 2003, Oleg has begun designing and building its successor, the Neon (<http://neon.skydan.in.ua>).

Notes

- ¹Oleg Skydan, UR3IQO, "T03DSP," <http://t03dsp.skydan.in.ua>.
- ²Colin Horrabin, G3SBI, "G3SBI's High Performance Mixer," Technical Topics, *RadCom*, Oct 1993.

- ³Colin Horrabin, G3SBI, "G3SBI's H-Mode FST3125 Mixer – Constructional Details," Technical Topics, *RadCom*, Sep 1998.
- ⁴Colin Horrabin, G3SBI, Dave Roberts, G8KBB, and George Fare, G3OGQ, "The CDG2000 HF Transceiver," *RadCom*, June-Dec 2002.
- ⁵Martin Bakker, PA3AKE, "H-Mode Mixer Frontend," www.xs4all.nl/~martein/pa3ake/hmode/index.html.
- ⁶Jerry Sevick, W2FMI, *Transmission Line Transformers*, Fourth Edition, Noble Publishing Corporation, 2001.
- ⁷S.G. Bunin, L.P. Yailenko, *Spravochnik Radiolubitelja-Korotkovolnovika* (HF Amateur Radio Handbook), Kiev, Tehnika, 1984.
- ⁸Eric Tart Red, *Arbeitsbuch für den HF-Techniker: Daten, Fakten, HF-Grundhaltungen*, Franzis-Verlag GmbH, München, Germany, 1986.
- ⁹The details of the RF unit design can be found at the RF unit page on the Neon Web site: <http://neon/skydan.in.ua/RF.php>.



We Design And Manufacture To Meet Your Requirements
 *Prototype or Production Quantities
800-522-2253
This Number May Not Save Your Life...

But it could make it a lot easier! Especially when it comes to ordering non-standard connectors.


RF/MICROWAVE CONNECTORS, CABLES AND ASSEMBLIES

- Specials our specialty. Virtually any SMA, N, TNC, HN, LC, RP, BNC, SMB, or SMC delivered in 2-4 weeks.
- Cross reference library to all major manufacturers.
- Experts in supplying "hard to get" RF connectors.
- Our adapters can satisfy virtually any combination of requirements between series.
- Extensive inventory of passive RF/Microwave components including attenuators, terminations and dividers.
- No minimum order.

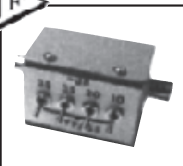
NEMAL
 Cable & Connectors
 for the Electronics Industry

NEMAL ELECTRONICS INTERNATIONAL, INC.
 12240 N.E. 14TH AVENUE
 NORTH MIAMI, FL 33161
 TEL: 305-899-0900 • FAX: 305-895-8178
 E-MAIL: INFO@NEMAL.COM
 BRASIL: (011) 5535-2368
URL: WWW.NEMAL.COM


NATIONAL RF, INC.




VECTOR-FINDER
 Handheld VHF direction finder. Uses any FM xcvr. Audible & LED display
 VF-142Q, 130-300 MHz \$239.95
 VF-142QM, 130-500 MHz \$289.95



ATTENUATOR
 Switchable, T-Pad Attenuator, 100 dB max - 10 dB min BNC connectors
 AT-100, \$89.95



TYPE NLF-2 LOW FREQUENCY ACTIVE ANTENNA AND AMPLIFIER
 A Hot, Active, Noise Reducing Antenna System that will sit on your desk and copy 2200, 1700, and 600 through 160 Meter Experimental and Amateur Radio Signals!
 Type NLF-2 System: \$369.95



DIAL SCALES
 The perfect finishing touch for your homebrew projects. 1/4-inch shaft couplings.
 NPD-1, 3 3/4" x 2 3/4", 7:1 drive \$34.95
 NPD-2, 5 1/8" x 3 5/8", 8:1 drive \$44.95
 NPD-3, 5 1/8" x 3 5/8", 6:1 drive \$49.95

NATIONAL RF, INC
7969 ENGINEER ROAD, #102
SAN DIEGO, CA 92111

858.565.1319 FAX 858.571.5909
www.NationalRF.com

Down East Microwave Inc.

We are your #1 source for 50MHz to 10GHz components, kits and assemblies for all your amateur radio and Satellite projects.

Transverters & Down Converters, Linear power amplifiers, Low Noise preamps, coaxial components, hybrid power modules, relays, GaAsFET, PHEMT's, & FET's, MMIC's, mixers, chip components, and other hard to find items for small signal and low noise applications.

We can interface our transverters with most radios.

Please call, write or see our web site
www.downeastmicrowave.com
 for our Catalog, detailed Product descriptions and interfacing details.

Down East Microwave Inc.
 19519 78th Terrace
 Live Oak, FL 32060 USA
 Tel. (386) 364-5529

The Shunt Method for Crystal Parameter Measurement

Here is a reliable, accurate way to obtain values for Q, R_m, C_p and frequency.

I have previously written an article in which I discussed measuring crystal parameters in shunt rather than in the conventional series configuration.^{1, 2} I believe that the shunt method has a number of advantages over the series method.

In a subsequent letter to the editor of *QEX*, Alan Bloom, N1AL pointed out that there is a difference between the frequency of maximum attenuation in the shunt method and the series resonant frequency of the crystal itself.³ This difference is due to the parallel capacitance of the crystal and the fixture in which it is measured.

This same error is also observed in the more usual series method of parameter measurement and so the problem of parallel capacitance is not unique to the shunt method of parameter measurement. Rather, it remains one of the impediments to careful measurement of crystal parameters. It can be difficult to measure parallel capacitance to the accuracy needed to correct for errors in series resonant frequency.

In the amateur literature, the shunt method has not had the analysis that the conventional series method has had, so I will discuss it in some detail. I will also discuss the parallel capacitance problem in the context of the shunt method and suggest additional measurements that will allow one to measure parallel capacitance with sufficient accuracy. Finally, I will describe how I've modified the algorithm used in the previous article to include a measurement of parallel capacitance and I will discuss how accurately crystal parameters may be measured in an automatic mode.

for a crystal is shown in Figure 1. The motional capacitance, C_m , and the motional inductance, L_m , are the equivalent electrical values for the piezoelectric effect of the mechanical vibrations of the crystal; hence the term "motional" in their name. The motional resistance, R_m , is an electrical equivalent to describe the mechanical losses

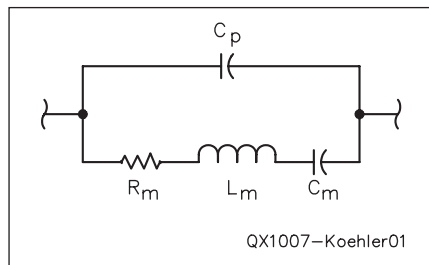


Figure 1 — The equivalent circuit for a piezoelectric crystal.

in the crystal. The total parallel capacitance of the crystal, C_p , is a physical capacitance, and can be thought of as having two parts; that of the crystal itself and that of the external circuit. The crystal capacitance is the actual capacitance of the two conducting plates on either side of the quartz dielectric and its holder. The external parallel capacitance is that of the fixture or circuit in which the crystal is placed plus stray external circuit capacitance.

The parallel capacitance, C_p , has an effect on the response of the crystal in a circuit. This means that the usual amateur practice of independently measuring the capacitance of a crystal with some sort of capacitance meter and then measuring the crystal response in a different instrument with, almost certainly, a different stray capacitance can cause significant errors. A few pF here or there can make a difference — especially for overtone crystals in the VHF region.

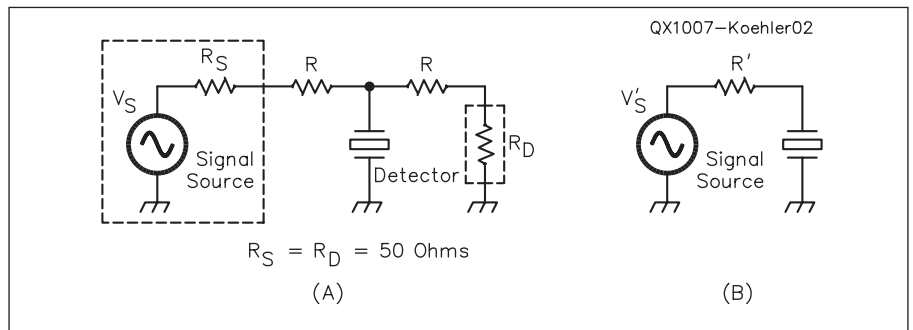


Figure 2 — The circuit for measuring crystal parameters in shunt is shown in Part A. Part B shows the equivalent circuit of circuit (A). R' is $R_s + R$ in parallel with $R_D + R$. V_s' is

$$\left(\frac{R_D + R}{R_D + R_s + 2R} \right) V_s$$

The Effect of Parallel Capacitance

The commonly used equivalent circuit

¹Notes appear on page 25.

The Crystal Circuit

As Bloom said, there are really three different resonant frequencies depending on how you define resonance. One is where the crystal has the least impedance magnitude, one is where the phase shift across the crystal is zero and one is the resonance defined by just C_m and L_m . For the discussion that follows, I shall define the latter as the series resonant frequency, f_0 ; it will be given by:

$$f_0 = \frac{1}{2\pi\sqrt{L_m C_m}} \quad [\text{Eq 1}]$$

The crystal is a series R-L-C circuit in parallel with a capacitance. The impedance of the series branch is:

$$Z_s = R_m + j\left(2\pi f L_m - \frac{1}{2\pi f C_m}\right) \quad [\text{Eq 2}]$$

and that of the parallel branch is:

$$Z_c = \frac{1}{j2\pi f C_p} \quad [\text{Eq 3}]$$

The total admittance of the crystal at all frequencies is thus:

$$Y_c = \frac{1}{Z_c} + \frac{1}{Z_s} \quad [\text{Eq 4}]$$

It will be obvious that, at the resonant frequency defined as in Equation 1, the crystal will actually have some capacitive susceptance due to C_p . The impedance will only become purely resistive at a somewhat higher frequency; this will be the parallel resonant frequency at which the phase shift through the crystal will be zero. The third resonant frequency referred to by Bloom will be the frequency at which the magnitude of the admittance is a maximum and this will be lower than f_0 .

Figure 2 shows a crystal in a shunt circuit, which we will now study in some detail. Figure 2A shows the actual circuit and Figure 2B shows the equivalent circuit. The frequency response of this circuit, the normalized voltage appearing across the crystal compared to the source voltage is given by:

$$\rho = \frac{1}{1 + Y_c R'} \quad [\text{Eq 5}]$$

With my signal generator/detector, I can only measure the magnitude of this response.⁴ The frequency at which Equation 5 has a minimum magnitude will *not* be that at which the magnitude of the crystal admittance is a maximum. It is not one of the three resonant frequencies mentioned previously;

instead it is yet another frequency whose value depends on the crystal admittance and the value of R' . It is worth noting that, in the conventional series method of crystal parameter measurement, the frequency of maximum transmission is also not any of these three resonant frequencies! Its frequency, as well, depends on the source and detector impedances of the measurement apparatus and the impedance of the crystal.

Figure 3 shows a typical frequency response for a crystal in the shunt mode; this is the actual response of a 55.25 MHz overtone crystal as measured with the equipment mentioned above using a fixture that I will describe later. If there were no parallel capacitance and if the frequency scale were logarithmic, the plot would be symmetrical in frequency.⁵

The presence of a parallel capacitance, C_p , causes two observable effects in the shunt response. Firstly, the response becomes asymmetrical and the lower frequency wing

of the response is lowered. The greater the parallel capacitance, the greater the asymmetry; this asymmetry is evident in Figure 3. Secondly, the frequency of maximum attenuation is reduced as the parallel capacitance is increased.

I will now describe how one may measure C_p accurately as part of the shunt method of measuring crystal parameters.

The Measurement Fixture and Determining C_p

A circuit diagram of my measurement fixture is shown in Figure 4. Figure 5 shows the fixture itself. It was built on a small scrap of double-sided FR4 printed-circuit board using a Dremel tool to grind out lands from the top copper surface. The input is a piece of RG-188 A/U coaxial cable and it goes to MiniCircuits PAT-10 attenuator. This attenuator, along with the 49.9 Ω 1% resistor at its output, was put in to provide a good match

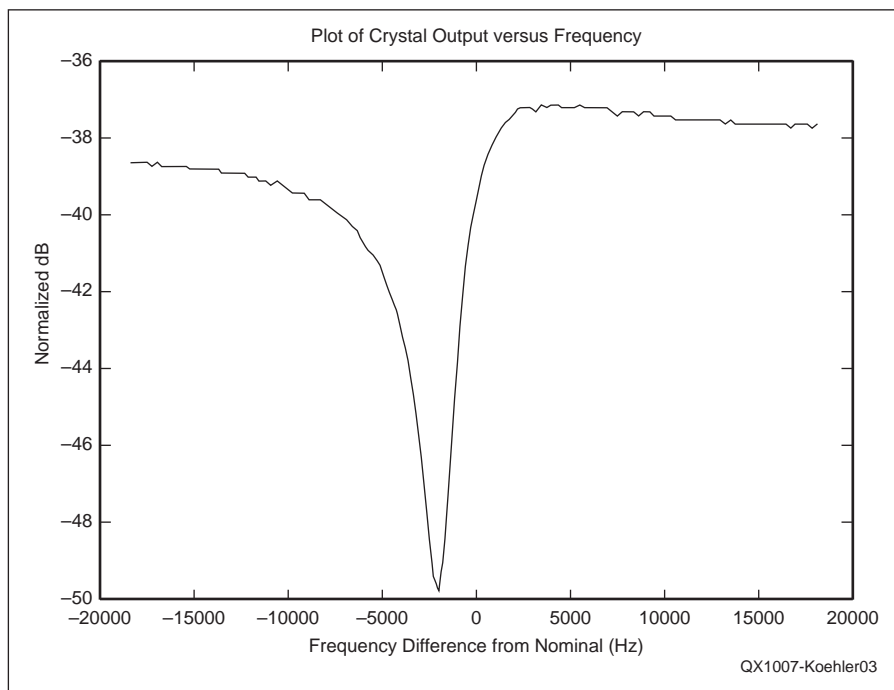


Figure 3 — The frequency response of a 55.25 MHz overtone crystal measured in shunt.

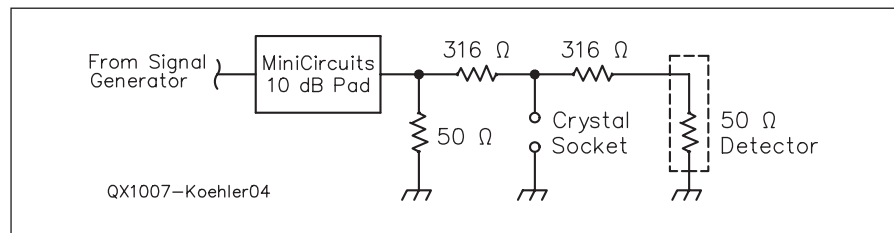


Figure 4 — Circuit diagram of a fixture for measuring crystal parameters in shunt.

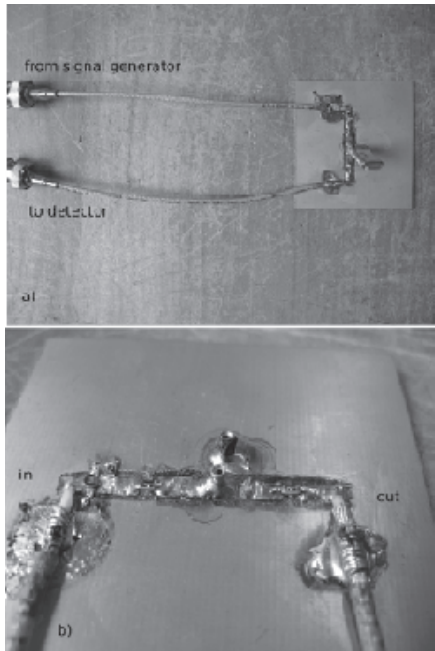


Figure 5 — Part A is a photo showing the fixture with a crystal in place. Part B is a close-up photo showing the circuit components.

to the signal generator, which is basically a DDS IC output going through a low-pass elliptical filter network. The junction of the attenuator and the $49.9\ \Omega$ resistor to ground provides a source to the series resistor with an impedance of $25\ \Omega$ resistive. The two 0805 size surface-mount $316\ \Omega$ 1% resistors are the shunt network to and from the crystal and the output is another length of RG-188 A/U cable going to the detector, which has a $50\ \Omega$ resistive input impedance. The crystal socket consists of two machined pins broken from an IC socket and spaced to fit an HC-49U crystal. The effective value of R' in Equation 5 is $176.5\ \Omega$. The loss of this fixture is considerable, but it is entirely resistive, except for stray capacitance and inductance, over a wide frequency range. The stray capacitance of this fixture is due to the capacitance of the wires and lands relative to the ground plane, and would be expected to be a few pF. The stray inductance would not be expected to be more than a few nH.

If a crystal is not plugged into the socket, then the equivalent circuit shown in Figure 2B is still valid but the place of the crystal is replaced by a single capacitor, the stray circuit capacitance, which we will call C_s . The normalized complex frequency response of this circuit is that of a classic R-C low-pass filter given by:

$$\rho_{RC} = \frac{1}{1 + j\omega\tau} \quad [\text{Eq 6}]$$

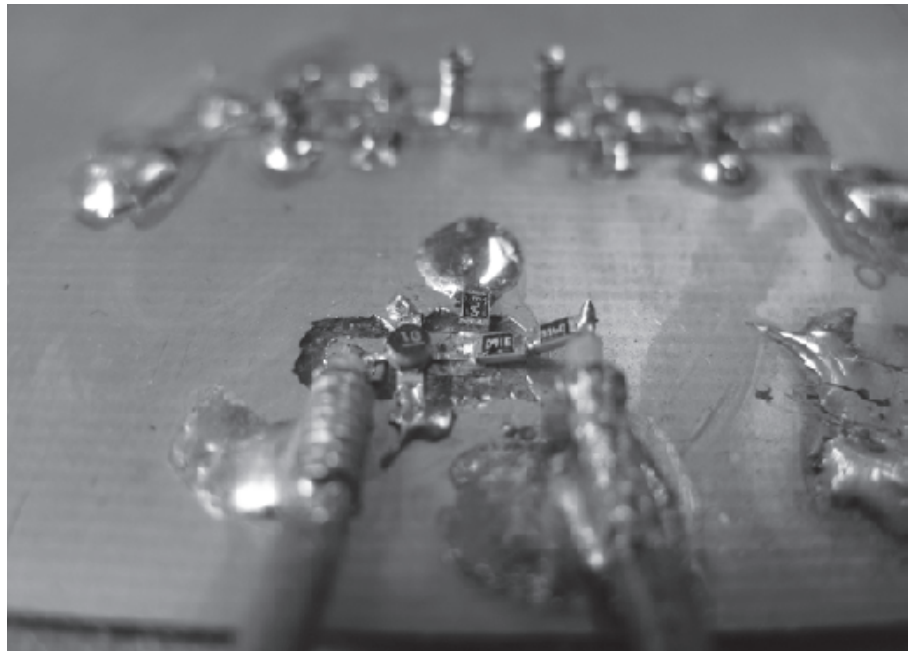


Figure 6 — Photo of the “zero-capacitance” reference fixture.

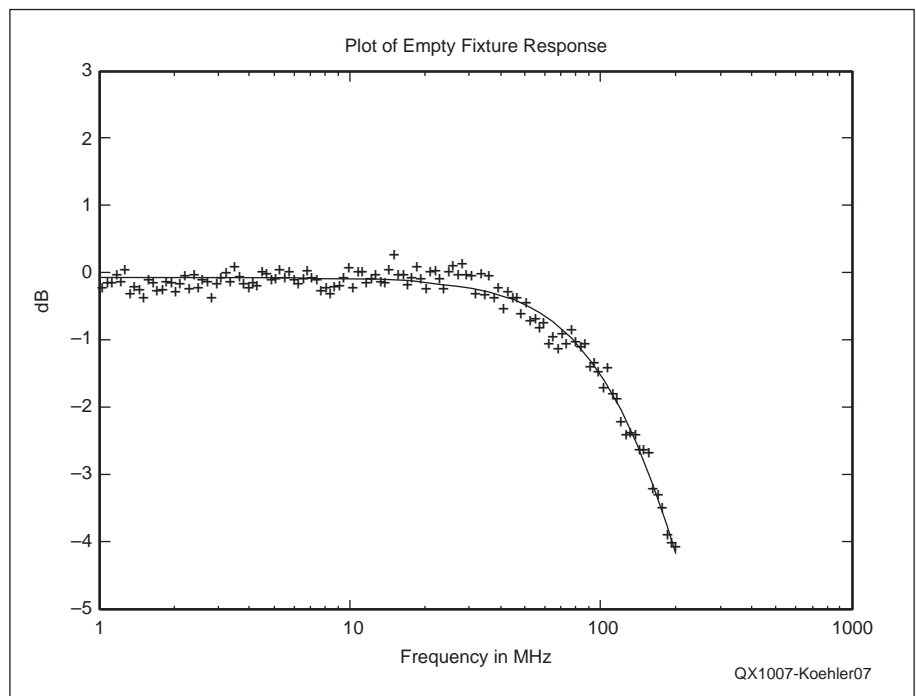


Figure 7 — Plot of the normalized frequency response of the measurement fixture with no crystal in place. This is the actual response of the measurement fixture, with no crystal minus the response of the “zero-capacitance” reference fixture. The solid line is the best fit to Equation 6 as determined by *gnuplot*.

where $\omega = 2\pi f$ and $\tau = R'C_s$. The “time constant,” τ , is given that name because it has dimensions of time.

Because my signal generator/detector covers the range from near zero to 200 MHz, it is possible to determine this normalized response and, knowing R' , we can thus calcu-

late C_s . To measure a normalized response, we must first measure the response of a similar circuit with no stray capacitance. I built a reference fixture, electrically identical to that of Figure 4 but with as little stray capacitance as possible. Figure 6 shows a close-up photograph of this fixture. The junction of

the two 316 Ω resistors is in the air and so should represent a capacitance to ground of zero; in reality, it may be a few tenths of a pF, but surely not much more. Then the ratio of the measured response of the fixture with the crystal socket (but with no crystal in place) to the reference fixture should be the response of a classic R-C low-pass filter. I measured the response at 128 frequencies for both the crystal fixture and the reference fixture spaced equally on a logarithmic frequency scale from 1 to 200 MHz. Figure 7 shows a plot of these normalized measurements where each data point is the average of 16 separate measurements. This plot of the measured values was made with a program called *gnuplot*.⁶ This is a very useful and free program available for *Windows*, *Linux*, *MacOS* and other operating systems. *Gnuplot* also has the capability of finding the best fit of arbitrary functions to data points. If the function is defined to be the response curve given by Equation 6, then the fit will give a value for the coefficients and hence the value for $R'C_S$. The best fit is shown in Figure 7 as a continuous line. From this best fit, it was found that C_S was 5.65 pF with an uncertainty of about 0.1 pF.

Except for frequencies near resonance (or its overtones), a crystal is simply a capacitance so, if a crystal (in this case, a 55.25 MHz overtone crystal) is placed in the fixture and the same relative amplitude response is measured, as shown in Figure 8, the value of the sum of the crystal capacitance plus the stray capacitance can be measured in the same way. From the best fit in Figure 8, the value of the total parallel capacitance is 10.10 pF. The crystal capacitance alone is thus $10.10 - 5.65 = 4.45$ pF; again the uncertainty in this value is approximately 0.1 pF.

Note that in both Figures 7 and 8, the response at low frequencies is not asymptotic to 0 dB as would be expected, but rather to about -0.05 dB. This is a result of the fact that the reference fixture and the measurement fixture do not have exactly equal losses, caused, no doubt, by the tolerance in the attenuation of the PAT-10 attenuators. This trivial difference has no effect on the calculated values of capacitances.

To summarize, it is apparent that measurements can be made, in the shunt mode, which allow one to infer the total parallel capacitance of a crystal while it is in its measurement fixture; this is C_p . I emphasize that this is the value with the crystal in the same fixture that will be used to measure the crystal parameters.

Modeled Crystal Responses in the Shunt Mode

With modern mathematical tools such as *Matlab*⁷ or *Scilab*⁸ for numerical modeling

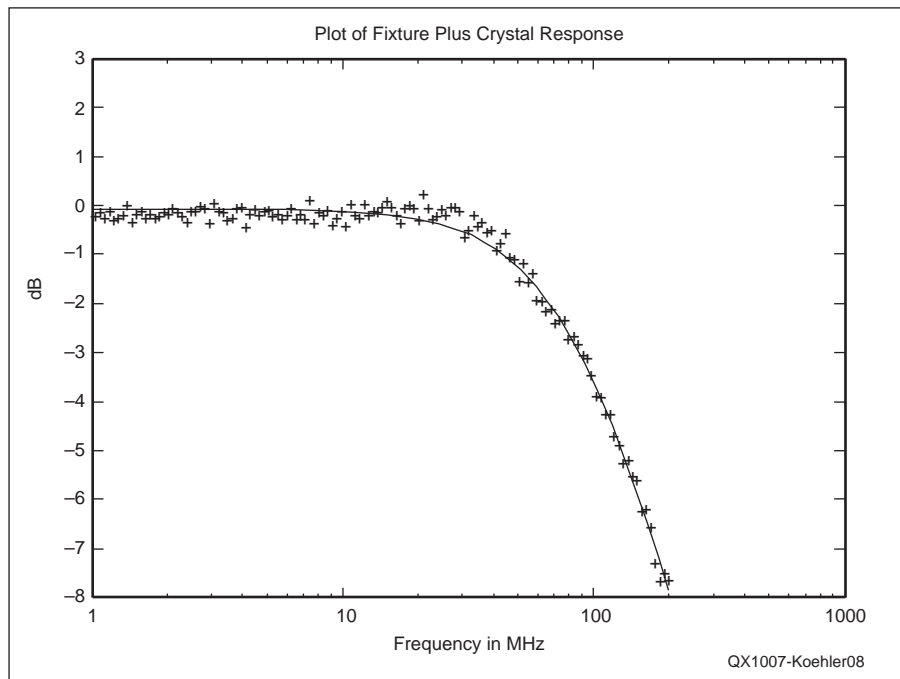


Figure 8 — Plot of the normalized frequency response of the measurement fixture with a 55.25 MHz crystal in place. Again, this is the actual response minus the “zero-capacitance” reference response. The solid line is the best fit to Equation 6 as determined by *gnuplot*. The dip due to crystal resonance, with a width of less than 0.01% of the 199 MHz plot width, falls between the measured frequencies and so does not appear in the diagram.

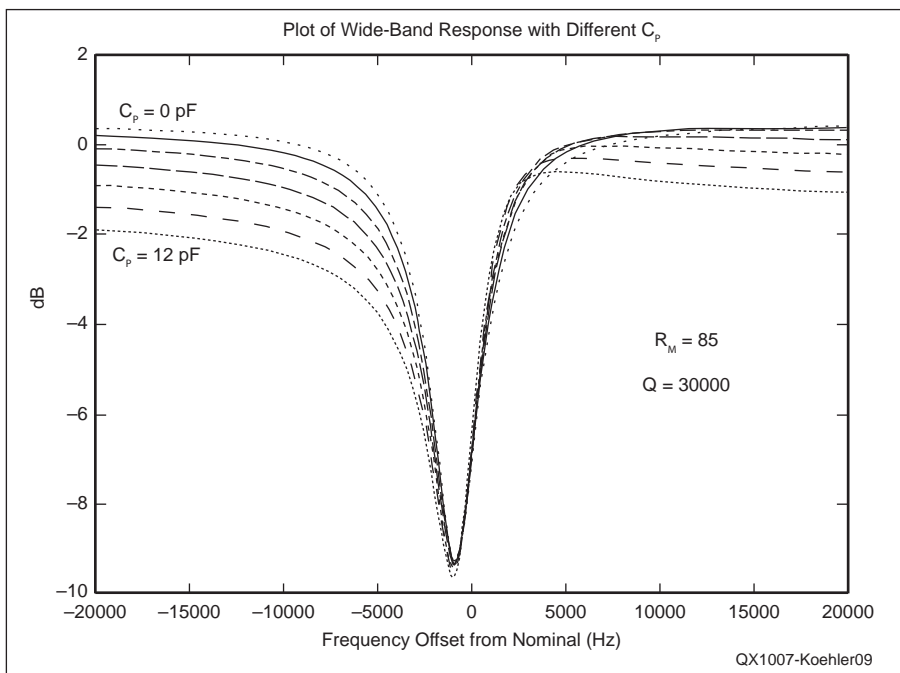


Figure 9 — Modeled frequency responses for an overtone crystal in shunt configuration for different values of C_p .

or, alternatively, *Maple*⁹ or *Mathematica*¹⁰ for symbolic manipulation, it is possible to make accurate models of circuit behavior. These tools allow us to examine effects such as that of parallel capacitance in more detail and this, in turn, allows us to understand exactly how this capacitance affects the measurements.

I used *Scilab* to study these effects because it is open software and thus free to install and to use. *Scilab* is very comparable to *Matlab*. The other mentioned mathematical tools are commercial products and quite expensive.

I had previously measured the parameters

of the same 55.25 MHz overtone crystal used in the C_p measurements above. This particular crystal had an R_m of 84Ω and a Q of 2.85×10^4 . I chose this crystal to be the basis of a model because, with high R_m and low Q , the effects of parallel capacitance would be easily demonstrable; a high R_m and a low Q are needed to make the frequency correction cited by Bloom significant. The frequency response of a crystal with these parameters (rounded off to 85 and 30,000, respectively) in a shunt measurement fixture with the same circuit as that of Figure 4 was modeled exactly using *Scilab*. The equations used in *Scilab* for this purpose are given in the “*Scilab Equations*” sidebar.

The results of this modeling are shown in Figure 9 as a family of curves for different values of C_p . These models were calculated using Equation 4 to represent the crystal. You can see that, for $C_p = 0$, the response curve is very symmetrical, while for $C_p = 12$ pF, the curve is asymmetrical, as in Figure 3. The reference level in Figure 9 is the level expected from the fixture with no crystal in place. As C_p is increased, the lower frequency side of the response curve has decreased magnitude while, on the higher side, the band-pass shape becomes sharper and, with C_p having a value of 12 pF, there is a marked “hump” in the response curve.

It is harder to see the effect of C_p on the frequency of maximum attenuation in this graph so Figure 10 shows the central region in more detail. As C_p increases, the attenuation increases and the frequency at which the maximum attenuation occurs moves to lower frequencies. When C_p has a value of 12 pF, the frequency offset from f_0 is some 160 Hz lower than when C_p is zero. Recall that when C_p is zero, the frequency of maximum attenuation is the true series resonant frequency defined by Equation 1. The maximum attenuation has also increased by about 0.5 dB; this additional attenuation is just due to the low-pass filter effect of C_p being superimposed on the crystal series circuit.

If I use the equations that Bloom gave, and put in the modeled parameters for this crystal, the frequency offset for 12 pF of parallel capacitance should move the frequency of maximum admittance magnitude (of the crystal alone!) down about 330 Hz. In the actual modeled response, however, which is the response of the crystal in the fixture, the shift was only about 160 Hz. I will come back to this discrepancy later.

Finally, Figure 11 shows the wide-band response of the actual crystal in the actual fixture compared to a modeled equivalent crystal with the same total C_p of 10.1 pF. This model was made with the parameters shown in the graph; these parameters were measured by the technique that I described

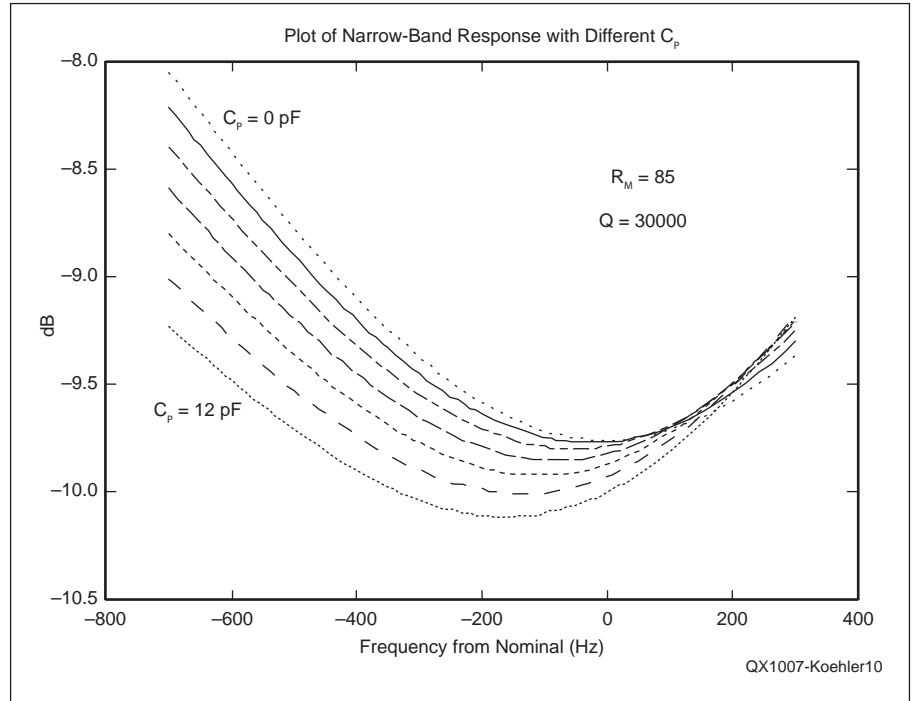


Figure 10 — Modeled responses in a smaller frequency interval near the minima of the plots for various values of C_p . This plot shows how the frequency of maximum attenuation is affected by C_p .

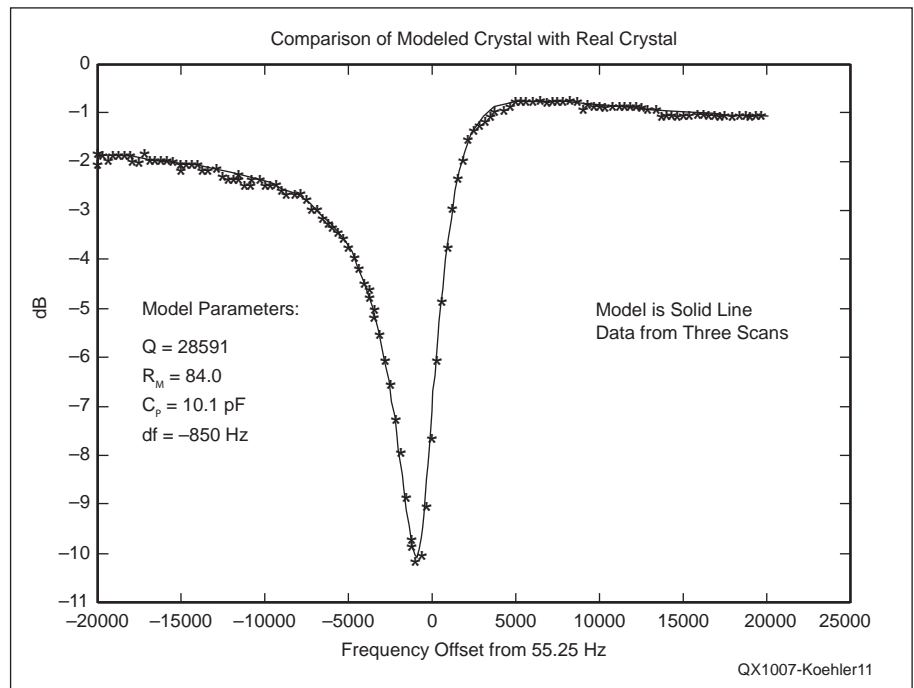


Figure 11 — Plot of the measured frequency response of a real crystal in the fixture shown in Figure 5 compared to a model crystal using parameters measured for the same crystal. The cross symbols are the measured points while the straight line is the modeled response. The measured points are from three separate scans of the same crystal.

in my earlier article. Since the exact value of the resonant frequency is not known in this graph, I arbitrarily “slid” the model in frequency till it matched the measured points as closely as possible. The frequency offset,

df , of -850 Hz is the difference between the measured frequency of the central minimum and the nominal crystal frequency of 55.250 MHz.

Figure 11 is very instructive because the

fit between modeled points and measured points is so good. Most importantly, it shows that characterizing the crystal by parameters as measured with an algorithm that I developed in my previous article, results in a very good fit to the actual crystal behavior.

Secondly, because of the good fit in the wings of the response plot, it shows that the value of C_p measured by the technique described above is an accurate measure of the true parallel capacitance of the crystal in that fixture.

Finally, it shows that the crystal equivalent circuit in Figure 1 is really a very good approximation to the behavior of a real crystal. The measured points were from an overtone crystal in the lower VHF region, and the effects of possible other crystal parameters such as lead inductance, leakage resistances and so on are obviously not significant. Therefore, for the crystals most commonly used for building filters in the MHz region, these second-order effects may certainly be neglected for most purposes; the simple model of Figure 1 is sufficient.

Before leaving the topic of modeling crystal responses, let me demonstrate one of the other mathematical tools that are available to users of personal computers. I try to use only open software myself, but a local community college has *Maple* installed on its computers. I took a course at this college and so, as a student, was able to use it. A *Maple* worksheet for the same crystal modeled with *Scilab*, is given in the sidebar “Modeling with *Maple*.” In this worksheet, a three dimensional plot was made of response versus frequency with the third dimension being the value of this parallel capacitance from 0 to 12 pF. You can see that as the parallel capacitance is increased, the low frequency wing of the response is lowered and the hump on the high side of resonance gets more prominent and moves to lower frequencies. If you run this worksheet in *Maple* on a computer, you can rotate the 3D shape by dragging it with a mouse so that you can readily see more details about how the shape is altered as a function of C_p . The power of these mathematical tools never ceases to astonish me; you basically just have to type in the equations describing the response and the program does all the rest. It makes it so easy to visualize what is going on.

The Signal Generator/Detector Measurement Algorithm

My signal generator is capable of setting the frequency to an accuracy of about 1 Hz and the detector can measure levels with an accuracy of, probably, better than 0.2 dB. The algorithm was developed to provide an automatic way of measuring crystal parameters using this signal generator/detector combi-

nation. I shall refer to frequency “scans,” by which I mean that the signal generator was stepped through a range of frequencies and at each step, after waiting for the detector output to settle, the amplitude was measured. Most scans had 128 discrete frequencies and the separation of points was logarithmic.

The procedure was as follows: with the crystal in the fixture, the scan was set to cover a range from 1 to 200 MHz. The measured amplitude points were used to determine the value of C_p . I did not fit all the data points to Equation 5 but, rather, used the fact that at the -3 dB point, the value of $\omega R' C_p = 1$. I used a polynomial fit of the data points in the vicinity of the -3 dB level to find the frequency at which the attenuation is -3.01 dB and then solved for C_p .

After determining C_p , a second scan was done over a relatively wide region around the crystal's expected resonant frequency. Once the central dip was located approximately, a third, much narrower scan was made and the data from this narrow-band scan was then used to determine the crystal parameters as described in my first article. The entire procedure, including the C_p measurement, takes about one second or less for each crystal and is initiated by pressing a single button. It couldn't be much easier.

Accuracy

One might ask what sort of accuracy one can expect from an automatic measurement technique such as that used in my signal generator/detector. Frequency errors can probably be disregarded because the signal generator frequency is well determined. Errors will essentially all be in the determination of the amplitude as the response is measured. The A/D conversion in the detector is in steps of, very roughly, 0.1 dB and there may be systematic errors in the conversion from A/D level to absolute dBm. These will limit the ultimate accuracy. In my discussion about calibrating the attenuator in my article describing the signal generator, I argued that the ultimate accuracy is probably no better than 0.2 to 0.3 dB. Perhaps the final word on accuracy is given by Figure 11, which shows how well a modeled response, using parameters as measured with the technique described, fits the measured data points.

Frequency Offset of the Admittance Maximum

I have left begging the question of the measured frequency given by my algorithm, which is the frequency of minimum transmission and how it is related to the series resonant frequency, f_0 . According to Bloom, the frequency of minimum impedance magnitude of the crystal alone should be lower than the series resonant frequency, f_0 , by an amount given by:

$$df = f_0 \frac{C_p}{2Q^2 C_m} \quad [\text{Eq } 7]$$

Since C_m is a derived quantity from the measured parameters, I prefer to rearrange this formula so that it only uses measured parameters; this gives me:

$$df = f_0^2 \pi C_p \frac{R_m}{Q} \quad [\text{Eq } 8]$$

Putting in the values for the crystal used here, df , which is $f - f_0$, should be about 285 Hz. For comparison, in the simulated responses of the crystal in the measurement fixture, the frequency of the minimum of the response was about 160 Hz lower than f_0 .

It is possible to measure the series resonant frequency directly and that is done by putting the crystal in a half-lattice circuit and then measuring the frequency of maximum transmission. The circuit used is shown in Figure 12. The trimmer capacitor is adjusted to produce a minimum response in the vicinity of the crystal resonant frequency but at least several tens of kHz away. This has the effect of cancelling out any parallel capacitance. I made up a small fixture using a balun “binocular” core to make a transformer and the completed circuit was made on a scrap of circuit board material, as shown in Figure 13.

The measured transmission of this circuit is shown in Figure 14. The range of the scan was from -600 Hz to +150 Hz from the nominal crystal frequency of 55.25 MHz. Since there are 128 discrete frequencies in the scan, the interval, in frequency, between data points was about 6 Hz. I made this measurement several months after previous measurements of the same crystal and I had, in the meantime, added some additional dither to the A/D circuit in my signal gen-

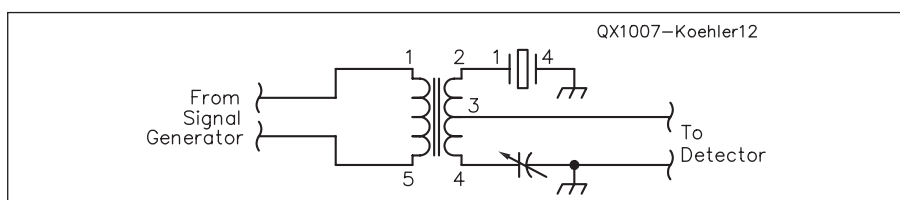


Figure 12 — Circuit diagram of a half-lattice filter.

erator/detector. Without dither, every scan gives exactly the same numbers so there is no advantage or improvement in accuracy by making repeated measurements. Figure 14 shows the superimposed data points from five separate, independent frequency scans.

Also shown in this figure is the best fit curve of a parabola to the points. The best fit coefficients were calculated by *gnuplot*. From the coefficients, it is possible to calculate the frequency of the maximum of the best fit curve, and it is -693 Hz from the nominal frequency of 55.25 MHz. From the statistics of the best fit, the estimated accuracy in frequency would be about $\pm 1.2\%$; or about ± 10 Hz. This frequency is the true series resonant frequency, f_0 , for this particular crystal.

When the crystal was measured in the shunt fixture, the frequency of maximum admittance magnitude was measured to be -850 Hz from 55.25 MHz. The series resonant frequency, as measured in the half-lattice filter was -693 Hz from 55.25 MHz; the difference is thus 157 Hz. This does not agree with the value, calculated by Bloom's equation, of 285 Hz but it does agree well with the simulated responses as calculated using *Scilab*.

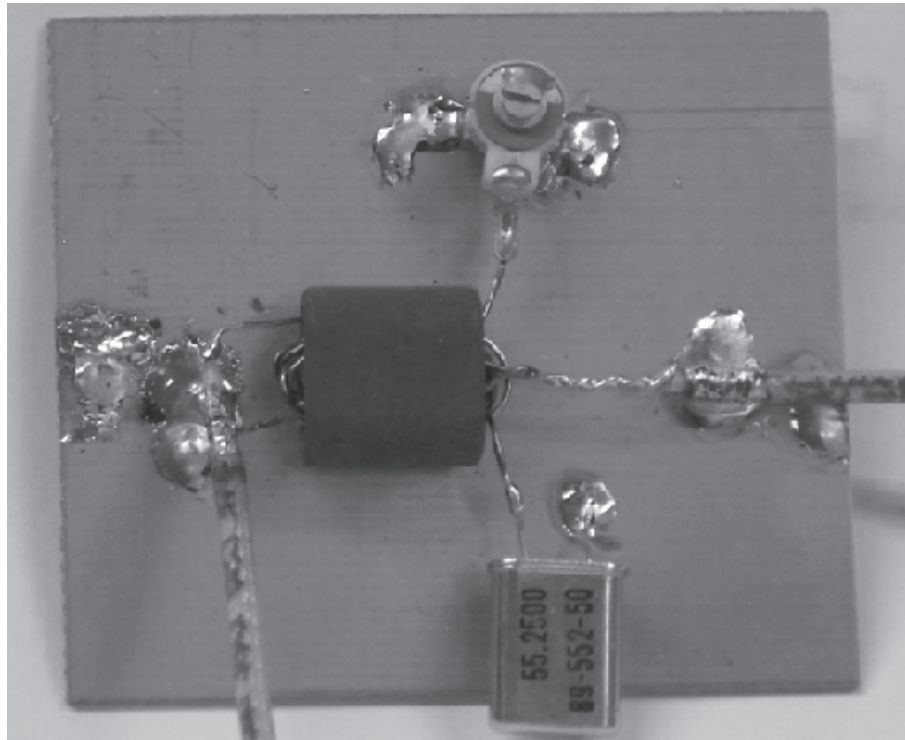


Figure 13 — Photo of the half-lattice filter made using a balun-core transformer. The braid of the input coaxial cable, on the left of the picture, is not connected to the circuit ground.

What is the Correct Frequency Offset?

We already know that the frequency of the minimum of the response as measured in the fixture will not be that of the frequency of minimum transmission for the crystal alone. The question is; how much of that difference is due to the fixture and how much is due to any approximations used by Bloom in arriving at his equation?

Let us first consider the latter of these two possibilities. I spent some considerable time working at the algebra both with pencil and paper and using tools like *Maple*. It is easy to get an equation for both the other resonant frequencies but they are quite complex with many terms and it is much harder to simplify them. I was able to derive an *approximate* expression for the offset between f_0 and the frequency of zero phase-shift, which agrees with that given by Bloom. Let me first go through the algebra; then I shall discuss the approximations used to arrive at it.

Over a small frequency range near resonance, we may replace Z_s , the impedance of the series branch of the equivalent circuit, by an approximation:

$$Z_s \approx R_m(1 + j\delta) \quad [\text{Eq 9}]$$

where:

$$\delta = 2Q \frac{(f - f_0)}{f_0} \quad [\text{Eq 10}]$$

and

$$Q = \frac{2\pi f_0 L_m}{R_m} \quad [\text{Eq 11}]$$

Equation 9 is a very good approximation only for frequencies in the vicinity of reso-

nance where $(f - f_0)$ is small compared to

$$\frac{f_0}{2Q};$$

that is, where δ is much, much less than

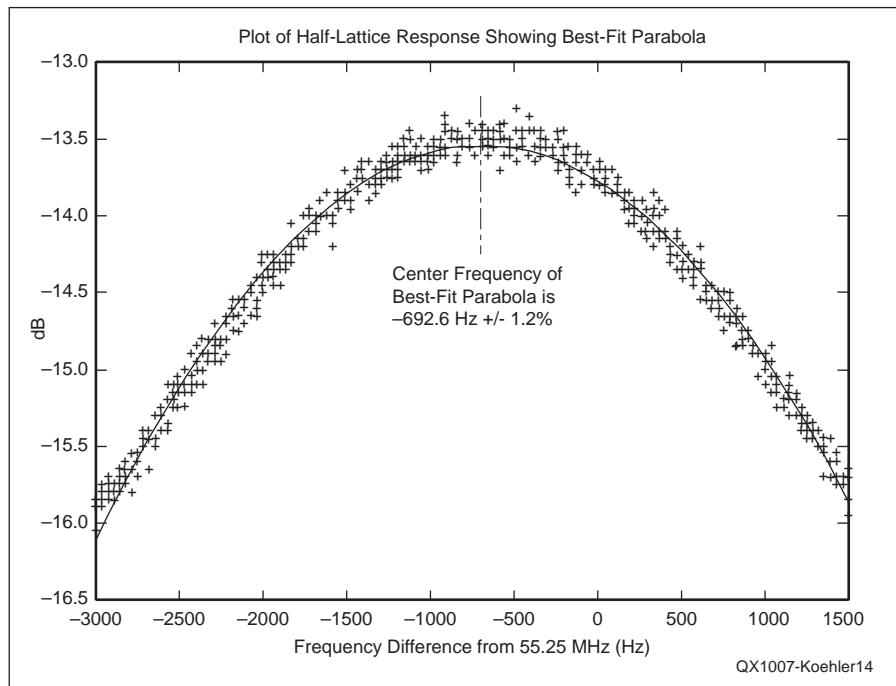


Figure 14 — Plot of the measured response of the half-lattice filter. The data points are from five separate scans. The best fit to a parabola is shown as a solid line. From the coefficients of this fit, the center frequency of the parabola was calculated to be -693 Hz.

one. So, let us now replace Z_s in Equation 4 with the expression in Equation 9. At the frequency of zero phase-shift, the imaginary terms must vanish and, making the assumption that

$$\frac{1}{1 + j\delta} \approx 1 - j\delta,$$

we quickly arrive at Bloom's equation.

For the crystal studied in this discussion,

$$\frac{f_0}{2Q}$$

is equal to about 10^3 so δ is much less than unity only for $(f - f_0)$ less than about 100 Hz. That is to say, Equation 9 is only valid for frequencies closer to f_0 than about 100 Hz. The calculated value of $(f - f_0)$, however, had a magnitude of 285 Hz, so it does not conform to the assumption used to make it. I conclude that, if Bloom derived his equation in the same way that I did, then it is not really a very good approximation for the difference between the frequency of zero phase shift and the series resonant frequency. It is, however useful; in physics, we would say it is a good first-order-of-magnitude approximation.

I was not able to come up with a simple expression for the difference between the series resonant frequency and the frequency of maximum admittance magnitude but, assuming that Bloom used the similar approximations, I think it likely that this expression is also not a very good approximation.

The other thing to consider is how close we might expect the frequency of the minimum of the response to be to the frequency of the maximum of the admittance magnitude. Looking at Equation 5, we see that the two frequencies would coincide only if the value of R' is infinite. That is, the two frequencies should approach one another only if $R'Y_C \gg 1$. In other words, we should expect agreement only if $R' \gg |Z_{min}|$. Note that Z_{min} is the minimum impedance magnitude of the crystal alone. As an aside, in the series method of measuring crystal parameters in which the crystal is in series with a source resistance, R_s , and a detector resistance, R_i , the peak of the response will approach the frequency of Z_{min} only if $(R_s + R_i) \ll Z_{min}$.

It seems to me that these conditions are not likely to occur in practice. For my fixture, R' was roughly 177Ω while Z_{min} was about 84Ω ; so R' was not much, much greater than Z_{min} . Using my fixture for a crystal in the HF region where we might expect Z_{min} to be in the neighborhood of 10Ω or so, the approximation is a lot better, but still not really good. For the usual series measurement described in the literature, the sum of source and detector resistance is usually 25Ω and so, for a typical HF crystal with Z_{min} of about 10Ω ,

that approximation is very poor indeed.

If a shunt measurement fixture had an R' of $1 \text{ M}\Omega$, the approximation would be satisfied very closely, but the response would be down some 80 dB and might be very difficult to measure. We can simulate it, however, to see how closely the simulated frequency of minimum response corresponds to the frequency given by Bloom's equation. In Figure 15, I have plotted the response for this same crystal in a fixture with $R' = 176.5 \Omega$ and $C_p = 0$ and 10.1 pF . These two curves have a frequency difference of 163 Hz, which agrees very closely with the measured difference of 157 Hz. Also shown in Figure 15 is the response of a fixture with $C_p = 10.1 \text{ pF}$ and $R' = 1 \text{ M}\Omega$. I have added +72 dB to this curve in order to bring it up into the same region as the other two. The frequency difference from 0 for this curve is 263 Hz. This is not 285 Hz as Bloom's equation would give but it is much closer. I redid the same plot with $R' = 1000 \text{ M}\Omega$ and the frequency of minimum response did not appear to change measurably.

I conclude from all this that Bloom's equation is a fairly good approximation for calculating the frequency of maximum admittance magnitude for a crystal (indeed, better than I would have expected), but I also conclude the usual circuits for both the series and shunt method for measuring crystal parameters do not really measure

this frequency. That is, most of the discrepancy between the calculated frequency of maximum admittance magnitude of roughly 285 Hz and the observed minimum of transmission observed of about 157 Hz is due to the finite fixture resistance, not to Bloom's equation being a poor approximation.

The particular crystal used in all these measurements is not a particularly good one as the value of R_m is so high and the Q is so low and we are in the VHF region. For crystals in the mid HF region that one might choose to use in a crystal filter, the value of Q is typically greater than 50,000 and R_m is usually less than 20Ω . For these crystals, Bloom's equation gives a maximum difference between the measured frequency (measured in either the shunt or series method) and the true $L_m C_m$ resonant frequency of no more than a few Hz, perhaps even less than 1 Hz. The corrections to the offset due to fixture finite series resistances or non-infinite shunt resistance, depending on whether you use the series method or the shunt method to measure parameters, will be less than this maximum so they will be truly negligible in either case.

So, What Does it All Mean?

I have shown, I hope, that it is possible to measure parallel capacitance quite accurately and so, in principle, one could calculate the

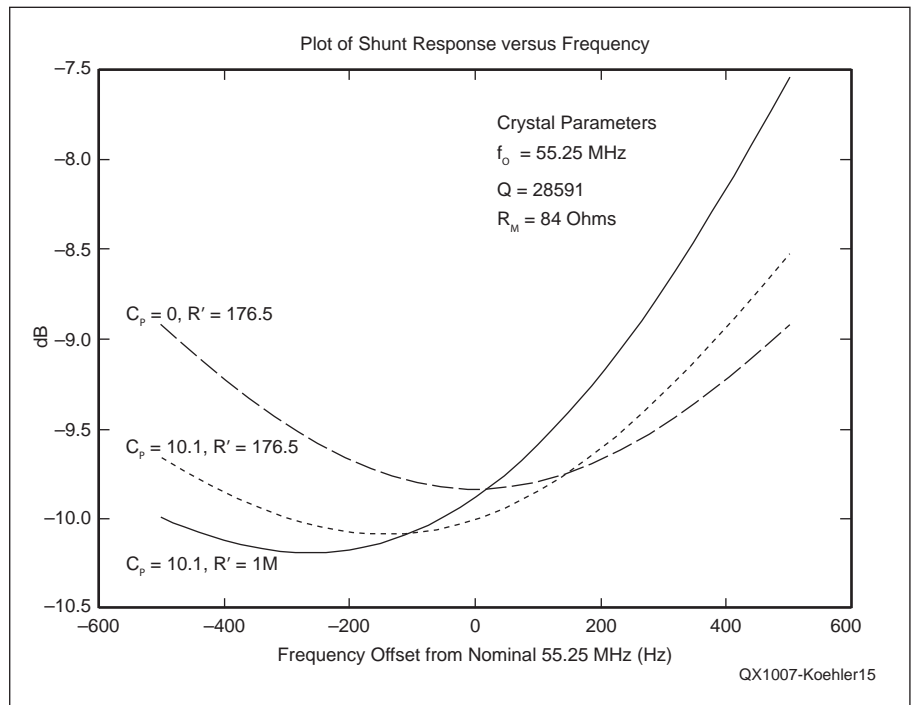


Figure 15 — Plot of the modeled response of a crystal in a shunt fixture with the parameters shown on the diagram. For a parallel capacitance of 10.1 pF and an R' of 176.5Ω , the frequency of minimum response is about -163 Hz . For an R' of $1 \text{ M}\Omega$, the frequency of minimum response is about -263 Hz .

true series resonant frequency of the crystal once the other parameters of the crystal have been measured and *assuming that one has the correct formula*. The question is; is it necessary? In the HF region for good crystals with high Q , probably not; in the VHF region with lower Q crystals, maybe.

Normally, in order to make a crystal filter, one buys a large batch of crystals and measures their parameters. Having done that, then the usual procedure is to select the number needed by looking only at the Q and the center frequency, picking those with the highest Q and the closest to one another in frequency and near to the desired frequency. The final filter may not be centered precisely

at the frequency you desire, but you live with that as long as the band-pass characteristics are what you want. Indeed, it is common to read in the amateur literature that the final filter is slightly off in frequency from what was expected from the measured parameters. This might be expected, partially, because crystal Q values were not infinite as is usually assumed in the design but it could also be because C_p was either not taken into account, wasn't measured properly or because there were other measurement errors.

I would argue that, if you have shunt measurements of crystal Q and frequency, it doesn't matter if the actual internal series resonant frequency is not exactly the same as

the measured frequency of maximum admittance, because you are only using those numbers to choose crystals from a batch. To be sure, the measured frequencies of minimum response will not be the frequencies of series resonance for the crystals but, if the crystals all have a similar R_m , Q and C_p , they will have similar frequency offsets.

Summary

The shunt method of measuring crystal parameters gives you a value for crystal Q , R_m , C_p and a frequency close to that of maximum admittance magnitude. This latter frequency is not the internal series resonant frequency of the crystal motional LC , but the conventional

Scilab Equations

In this function, v , is the complex response of a crystal. The input parameters are;

f = the frequency array for which the impedance is desired

f_0 = the series resonant frequency of the crystal

R_m = the series resistance of the crystal

Q = the crystal Q

R = the series resistance of the measurement fixture; this is R' in the equations used in the text

C_p = the total parallel capacitance of the crystal and fixture.

This function returns v , which is a complex array of the relative voltage at the crystal compared to the voltage from the generator. It is equal to p in Equation 5.

```
function [v] = complex_response_2(f, fo, Rm, Q, Cp, R);
```

```
//
```

```
// there are no approximations in this calculation
```

```
//
```

```
  Zo=1/(2*%pi*%i*Cp.*f);
```

```
  fterm=((f+fo).*(f-fo))./(fo.*f);
```

```
  Zs=Rm*(1 + (%i*Q.*fterm));
```

```
  Zt=(Zo.*Zs)./(Zo+Zs); // total impedance of xtal
```

```
  v=Zt./(R + Zt);
```

```
endfunction
```

As an example, to generate the points that go into the production of one model used in Figure 10 (the narrow-band modeled response for a 12 pF value of C_p), after loading the function, the *Scilab* program would be:

```
// first, define the frequency array as points from 55.2493 to 55.2503 MHz with a 10 Hz interval
```

```
f=[55249300:10:55250300];
```

```
// then, open a file to write the result, the file name being 'n_12.txt'
```

```
xd = mopen('n_12.txt', 'w');
```

```
// then, calculate the response array and write it to the file
```

```
for k=1:101, mfprintf(xd, '%f\n', 20*log10(abs((complex_response_2(f(k), 55.25e6, 85, 30e3,12e-12,176.5))))), end;
```

```
// finally, close the file
```

```
mclose(xd);
```

The file would subsequently be plotted using *gnuplot*. *Scilab* has built in plotting commands, but I wanted to do other things with the resulting data as well as just plotting them. Therefore, I used *Scilab* to do the calculations alone.

series measurement doesn't give you that frequency either. The shunt method, modified as described here, does give you C_p , which the series method does not.

To summarize, this detailed study of the shunt mode shows three things:

- The shunt mode is an accurate method for determining the crystal parameters,
- It is possible to precisely and quickly measure crystal parameters, including C_p , with an accurate signal generator and magnitude detector,
- The simple model of a crystal is a very good approximation to a real crystal.

The shunt mode has a further advantage, not mentioned previously, that the signal levels through the crystal during the parameter measurement are quite low. For example, in my fixture with my signal generator/detector system, the levels at the crystal are in the vicinity of -40 dBm. These levels are more representative of the voltages that a crystal filter experiences in a receiver than the levels, of the order of volts, normally used in the series measurement method.

Notes

¹Jim Koehler, VE5FP, "Some Thoughts on Crystal Parameter Measurement," QEX, Jul/Aug, 2008, p 36.

²See, for example, Jack Hardcastle, "Quartz Crystal Parameter Measurement," QEX, Jan/Feb, 2002, p 7 or Jack Smith, K8ZOA, "Designing the Z90's Gaussian Crystal Filter," QEX, May/June, 2007, p16.

³Alan Bloom, N1AL, Letters to the Editor, QEX, Sep/Oct 2008, p 41 and Jan/Feb 2010, p 37.

⁴Jim Koehler, VE5FP, "A DDS-based Signal Generator," Nov/Dec, 2009, p 3.

⁵Over a restricted frequency range as shown in this plot, the difference between a logarithmic frequency scale and a linear one is negligible.

⁶www.gnuplot.info/

⁷www.mathworks.com

⁸www.scilab.org

⁹www.maplesoft.com

¹⁰www.wolfram.com

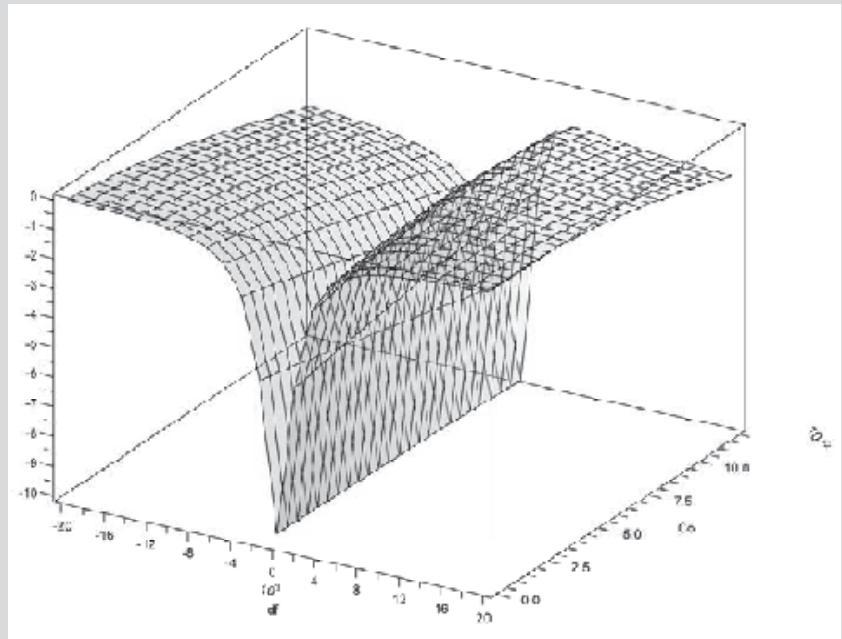
An ARRL member, Jim Koehler was first licensed as VE5AL in 1952 at the age of 15. He has been VE5FP since returning to Canada in 1966 after studying abroad. He was a Professor of Physics and Engineering Physics at the University of Saskatchewan in Saskatoon until his retirement. Jim and his wife now live on Vancouver Island where he dabbles in the design of electronic test equipment and proton-precession magnetometers.

Modeling with Maple

```

> Q := 30000;                                     (1)
                                                    Q ≈ 30000
> R := 176.5;                                     (2)
                                                    R ≈ 176.5
> r := 85;                                        (3)
                                                    r ≈ 85
> fo := 55.25e6;                                  (4)
                                                    fo ≈ 5.525 107
> δ :=  $\frac{2 \cdot Q \cdot df}{fo}$ ;                    (5)
                                                    δ ≈ 0.001085972851 df
> Yo := 2 · π · fo · ICo;                          (6)
                                                    Yo ≈ 1.1050 108 π Co
> Zs := r (1 + Iδ);                               (7)
                                                    Zs ≈ 85 + 0.09230769234 Idf
> Y := Yo +  $\frac{1}{Zs}$ ;
                                                    Y ≈ 1.1050 108 π Co +  $\frac{1}{85 + 0.09230769234 Idf}$  (8)
> ρ := 20 · log10  $\left( \text{abs} \left( \frac{1}{1 + R \cdot Y} \right) \right)$ ;
                                                    ρ ≈  $-\frac{20 \ln \left( \left| 1 + 1.9503250 10^{10} \pi Co + \frac{176.5}{85 + 0.09230769234 Idf} \right| \right)}{\ln(10)}$  (9)
> plot3d(ρ, df = -20000 .. 20000, Co = 0 .. 12e-12);

```



QEX

Using *QuickSmith* — Part 1

Allow this software to draw the circles and lines on a Smith chart for your next RF design project.

An understanding of RF technology is essential to hams who wish to go below the surface and explore the depths of RF as applied to this amazing hobby called “Amateur Radio.” Often, well-developed software can be a great tool for learning and/or reinforcing what we already know or think we know about the subject. This article will explore the use of an excellent “free-ware” software package called *QuickSmith*. *QuickSmith* was developed by Nathan Iyer. The software can be downloaded from Nathan Iyer’s Web page at www.nathan-iyer.com. As the name implies, *QuickSmith* involves the use of the Smith chart.¹ The package also includes a circuit design tool that allows the user to design impedance-matching networks and even design low-noise small-signal amplifiers using S parameters and noise parameters found in manufacturers’ data sheets. The software not only has practical value in designing circuits but, perhaps more importantly, the software is very educational and intuitive to use. In order to get the most benefit from this article you should download *QuickSmith* and use the software to follow the examples presented here.

Now, let’s jump right into *QuickSmith* and look at several examples, showing just what this software can do for us. In his book, *Electronic Applications of the Smith chart*, Phillip H. Smith wrote “The single open- or short-circuited shunt matching stub whose length is continuously adjustable over a range of one-quarter wavelength, and whose position along the main line is adjustable over a range of one-half wavelength, is capable of correcting any mismatch condition whatsoever along the main line.” This is quite a profound statement! Using *QuickSmith*, let’s put it to the test.

Example 1

Start *QuickSmith* software. You will see two panes on the screen. The left pane is the Smith chart and the right pane is a schematic editor tool that allows you to place components in the circuit using the drag-and-drop technique. There are spaces for nine components on the schematic — five series-connected components and four shunt-connected components. Shunt-connected components are placed in the vertical white spaces while series-connected components are placed in the horizontal white spaces. Initially, the load impedance is set to $50 + j0 \Omega$; that is, $R = 50$ and $X = 0$.

I arbitrarily selected a load impedance of $35 - j20 \Omega$ for this example. Using the up/down arrows near the load impedance value, set the resistive part (R) to 35Ω and the reactive part (X) to -20Ω . (The step size of any of the figures shown can be changed by simply double-clicking on the figure and typing the desired step size into the pop-up window.) Figure 1 shows the resulting display with the blue dot on the Smith chart indicating the resulting input impedance. [Throughout this article the author refers to a blue dot on the various figures. Although *QEX* is not printed in color, we left the color reference in the text. When you are looking

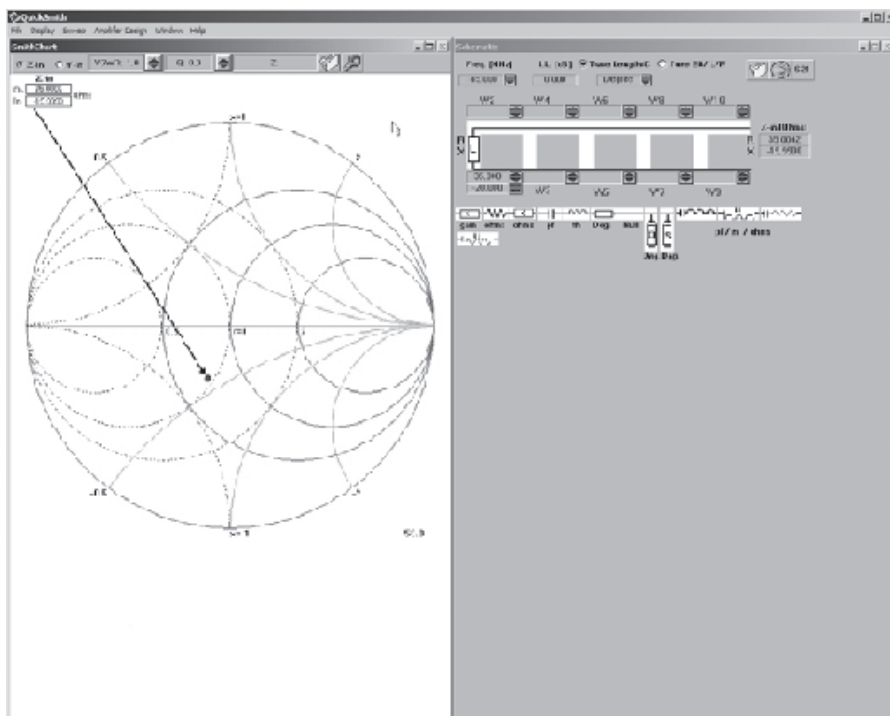


Figure 1 — The load impedance of the circuit at the right is $35 - j20 \Omega$. The location of the point representing this impedance is shown by the blue dot on the Smith chart at the left.

¹Notes appear on page 33.

at the software on a computer screen, you will be looking for this blue dot. — Ed.] Be sure to have the *admittance* circles shown by selecting *Admittance circles* under the *Display* tab. You'll see why shortly.

Next, using the *Assign values* tab, set the frequency to 145 MHz, the velocity factor to 1, the characteristic impedance to 50 and the T-line design frequency to 145 MHz. Next, check the *Line Length/C* radio button at the top of the right pane (schematic editor) and set the measuring unit to *degrees*.

Next, drag and drop a series-connected transmission line and place it at position 4 on the schematic as shown in Figure 2. Then, drag and drop a shorted stub to position 5 on the schematic. Set each line to a characteristic impedance of $50\ \Omega$ and the length to 45° initially. The dot representing the input impedance on the Smith chart is shown in Figure 2. Increase the value of T4 from 45° to 70° to place the blue dot on the *unity conductance circle* that passes through the center of the chart. See Figure 3. Then, increase the length of the shorted stub from 45° to 121° to place the dot at the center of the Smith chart, as shown on Figure 4. At this point the load impedance of $35 - j20\ \Omega$ has been matched to $50\ \Omega$.

We know that a good match has been achieved at the frequency of 145 MHz, but what about frequencies just above or below 145 MHz? Click on *Sweep Setup* on the menu and type in the desired range of frequencies to be swept and the number of points. Left-click on the Smith chart and click on *Sweep* on the menu and then *Generate sweep* under this menu. If the bandwidth of the matching circuit is broadband, you will see a very short line or maybe none at all. If you don't see a line representing the swept frequency response go back to the *Sweep setup* menu, increase the sweep frequency range and repeat the process until a line is visible on the chart. You can determine the SWR over this frequency range by increasing the SWR figure on the toolbar to draw SWR circles around the center of the chart. Figure 5 shows that the swept frequency range of 140 MHz to 150 MHz is entirely contained in the 1.2:1 SWR circle and nearly contained within the inner (1.1:1) SWR circle. Thus, a very good impedance match is obtained over the frequency range being swept.

Example 2

Just as transmission line stubs can be used to achieve an impedance match, so too can "lump" components. Figure 6 shows an L network using a series-connected inductor and a shunt-connected capacitor to achieve the desired match to $50\ \Omega$. First, increase L4 from 20 nH to 47 nH, to place the blue dot on the *unity conductance circle*. Then, increase

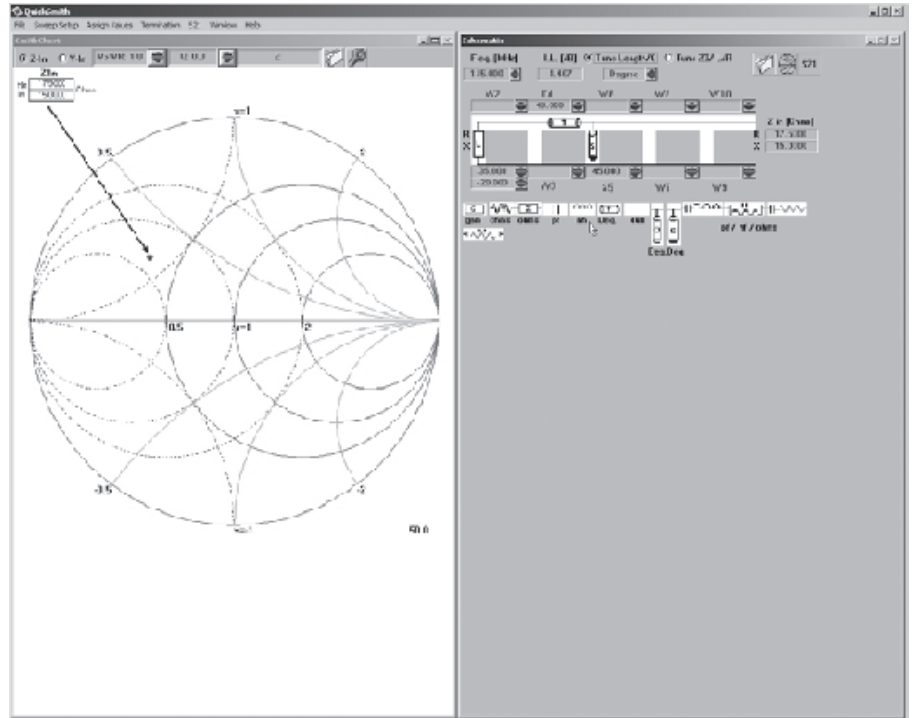


Figure 2 — In order to design an impedance-matching circuit, a transmission line (T4) and a shorted stub (S5) are placed on the schematic and both are initially set to 45° (one-eighth wavelength). This changes the impedance to $17 + j15\ \Omega$, represented by the location of the blue dot on the Smith chart at the left.

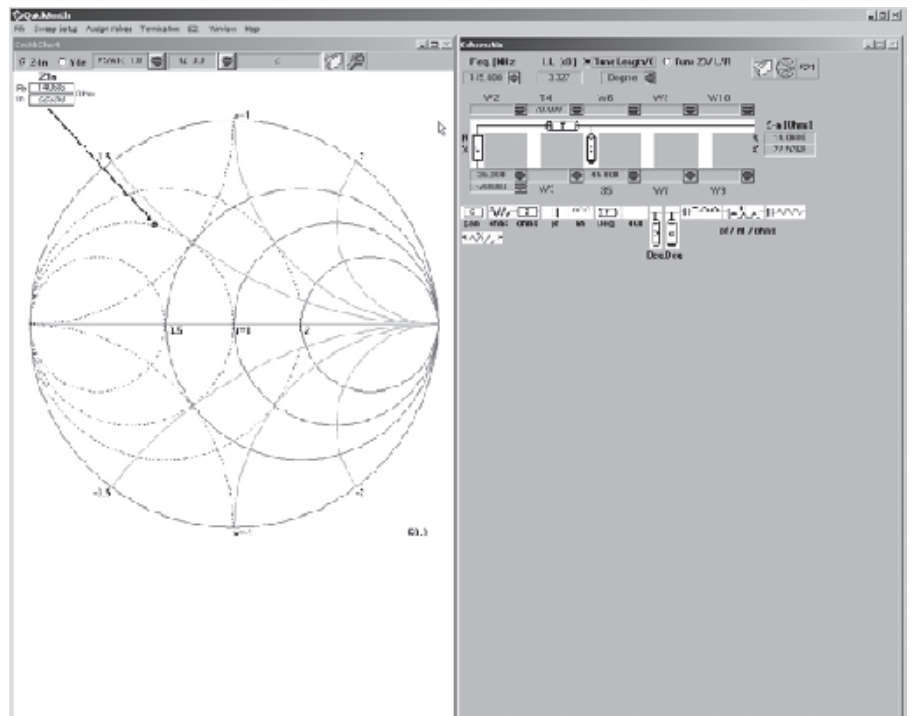


Figure 3 — With the length of T4 increased from 45° to 70° the blue dot is placed directly over the *unity conductance circle*.

C5 from 10 pF to 14 pF, to place the blue dot directly at the center of the chart. Just as in the previous example, check the bandwidth of the match by sweeping over the frequency range of 135 MHz to 155 MHz. The SWR over this range is less than 1.1:1.

Example 3

It is one thing to achieve an impedance match over a range of frequencies with the load impedance held constant, as in the previous example, but what if the load impedance changes with frequency? This is what happens with an antenna — the load impedance changes with changes in frequency. Achieving a match over the entire frequency range is like trying to hit a moving target while riding on a merry-go-round! With *QuickSmith*, we can sweep the frequency range of interest to find the resultant bandwidth of the impedance-matching circuit. A new feature of *QuickSmith* is called into play. First, a gamma (Γ) file must be created. This file simply provides the gamma (Γ) magnitude and angle of the equivalent impedance at each test frequency. The gamma file is simply an ASCII file and can be created in Notepad and saved with the file extension “GAM.” The basic protocol for creating a gamma file is as follows:

- 1) The first line in the file should be “QuickSmith GAM”.
- 2) The second line is the characteristic impedance, Z_0 , usually 50 Ω .
- 3) The remainder of the file contains the values of frequency in MHz, the reflection coefficient (Γ) magnitude and angle in degrees.
- 4) The components on each line are separated by a space, with a carriage return at the end of each line.

Here is a typical gamma file:

```
QuickSmith GAM
50
30 0.71 45
31 0.72 35.5
32 0.75 26.6
```

In this gamma file the “50” indicates a 50 Ω system impedance and the three frequencies are 30 MHz, 31 MHz and 32 MHz with the gamma magnitude and angle listed beside each frequency. We will use this as an example in a moment, but first we need an explanation of how we calculate the gamma magnitude and angle from given complex impedance values.

The complex impedance values in Table 1 are for a 30 MHz antenna as adapted from an example on page 5-5 of *Antenna Impedance Matching*, first edition, by Wilfred N. Caron, published by ARRL.²

While the *normalized* complex impedance (R and X) values were given for each

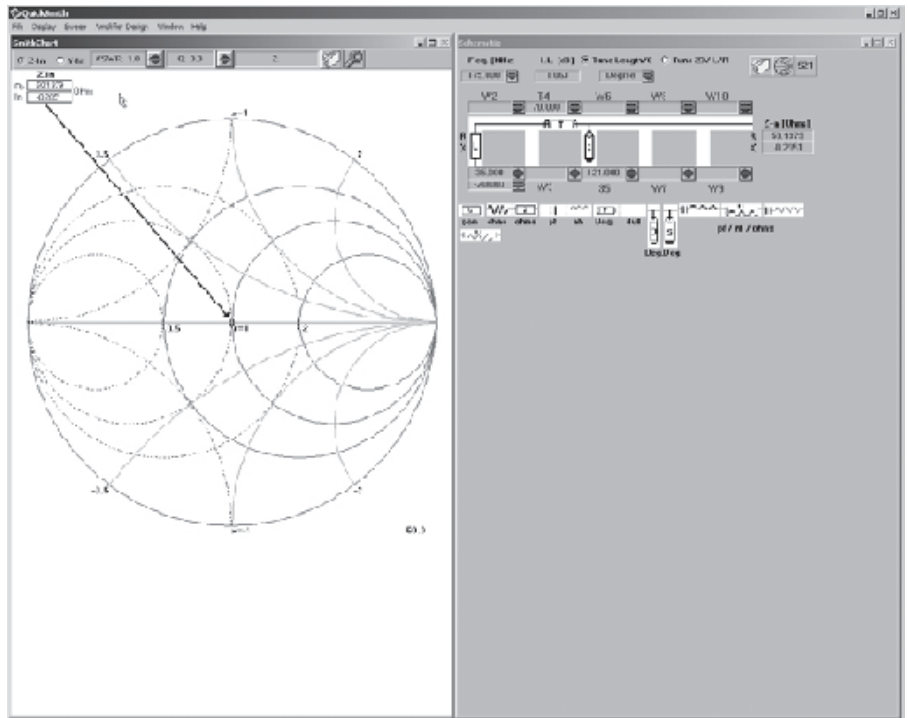


Figure 4 — By increasing the length of the shorted stub (S5) the blue dot is “walked” around the unity conductance circle to the center of the Smith chart (50 ± j0 Ω).

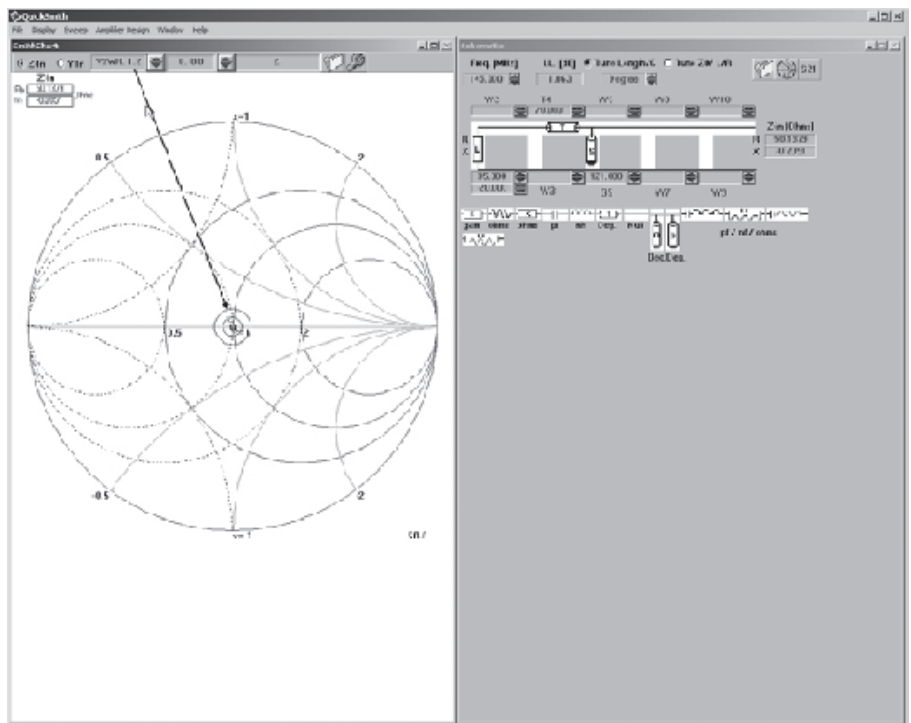


Figure 5 — The swept-frequency response shows that the matching circuit is broadband enough to provide a low SWR over the frequency range of 140 MHz to 150 MHz. The inner SWR circle represents an SWR of 1.1:1 and the outer circle represents an SWR of 1.2:1. The sweep, represented by the line through the center of the chart is fully contained within the 1.2:1 SWR circle and nearly contained within the 1.1:1 SWR circle.

Table 1

Freq (MHz)	R Ω	X Ω	Γ mag	Γ angle	SWR
30	50	100	0.71	45°	5.82
31	70	120	0.72	35.5°	6.06
32	100	150	0.75	26.6°	6.85

frequency, the gamma magnitudes and angles along with the SWR were calculated from these R and X values. The complex impedance for each frequency was converted to the equivalent gamma magnitude and angle as described below.

First, the complex gamma figure was obtained by using Equation 1:

$$\Gamma = \frac{Z_L - Z_0}{Z_L + Z_0} \quad [\text{Eq 1}]$$

where Γ is in complex form
 Z_L is the complex impedance
 Z_0 is the system impedance.

Using the given impedance at 30 MHz as an example, the complex form of gamma is calculated as shown below:

$$\Gamma = \frac{50 + j100 - 50}{50 + j100 + 50} = \frac{j100}{100 + j100}$$

$$\Gamma = \frac{j100}{100(1+j)} = \frac{j}{(1+j)} \times \frac{(1-j)}{(1-j)}$$

$$\Gamma = \frac{(j-j^2)}{(1+j-j-j^2)} = \frac{j(1-j)}{(1-j^2)}$$

$$\Gamma = \frac{j(1-j)}{2} = 0.5j(1-j)$$

$$\Gamma = 0.5j - 0.5j^2 = 0.5j + 0.5$$

Figure 7 shows how this gamma value is plotted on a rectangular chart. The vertical axis represents the imaginary or j value and the horizontal axis represents the real value. The angle of gamma is equal to the *arctangent* of $0.5/0.5 = 1$ or 45° . The magnitude of gamma is:

$$\Gamma = \frac{j}{\sin \theta} \quad [\text{Eq 2}]$$

Then:

$$\Gamma = \frac{0.5}{\sin(45)} = \frac{0.5}{0.7071} = 0.7071$$

The SWR is determined by Equation 3:

$$\text{SWR} = \frac{1+\Gamma}{1-\Gamma} \quad [\text{Eq 3}]$$

For 30 MHz:

$$\text{SWR} = \frac{1+0.7071}{1-0.7071} = \frac{1.7071}{0.2929} = 5.83$$

In like manner, the magnitude and angle of gamma and the SWR values are calculated for

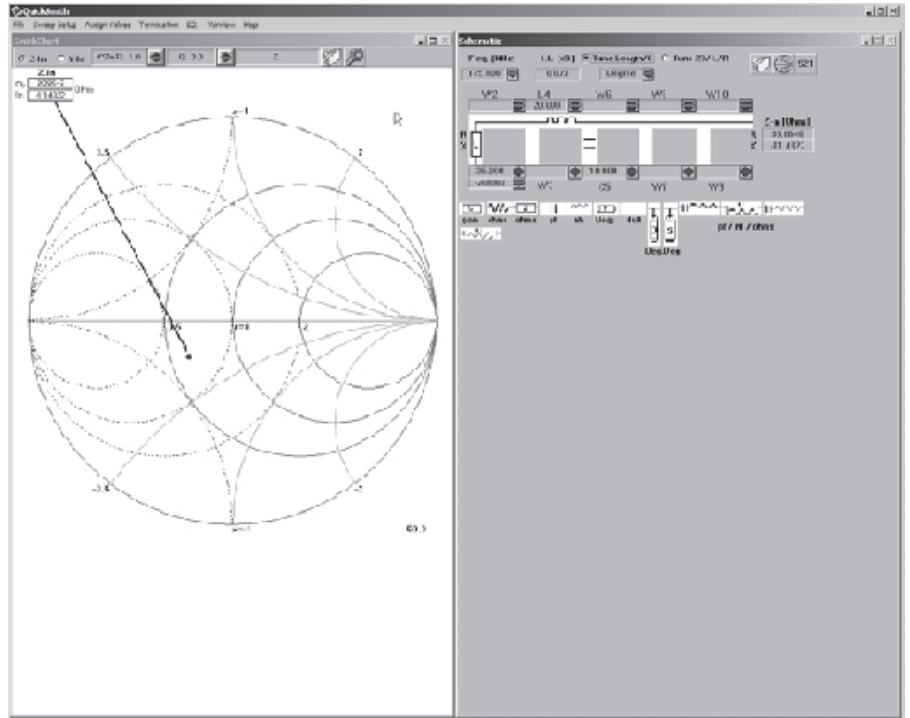


Figure 6 — An L network consisting of “lump” components can also be used to design an impedance matching network for the same load shown in the previous example. Here, a series inductor and a shunt capacitor are used to provide the necessary match so that the input “sees” a 50Ω impedance. With L_4 set to 20 nH and C_5 set to 10 pF, the input impedance is approximately $30.9 - j11.4 \Omega$. By increasing L_4 from 20 nH to 47 nH, the blue dot is placed on the *unity conductance circle*. Then, increasing C_5 from 10 pF to 14 pF moves the blue dot directly over the center of the Smith chart ($50 \pm j0 \Omega$).

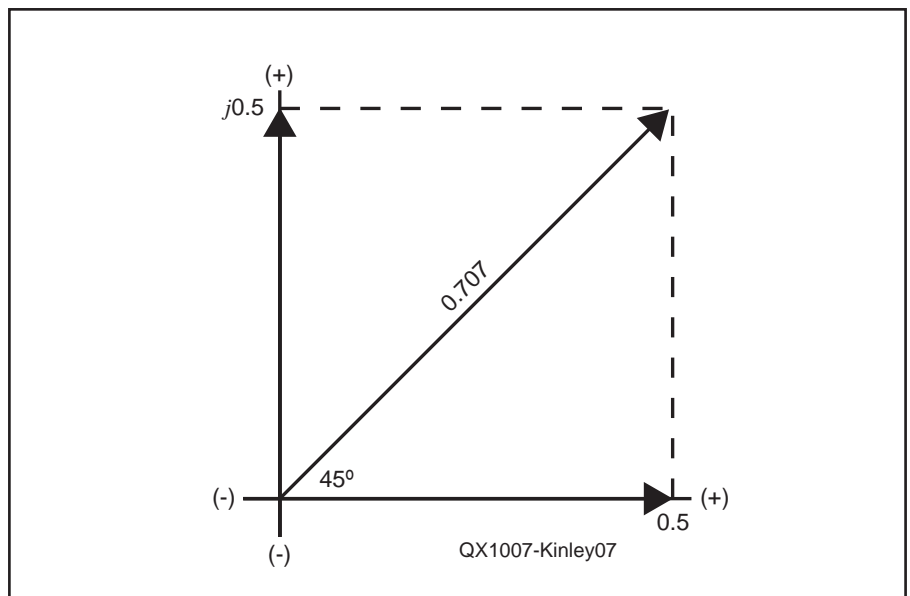


Figure 7 — This is a graph representing the rectangular coordinates of the complex gamma of $0.5 + j0.5$. The vertical scale represents the imaginary part of the complex number and the horizontal scale represents the real part. The resultant gamma angle is 45° and the gamma magnitude is 0.707.

31 MHz and 32 MHz.

In order to use the gamma file you must create it as described above and save it as a GAM file with a name you can recognize and in a location you can find when importing it into *QuickSmith*. Create the file described above and save it as “30mhzdip.GAM” in the *QuickSmith* folder. Start *QuickSmith* and follow the steps below:

- 1) Click on the wrench icon on the toolbar.
- 2) On the menu, click on *Termination* and check *Gamma*.
- 3) Click on *Termination* on the menu again and select *Multiple > Link*.
- 4) From the files listed select *30mhzdip.GAM*.
- 5) You will see the start frequency, stop frequency and number of points, click OK.
- 6) On the schematic editor set the frequency to 31 MHz.

7) The blue dot representing the impedance point on the Smith chart will appear as shown in Figure 8.

8) Drag and drop a parallel capacitor in the vertical space next to the load and set the initial value to 100 pF. See Figure 9.

9) Decrease the value of the capacitance until the blue dot is placed on the *unity resistance circle*. This occurs at a capacitance of 71 pF. See Figure 10.

10) Drag and drop a series inductance into position 4 and set the initial value to 300 nH.

11) Increase the value of L4 to “walk” the blue dot to the center of the Smith chart. You can increase the step size of L4 to speed up the process. The final inductance of L4 is approximately 553 nH.

12) Set the SWR circle to 2.0.

13) Under *Sweep setup* set the start frequency to 30 MHz, the stop frequency to 32 MHz and the step to 0.1 MHz.

14) Click anywhere on the Smith chart and click on *Sweep > Generate sweep* on the menu.

15) The result should look like Figure 11, indicating that the entire frequency range is within the 2.0 SWR circle.

Example 4

The preceding example was a simple case since no special technique was used to make the impedance-matching circuit broad band enough to cover the frequency range of 30 MHz to 32 MHz while keeping the maximum SWR within the 2.0 circle.

The author of *QuickSmith*, Nathan Iyer, included an example of using special techniques to increase the bandwidth of the matching circuit in order to keep the SWR within a predetermined limit. Using the previously described procedures, load the gamma file with the name *dipole.gam*. Under the sweep setup, set the start frequency to

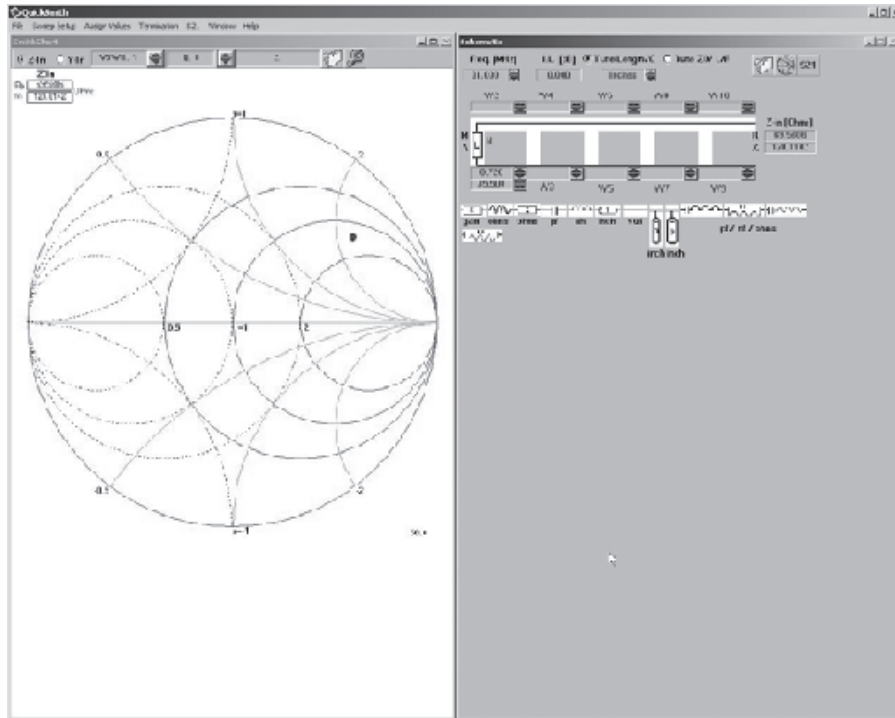


Figure 8 — The blue dot on the Smith chart represents the impedance of the 30 MHz dipole at 31 MHz with no matching components placed on the schematic editor.

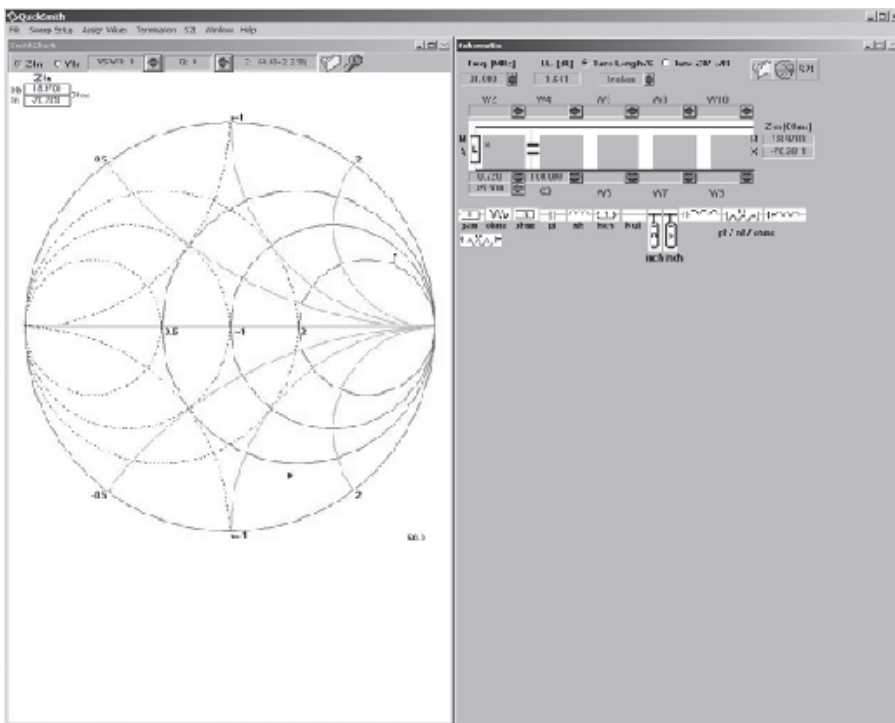


Figure 9 — With a shunt capacitor placed on the schematic, the input impedance at 31 MHz has changed to the new impedance represented by the blue dot on the Smith chart.

100 MHz, the stop frequency to 200 MHz and the step to 10 MHz.

Set the SWR circle to 2.0 and run the frequency sweep. Your result should look like Figure 12 with no components on the schematic editor. Next, click in the gray area of the schematic editor and then click on *File* on the menu. Open the file labeled *dipole.sch*. Run a frequency sweep and the result should look like Figure 13. Notice that the entire sweep trace is contained well within the 2.0 SWR circle.

Example 5

In order to clear out the previous entries, exit and restart *QuickSmith*. Recall that a quarter-wave matching section can be used to match two impedances. The quarter-wave matching section must have a characteristic impedance that is determined by Equation 4:

$$Z_0 = \sqrt{Z_1 \times Z_2} \quad [\text{Eq 4}]$$

If Z_1 is 100 Ω and Z_2 is 50 Ω , a quarter-wave matching section of 70.7 Ω will do the trick. Using *QuickSmith*, set the load impedance to $R = 100 \Omega$ and $X = 0 \Omega$. Place a series-connected transmission line in the circuit. Set the impedance to 70.7 Ω and initially set the length to 45°. At this point, the input impedance is roughly $66 - j23 \Omega$. Now, increase the length of the transmission line until the input impedance is 50 Ω and the blue dot is over the center of the Smith chart. At this point, the length of the transmission line should be 90° (one-quarter wavelength).

Example 6

One popular lightning protection scheme is to place a shorted quarter-wave stub across the transmission line. At the operating frequency, the shorted quarter-wave stub has no effect on the impedance. This can be observed using *QuickSmith* and the circuit editor. Clear the old circuit by placing the “null” components over the old components. Set the load impedance to $R = 50$ and $X = 0$. Place a shorted stub shunt-connected across the circuit. Set the characteristic impedance of the cable to 50 Ω and the cable length to 45° initially. Notice that the blue dot is located on the *unity conductance circle* but far from the 50 Ω point on the Smith chart. Increase the length of the stub and you will see that the input impedance is 50 Ω at a stub length of 90° ($1/4 \lambda$).

Example 7

Restart *QuickSmith* and set the load impedance to $R = 85 \Omega$ and $X = -250 \Omega$. You should see a display like Figure 14. To achieve an impedance match of 50 Ω , the first step is to move the dot to the *unity resistance*

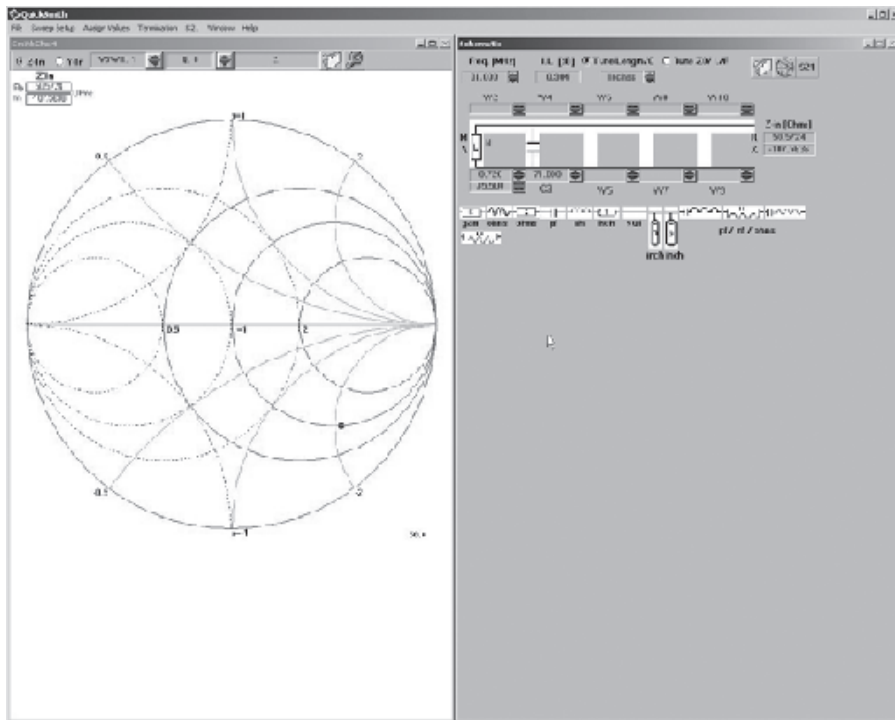


Figure 10 — Decreasing the capacitance from 100 pF to 71 pF has moved the blue dot to the *unity resistance circle* on the Smith chart.

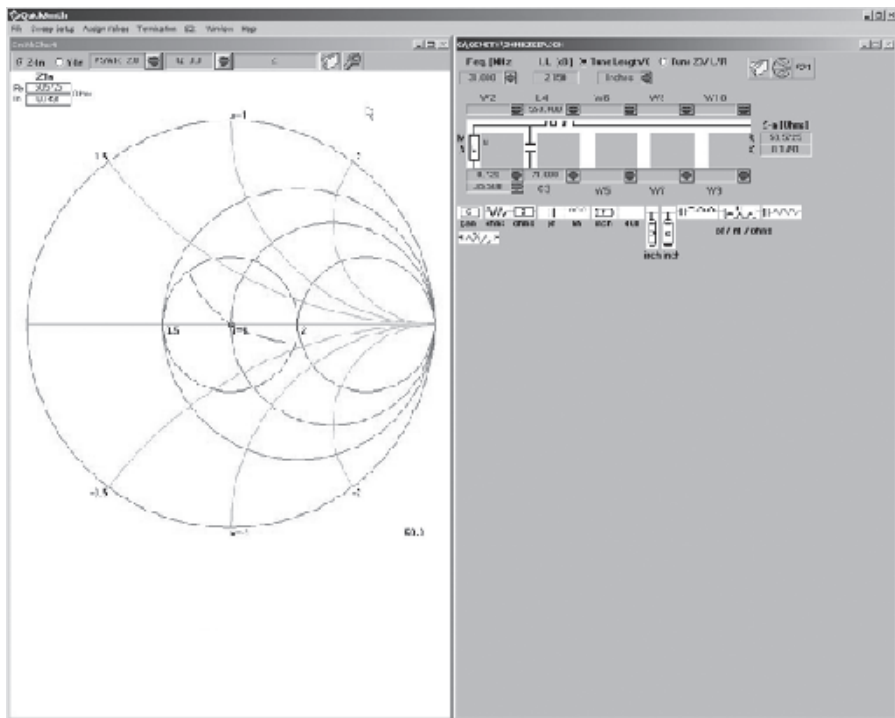


Figure 11 — Placing a series inductance on the schematic and adjusting the value to 553 nH moves the blue dot along the *unity resistance circle* to the center of the Smith chart at $50 \pm j0 \Omega$. The sweep plot shows that the input SWR is within the 2.0 SWR circle over the frequency range of 30 MHz to 32 MHz.

circle. This can be achieved by inserting a short section of transmission line as shown in Figure 15. First, set the measurement unit to degrees and initially set the length to 10° . Set the incremental value to 0.1° and adjust the line length until the blue dot is placed on the *unity resistance circle*. Next, place a series-connected inductor on the schematic and set the initial value to 100 nH and set the incremental value to 10 nH. Adjust the inductance to “walk” the blue dot to a position directly over the center of the Smith chart ($50 \pm j0 \Omega$). This occurs at an inductance of 310 nH. See Figure 16.

Example 8

One last example of antenna matching is presented here. The impedance measurements were made with an antenna analyzer on the transceiver side of the coax cable that connects to my 40 meter inverted V antenna. The impedance measurements along with the converted gamma magnitude and angle and SWR are shown in Table 2. A gamma file was created as described previously. Then, the gamma file was imported into *QuickSmith*. The screen print in Figure 17 was taken with no matching circuit in place. The Sweep setup was set to a start frequency of 7.0 MHz, stop frequency of 7.3 MHz and a step frequency of 0.01 MHz (10 kHz). The incremental value of the frequency on the schematic editor was set to 0.05. The SWR circle was set to 2.0. With the frequency set to 7.15 MHz (the center of the 40 meter band) the sweep was run and resulted in the display shown in Figure 17. Notice that the upper end of the band at 7.3 MHz is outside the 2.0 SWR circle and the center of the band at 7.15 MHz is not at the minimum SWR at the center of the Smith chart.

Next, the matching circuit is designed on the schematic editor, resulting in the display shown in Figure 18. After the matching circuit is designed on the schematic editor, the *Sweep setup* is selected and again set to a start frequency of 7.0 MHz and a stop frequency of 7.3 MHz with a step of 0.01 MHz. Then, the *Sweep>Generate sweep* is selected. Notice in Figure 18 that the entire sweep plot is within the 2.0 SWR circle and the center of the band at 7.15 MHz is at $50 \pm j0$ on the Smith chart.

As shown in these examples, *QuickSmith* is a very useful aid in designing and testing impedance-matching circuits. The examples presented here cover just some of the capabilities of *QuickSmith*. The more you experiment with *QuickSmith*, the more you learn about its capabilities and about impedance-matching techniques using transmission lines, lump components or a combination of the two. There is much more that can be done

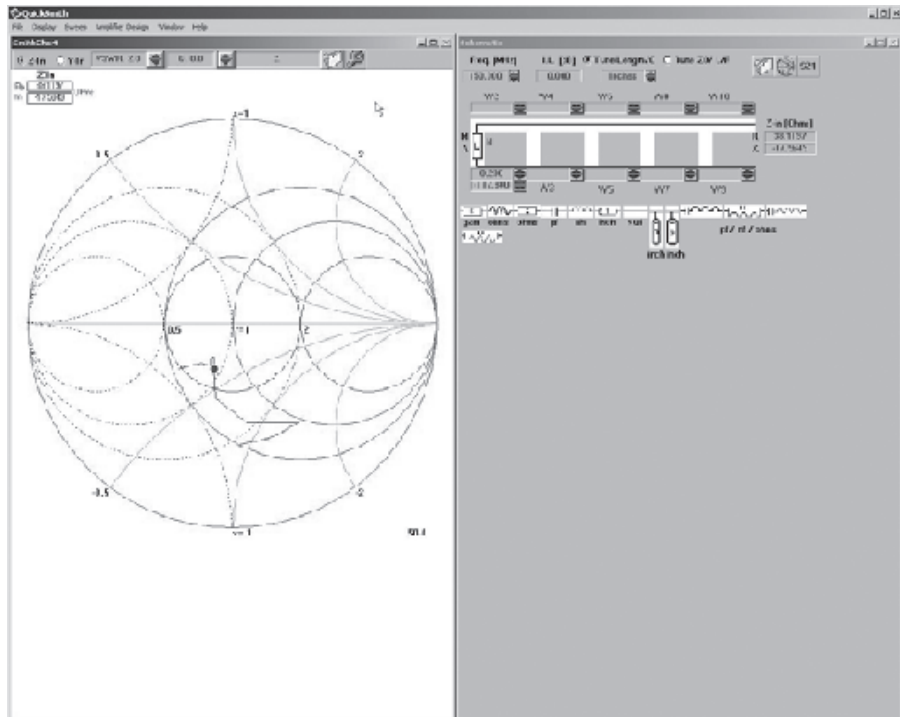


Figure 12 — Using the *dipole.gam* file, the sweep response over 100 MHz to 200 MHz indicates that a large portion of the response falls outside the 2.0 SWR circle.

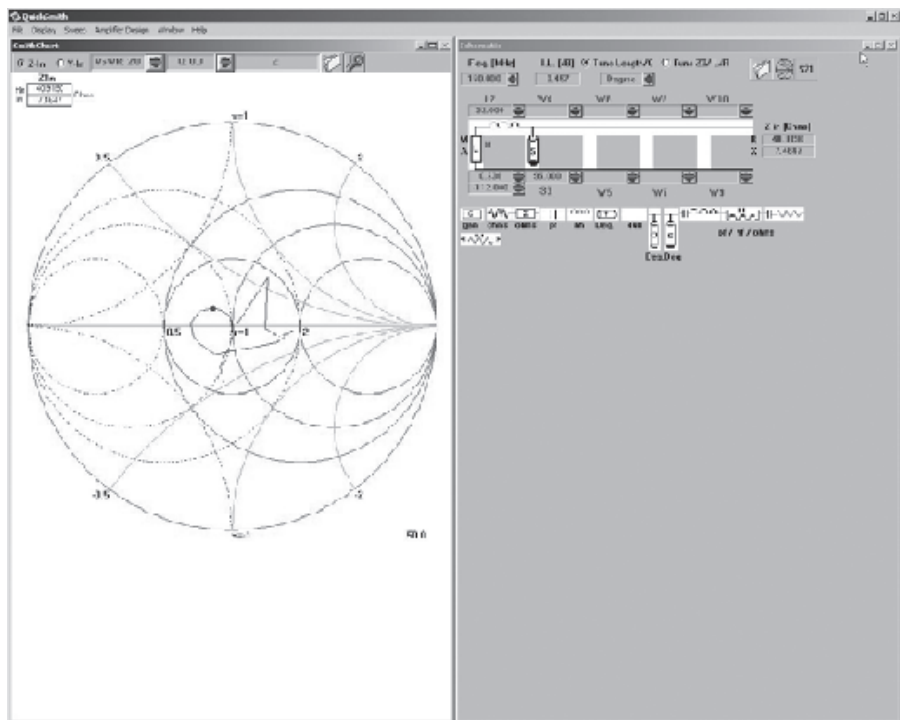


Figure 13 — The matching components on the schematic editor have the entire sweep response from 100 MHz to 200 MHz contained within the 2.0 SWR circle.

with *QuickSmith*. In Part 2 we will show how to use *QuickSmith* to design a small-signal, low-noise, single-stage RF amplifier using constant-gain and constant-noise circles.

Harold Kinley, WA4GIB, first studied electronics at a technical school, and is a Certified Electronics Technician. He held a First Class Radiotelephone License, which was later “downgraded” to a General Radiotelephone Certificate. Harold worked in radio and television broadcasting and later in commercial two-way radio. He started as a district radio technician for the South Carolina Forestry Commission, and 31 years later retired as Regional Communications Manager for the same agency. He has always enjoyed field work, installing, maintaining and repairing communication equipment.

Harold completed the NRI Complete Communications Course with high honors, studied a CIE electronics course and an MTI training course as well as much independent study for which there were no certificates or degrees — just the knowledge acquired.

An ARRL Member, Harold was first licensed as a Novice in 1962 and upgraded Conditional (General) in 1963. He finally upgraded to Extra class in 1998.

Harold first began writing for publication in 1976 for the NRI Journal, and later had many articles published in Popular Electronics, Electronic Servicing & Technology, EMC Technology and started a column called “Technically Speaking” for Mobile Radio Technology in the early 90s. Harold has written three books, The PLL Synthesizer Cookbook, Standard Radio Communications Manual and The Radiomans’s Manual of RF Devices, Principles & Practices. He recently revised and expanded the last title and renamed it The RF Desk Reference for Wireless Communications. That book is only available directly from the author. See www.haroldkinley.com for details.

Harold has been enjoying retirement since 2002, and still enjoys the wonderful hobby of ham radio.

Notes

¹The Smith chart was invented by Phillip H. Smith and first published in *Electronics*, Vol 12, No. 1, Jan 1939, pp 29-31. Today, Smith Chart® is a registered trademark of Analog Instruments Company.

²Wilfred N Caron, *Antenna Impedance Matching*, ARRL, First Edition, Second Printing, 1993, ISBN: 0-87259-220-0. (Out of print and no longer available from ARRL.)

Table 2

Freq (MHz)	R Ω	X Ω	Γ mag	Γ angle	SWR
7.00	36	-20	0.28	-112°	1.76
7.05	39	-16	0.21	-114.3°	1.54
7.10	46	-10	0.11	-105.9°	1.25
7.15	57	8	0.10	-44.5°	1.21
7.20	72	13	0.21	24.5°	1.52
7.25	88	21	0.31	20.3°	1.90
7.30	91	43	0.40	29.4°	2.35

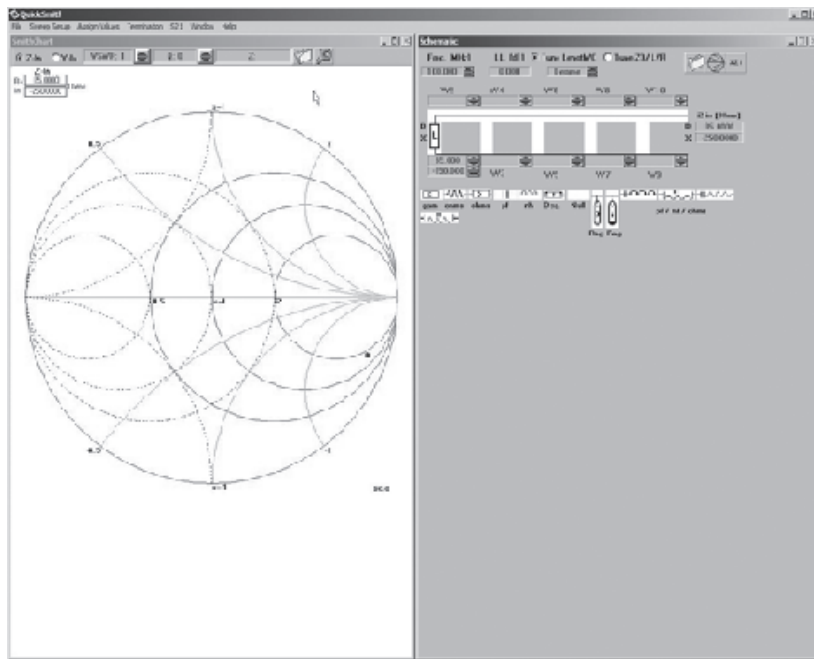


Figure 14 — A load impedance is set to R = 85 Ω and X = -250 Ω. The blue dot on the Smith chart indicates this impedance at the input.

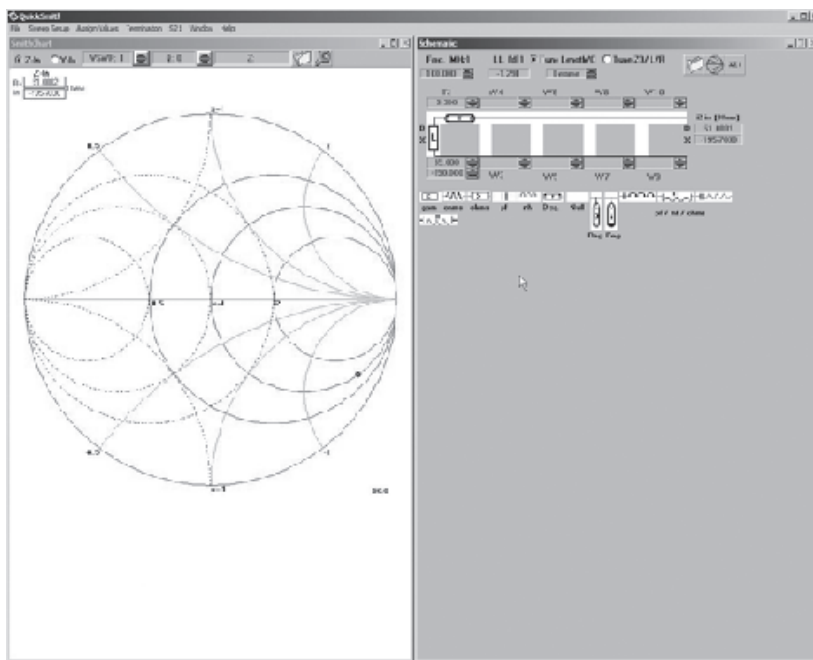


Figure 15 — Inserting a short transmission line in series moves the blue dot from the position in Figure 14 to a position over the unity resistance circle. The transmission line length is 3.4° or slightly less than 0.01 wavelength.

Figure 16 — Inserting a series inductance and setting the value to 310 nH moves the blue dot to the center of the Smith chart at $50 \pm j0 \Omega$.

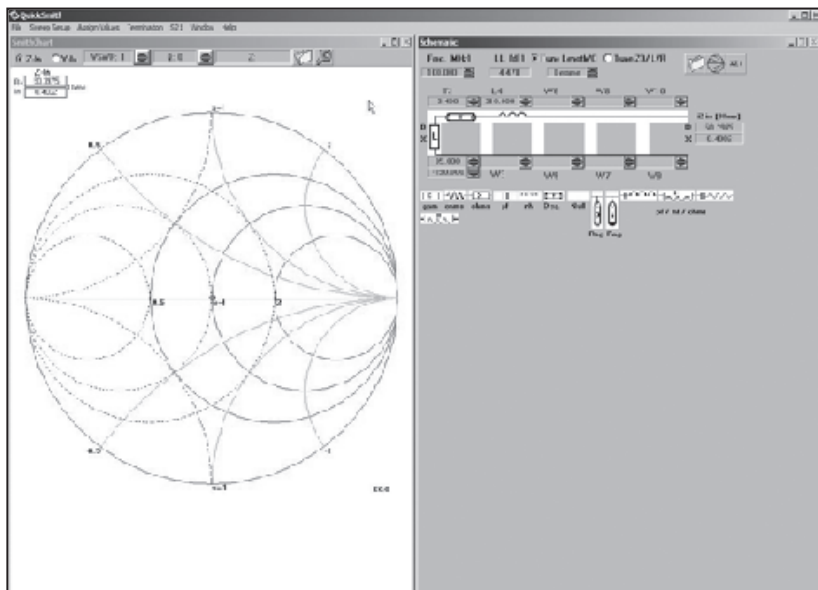


Figure 17 — Using the gamma figures shown in Table 2 for a 40 meter antenna (at the transceiver end of the coax) shows a swept-frequency response in which the upper frequency limit (7.3 MHz) falls outside the 2.0 SWR circle.

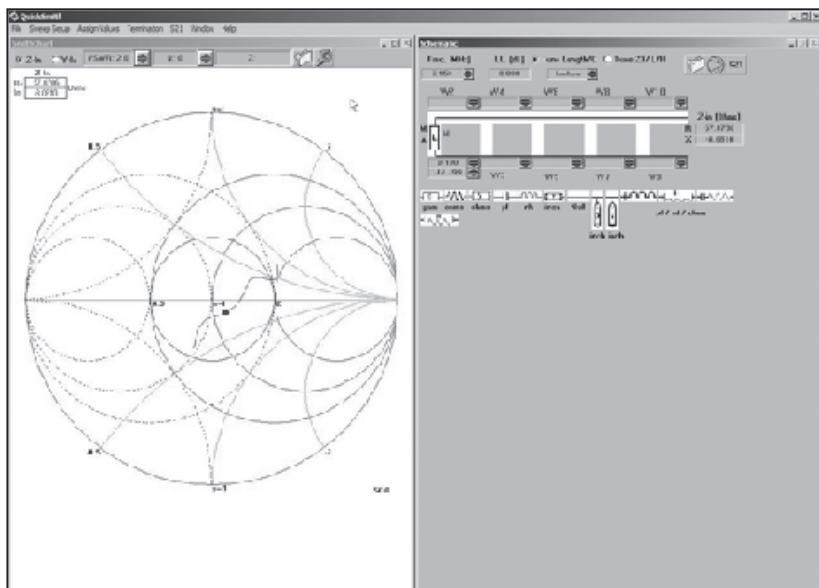
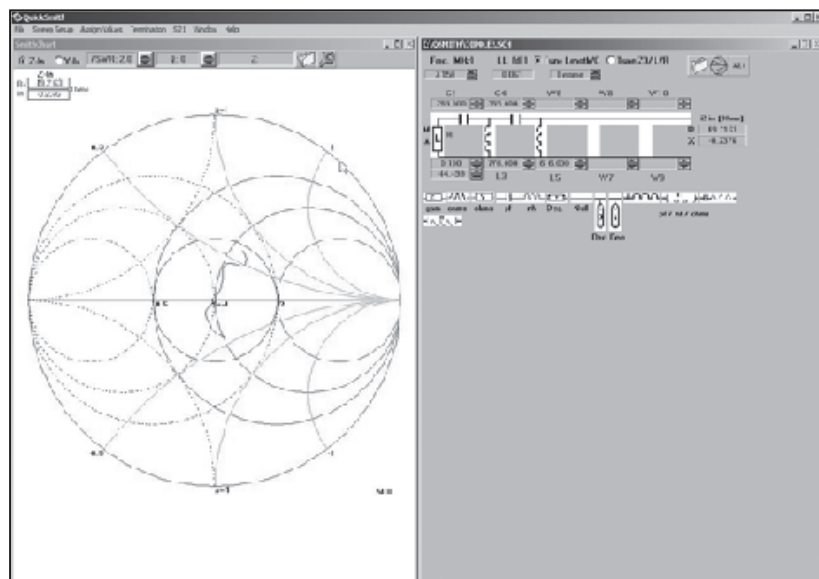


Figure 18 — With this matching network, the swept-frequency response shown in Figure 17 is moved completely inside the 2.0 SWR circle with the center frequency of 7.15 MHz is at dead center of the Smith chart.



A 20 Meter Sleeve Dipole Without the Sleeve

Here is a variation on the sleeve dipole for antenna experimenters to try.

Many *QEX* readers are familiar with the sleeve dipole concept, although it is likely few readers have built one. As shown in Figure 1, part A, the coaxial feed line going to the center of the dipole is routed through a quarter-wave conducting sleeve. The dipole sinusoidal RF current distribution is impressed on the sleeve and a quarter-wave wire forming the second half of the dipole. This geometry permits convenient feeding of the dipole from one end. Note that the electric field, E , at the ends of a dipole are maximum, so care must be taken with this high voltage feed point.

Despite the convenient geometry, a sleeve dipole is not all that convenient to construct, since it entails the tedious job of dressing a copper braid over a long piece of coax.

In this article I present a sleeve dipole equivalent antenna, minus the sleeve.

Concept

The feed end of the sleeve forms one end of the dipole RF current distribution. Radio frequency current cannot bridge the sleeve/coax gap, as the gap represents a very high RF impedance. I propose replacing the sleeve and high impedance gap with a high impedance current choke, as shown in Figure 1, Part B. The sinusoidal dipole current then may be impressed on the exterior surface of the coaxial shield and the same quarter-wave wire as before.

Modeling

To make an effective current choke, I wound the coaxial cable to form a coil, and bridged it with an air variable capacitor to form a high impedance parallel LC network. For such a choke, we need to have some idea of the effective inductance and capacitance

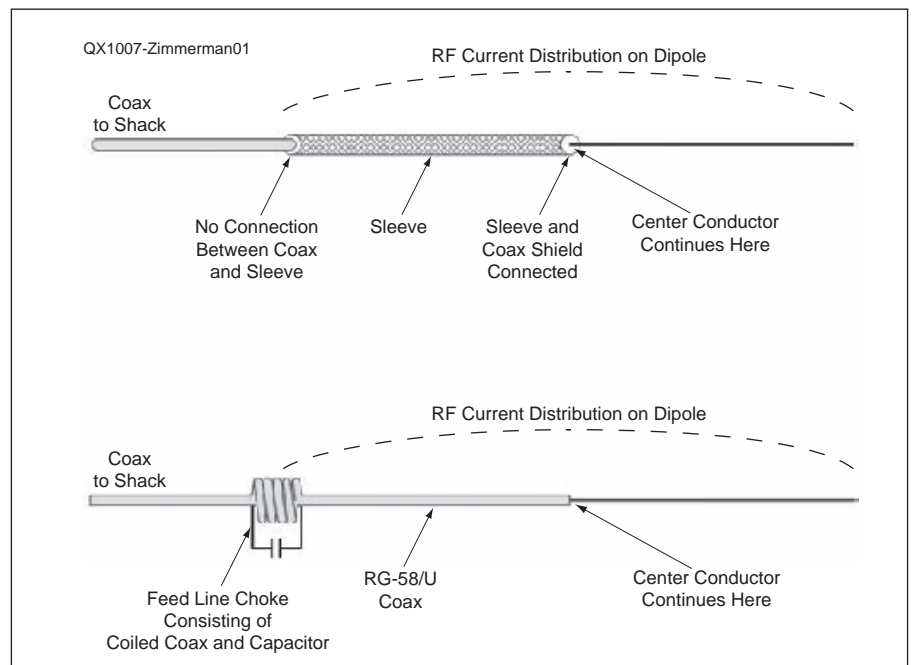


Figure 1 — Construction of a sleeve dipole (A) and the choke dipole (B).

of the dipole itself. That is to say, we need to know the equivalent circuit model of a resonant dipole antenna.

For this equivalent circuit, I first turned to *EZNEC* and modeled a half-wave dipole in free space for 14.200 MHz.¹ I used a 1/4 inch wire diameter to represent RG-58/U coax. A length of 10.181 meters provides the resistance and reactance values shown in Figure 2A and B. If this impedance, $Z = R + jX$, is plotted on a Smith Chart (Figure 3), we see

the locus is very nearly the real 72Ω circle. Well, not quite: the entire circle is rotated clockwise around the origin, as if bridged by a stray capacitance. Accordingly, I tested the candidate circuit model shown in Figure 4 with the impedance data in Figure 2A and B. The resulting component values R_{series} , L_{series} , C_{series} , and C_{stray} given in the Figure 4 caption reproduce the dipole impedance exactly (to within 0.01Ω for the antenna R and X) between 13.9 and 14.4 MHz.

For readers interested in using this model for another amateur band at frequency f (MHz), the inductor and two capacitors may

¹Notes appear on page 38.

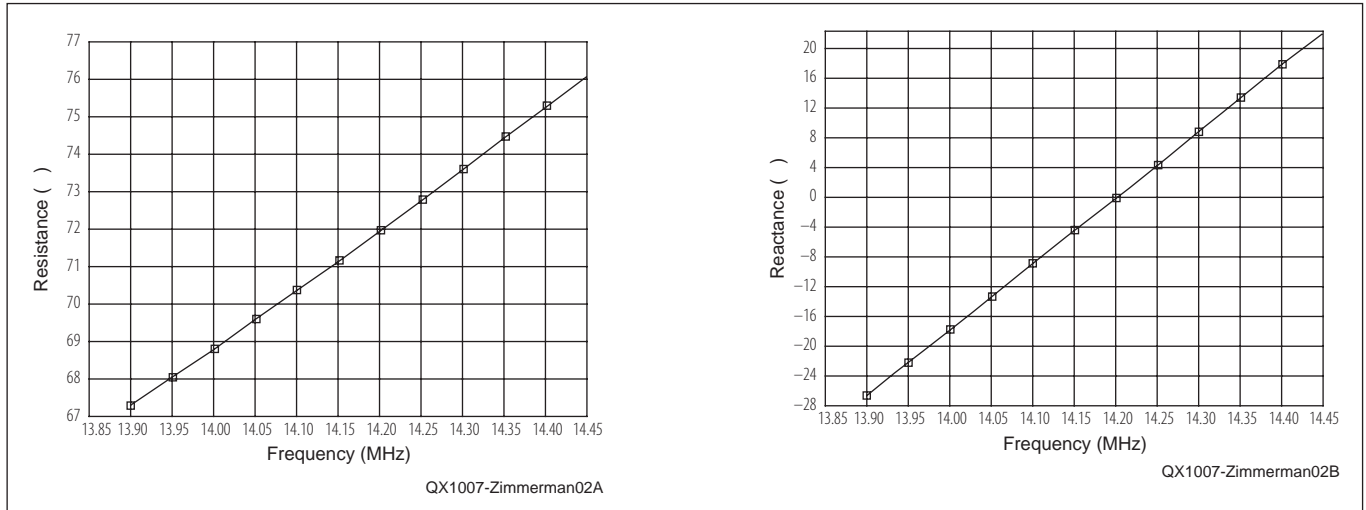


Figure 2 — Part A gives the resistance of the dipole as modeled on EZNEC for 14.200 MHz. The modeled reactance is shown at Part B.

be scaled by the ratio = $14.200 / f(\text{MHz})$. Of course there is no need to scale the resistance, R_{series} ; it remains the same independent of the dipole frequency.

Choke Construction

A good starting point for choke design is to use inductor and capacitor values approximately equal to those in the dipole itself. For my 20 meter inductor, I chose a target value of $7 \mu\text{H}$. The resonating capacitor for $7 \mu\text{H}$ and 14.200 MHz is 24 pF. Using the ARRL Single-Layer Coil Winding Calculator, I chose 10 turns of coax on a 3 inch diameter mandrel with a total coil length of 2.0 inches.² After winding the coil of coax, I bared a $\frac{3}{4}$ inch segment of coax braid on each end of the coil. Then, using a soldering gun (260 W), I bridged the coil with a 10-100 pF air variable capacitor, as shown in Figure 5. My coil form was a plastic drink bottle. You can see strips of duct tape holding the coax coil turns in place.

To be sure the choke had sufficient impedance to keep RF current off the feed line, I tested the choke with an AEA Bravo VIA impedance analyzer, using 1 inch test leads. The resulting series impedance of the parallel tank is 1000Ω , which was deemed satisfactory for 100 W operation. The data is shown in Figure 6.

The total length for the resonant dipole, from EZNEC, is 10.181 meters, half of which is RG-58/U coax and half of which is AWG No. 12 copper wire. The dipole center connection of the coaxial cable center conductor to the No. 12 wire is shown in Figure 7.

My backyard is small, and I had to install the dipole in a sloping manner. My installation is shown in Figure 8. The choke is on top of the bamboo pole at the left, and the No.

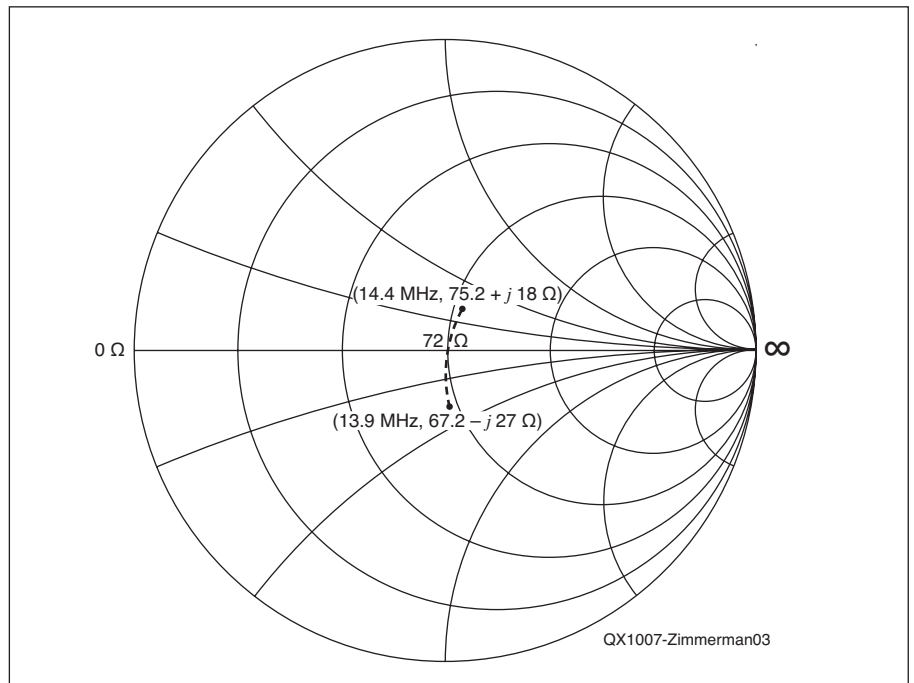


Figure 3 — Smith Chart with 72 Ω resistance at the center. The modeled dipole impedance is slightly shifted from the 72 Ω circle.

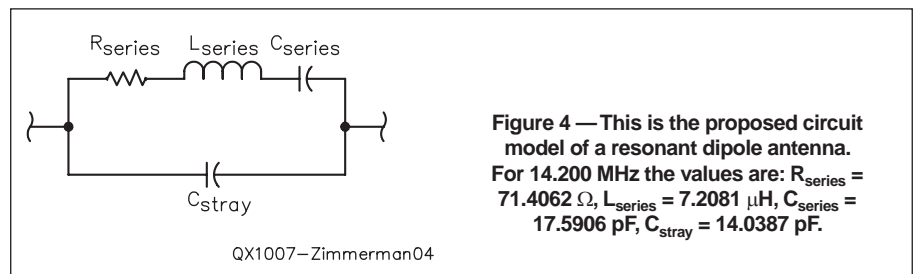


Figure 4 — This is the proposed circuit model of a resonant dipole antenna. For 14.200 MHz the values are: $R_{\text{series}} = 71.4062 \Omega$, $L_{\text{series}} = 7.2081 \mu\text{H}$, $C_{\text{series}} = 17.5906 \text{ pF}$, $C_{\text{stray}} = 14.0387 \text{ pF}$.

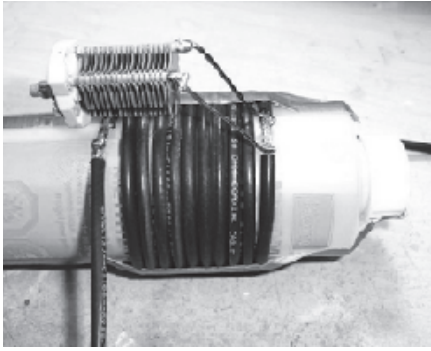


Figure 5 — This photo shows the 1000 Ω impedance current choke for 14.200 MHz.

12 wire is supported at the right on a 9 meter push-up mast.

TUNE-UP

The dipole initially resonated at 14.350 MHz with an SWR of 1.46:1. The passband is primarily dependent on the dipole length, and less so on the choke tuning. I lowered the choke briefly, and slightly increased the capacitance; this brought the antenna center frequency to 14.250 MHz as shown in Figure 9. After tune-up, the choke (or at least the variable capacitor) should be protected in a weather-proof plastic box; do not use a metal box, as there is high RF voltage across the choke.

You may want to measure the capacitance value after the antenna is adjusted for the best operation, and replace the variable capacitor with a fixed-value unit. You could also just build the antenna using a fixed value capacitor in the range of about 25 to 35 pF. Be sure to choose one that can handle the high voltage point at the end of the antenna.

Summary

Initial tests were made at 25 W PEP. I checked into the Maritime Mobile Net on 14.300 MHz, with net control W4YKY in southern Georgia. Carl came right back with a 59+10 dB report and said, "Don't change anything!"

There is no evidence of RF in the shack. The rig works stably, and I can grip the cable with my hands and observe no SWR change.

The choke dipole is convenient for city apartment dwellers, or anyone who may prefer an "end fed" antenna arrangement. Performance at the 100 W level has been pleasing. I easily keep regular schedules with WP4G in San Juan, Puerto Rico. I wish to recommend this design to other readers.

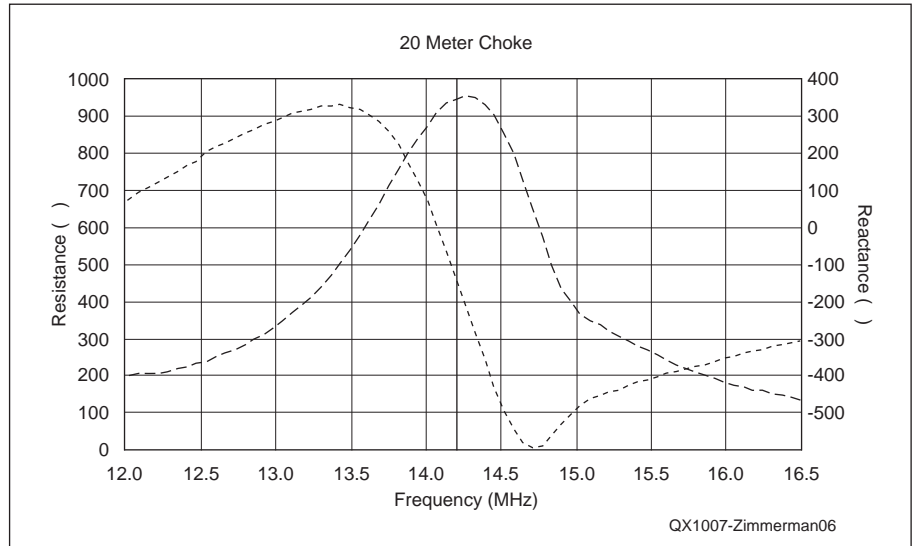


Figure 6 — Here is the measured plot of R and X for the current choke.

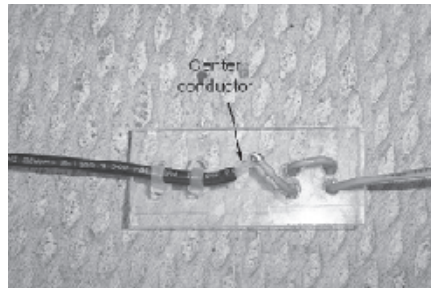


Figure 7 — This is the center feed point of my choke dipole.

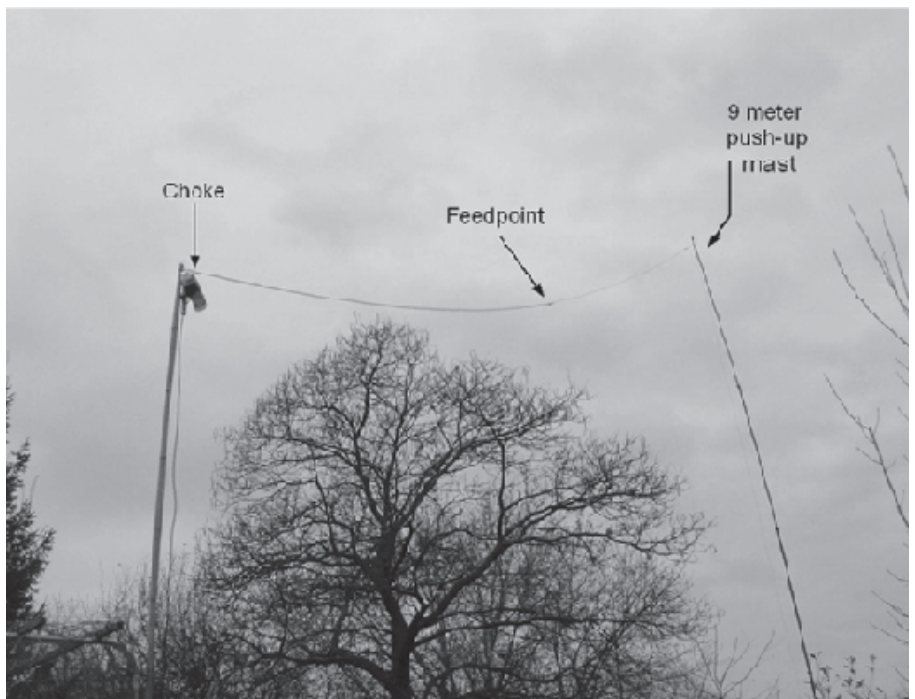


Figure 8 — The sloping dipole in my backyard. The push-up mast is 9 meters high.

Robert K. Zimmerman, Jr. was born in 1951 in Dupo, Illinois. He graduated from Southern Illinois University, Edwardsville, with BS and MS degrees in physics (1973, 1975) and then attended the University of Illinois, Urbana-Champaign, where he was awarded the MSEE degree in 1980. He has spent his entire career in radio science, working for Cornell University (Arecibo Observatory), NASA Goddard Spaceflight Center, Los Alamos National Laboratory (accelerator division), and most recently as a radar engineer on Kwajalein Atoll. He is presently involved in microwave antenna research at McMaster University, Hamilton, Ontario. An ARRL Life Member, Bob has been licensed as WN9PXXG (1965), WA9ZSF, NP4B, V73BZ, and now as VE3RKZ. He is active primarily on 40 m and 23 cm.

Notes

- ¹The author's EZNEC antenna model files for this antenna are available for download from the ARRL QEX Web site. Go to www.arrl.org/qexfiles and look for the file **7x10_Zimmerman.zip**.
- ²The ARRL L-C-F and Single Layer Coil Winding Calculator is available from your local ARRL dealer, or from the ARRL Bookstore. ARRL Order No. 9123, \$12.95. Telephone toll free in the US 888-277-5289 or call 860-594-0355, fax 860-594-0303; www.arrl.org/shop; pubsales@arrl.org.

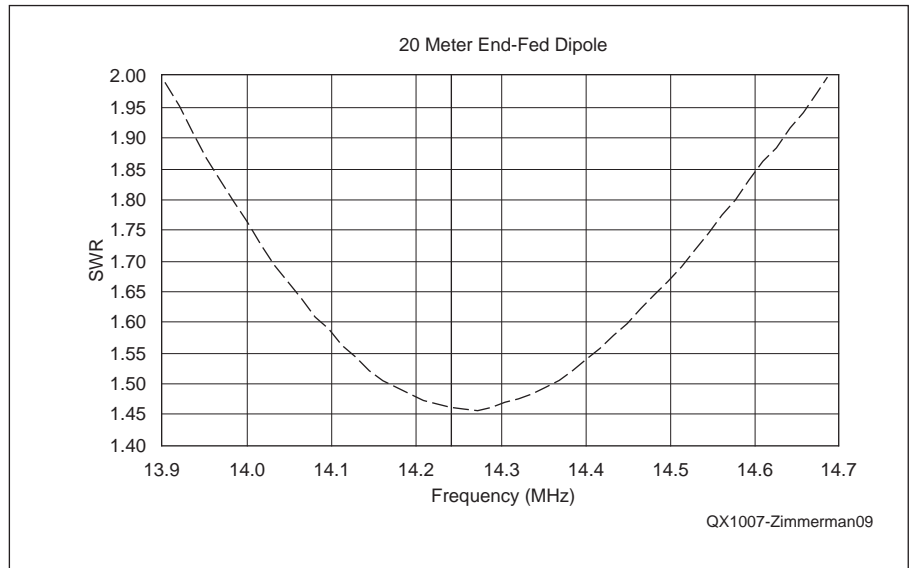


Figure 9 — The measured SWR plot of my finished choke dipole, after adjustment.



A Forum for Communications Experimenters

Subscription Order Card

QEX features technical articles, columns, and other items of interest to radio amateurs and communications professionals. Virtually every part of the magazine is devoted to useful information for the technically savvy.

Subscribe Today: Toll free 1-888-277-5289 • On Line www.arrl.org/QEX

Subscription Rates: 1 year (six issues)

ARRL MEMBER: for ARRL Membership rates and benefits go to www.arrl.org/join

US \$24.00 US via First Class \$37.00 Intl. & Canada by air mail \$31.00

NON MEMBER:

US \$36.00 US via First Class \$49.00 Intl. & Canada by air mail \$43.00

Renewal New Subscription

Name: _____ Call Sign: _____

Address: _____

City: _____ State: _____ ZIP: _____ Country: _____

Check Money Order Credit Card Monies must be in US funds and checks drawn on a US Bank

Charge to:

Account #: _____ Exp. Date: _____

Signature: _____



Published by:
ARRL, 225 Main St,
Newington, CT 06111-1494 USA

Contact circulation@arrl.org
with any questions or go to
www.arrl.org

Web Code: QEC

Project #350

Amateur Radio Astronomy Projects—Total Power Radio Telescope

Build your own radio telescope and copy signals from deep space!

My final project in this series is the total power radio telescope. This was the first astronomy project I built, and the most difficult. It took me many years to finally get a unit that worked. There are now dealers that carry very good total power receivers. I chose to build a radio that received radiation from the atomic hydrogen spectral line at 1420 MHz. Since hydrogen is the primary substance in the universe, this frequency is perfect for mapping objects in the universe.

Background

As most of us know, when you look at light from a light bulb with a prism or diffraction grating, you see the full spectrum. If you turn that prism/diffraction grating to a fluorescent bulb, neon bulb, or sodium lamp, however, you see quite a different spectrum with bright emission lines corresponding to the element creating the light — mercury for fluorescent bulbs, neon for neon bulbs, and sodium for sodium lamps. These spectra are distinct for each element. It turns out that these spectral lines also occur in the radio region of the electromagnetic spectrum and the line for neutral hydrogen is at 1420 MHz. The 1420 MHz line was first discovered in 1951 by Ewen and Purcell at Harvard University, and their horn antenna is on display at the National Radio Astronomy Observatory (NRAO) in Greenbank, West Virginia. Since most of the universe is made of hydrogen, this is a great frequency to use to map the radio objects in the universe.

I decided that this was to be my first radio project, and I wanted to create a radio map from my backyard. As mentioned above, I started this project in the 1980s, when

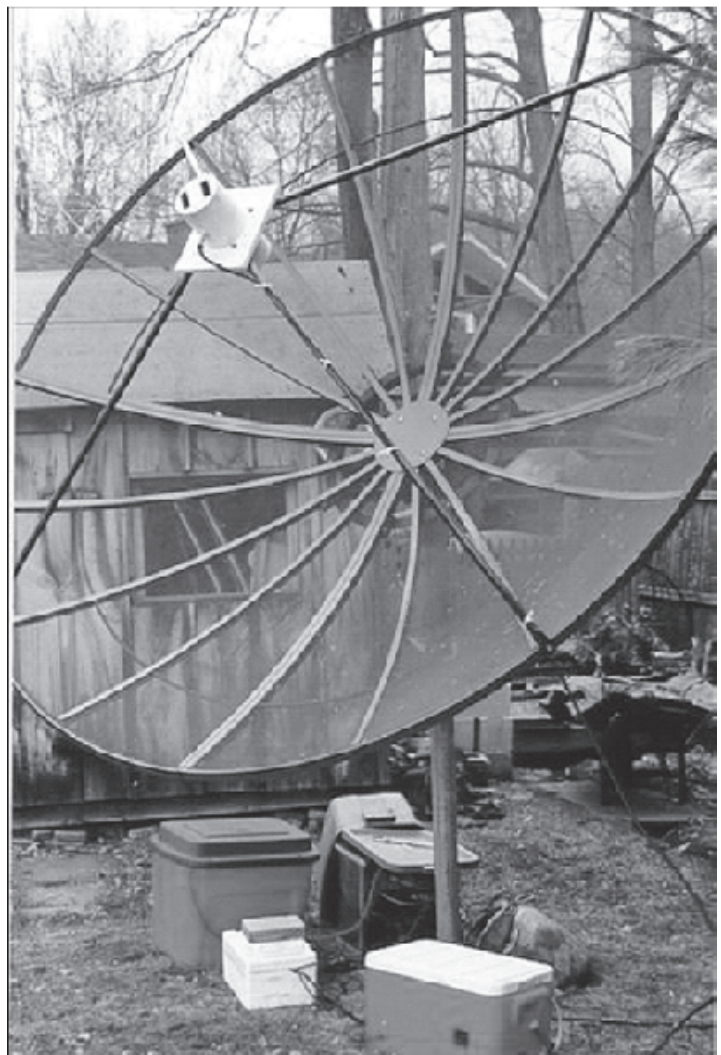


Figure 1 — My total power radio telescope system.

there were very few resources for making such a radio telescope. I am a high school science teacher and have some background in elementary electronics but this project was well beyond me. I found Bob Sickels, an amateur radio astronomer in Florida, and he helped me over the phone and also when I flew to Florida twice for help. I then received help from a Society of Amateur Radio Astronomers (SARA — www.radio-astronomy.org/) member, Paul Schuler, who lived near me. We worked for several years together, and I finally got the radio to work. My radio telescope was finally operational about ten years after starting the project.

Signals Detected

If you've ever taken a digital photo, you know that you can take millions of pixels with one shot. Unfortunately, radio astronomy uses a one pixel per observation instrument, and it takes a long time to compile enough data for a picture. The data in this case is a voltage that corresponds to an intensity of signal received. The receiver is calibrated with a known noise source. My final radio telescope is shown in Figure 1. Each day that I observed, I collected data at 10 second intervals at various altitudes (25° to 75°) using the drift scan method of collection; the objects in the sky "drift" by the antenna, which is pointed as close to due south as possible. Remember that I wanted to make a full sky map, so I needed data for the entire day and an entire year. Remember, also, that the sun and moon dominate any chart taken near them, and their signal swamps that data, so many charts needed to be collected to gather all the data I sought.

When and How to Observe

Radio objects are available all day and night and in all types of weather (lightning can destroy the equipment so I always packed up when a storm approached). There are lists of objects that amateurs can try to find, arranged by astronomical coordinates. One is available at: <http://adsabs.harvard.edu/full/1968AJ.....73..135G>. [Yes, that URL includes a group of 5 dots and another group of 2 dots. — Ed.]

To share information with others, a reference system must be adopted. The system used by astronomers is the celestial coordinate system. After years of teaching that the night sky is not a sphere that rotates around the earth, it is ironic that this is what we are going to envision for our coordinate system. Since both the surface of the earth and the celestial sphere are surfaces of spheres (or nearly so), we can define any point on those surfaces with two coordinates. In nearly the same way that we use Longitude and Latitude to find a point on the surface of

the earth, we use Right Ascension (RA) and Declination (DEC) to find objects on the celestial sphere.

This is where we should break to make sure that everyone who is about to use this has a radio telescope in which the pointing of the antenna is precisely known. With optical telescopes, we can verify our position with a quick glance through the scope, but with our radio antenna it's much more complicated. If you need to verify your pointing, here's a way of doing it with no extra cost than the time to complete some days of solar observation.

Verifying Your Pointing Position

I learned from Paul Schuler that you could use the sun as a pretty good point source and plot the width of the solar plot (left and right of center) versus the number of degrees away from the actual/calculated declination. For this, you must be sure to capture the entire solar peak since you will need the peak to find the center line. I looked up the sun's actual RA and DEC on the Internet (there are currently many sources for this information including: (faculty.physics.tamu.edu/krisciunas/ra_dec_sun.html) and pointed

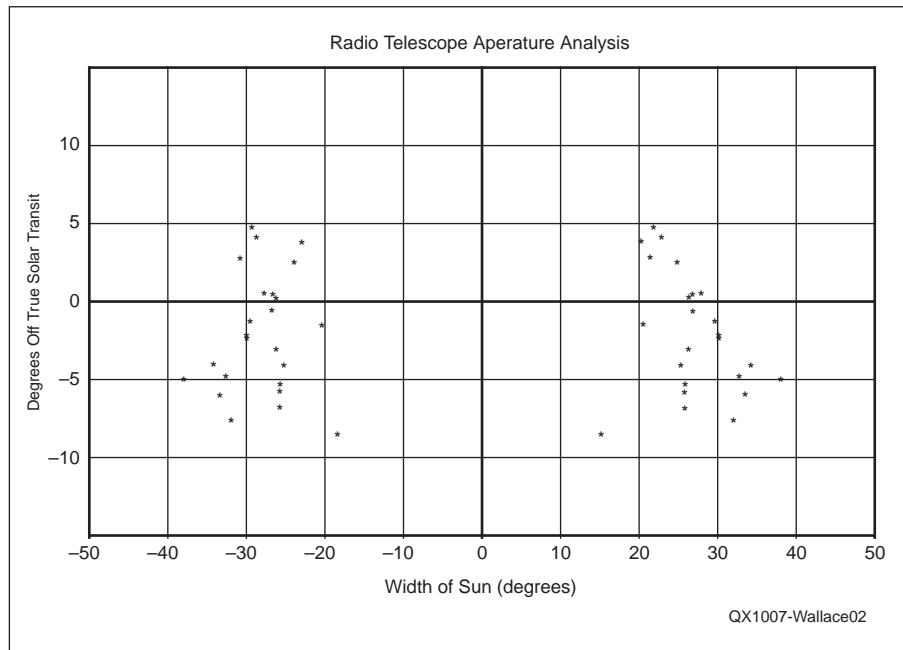


Figure 2 — An aiming chart for the 10 foot parabolic dish antenna.

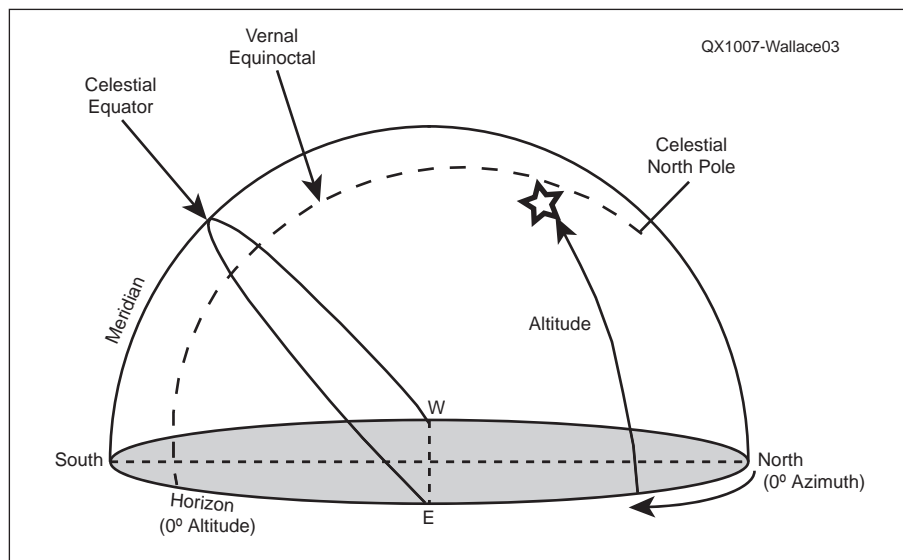


Figure 3 — Finding the altitude and azimuth for an object. (Graphic used by permission from Dr. Jim McDonald.)

my antenna directly at the sun and then progressively further away (above and below) over a period of days to get the plot shown in Figure 2. I found that my antenna is a little asymmetrical and my pointing is off by about 1.5°.

Azimuth and Altitude

If you were to go out tonight and try to show someone the “Big Dipper” you would probably point to the object and use Azimuth and Altitude. Azimuth is the angle around the horizon from due North and running clockwise. It corresponds to the compass directions with 0° representing due North, 90° due East, 180° due South, and 270° due West. Altitude is the height of the object in degrees above the horizon. Altitude can range from 0° (on the horizon) to 90° (directly overhead). A good approximation of these to use at night is your hand at arm’s length. Your whole hand (thumb through pinky) is about 10° and each finger is about 2°. Although Altitude and Azimuth are useful for observing at night and showing others constellations and other objects, it isn’t helpful for us. This is because none of us is at the exact same latitude and longitude, and so my altitude and azimuth information for the “Big

Dipper” would be different for you. Also, as the object rises and sets, it changes position in the sky. See Figure 3.

Right Ascension and Declination

As I mentioned earlier, Right Ascension

(RA) and Declination (DEC) are similar to longitude and latitude. If you picture Earth’s North Pole projected into the sky, this would correspond to the Celestial North Pole. And if you project Earth’s equator into the sky, this

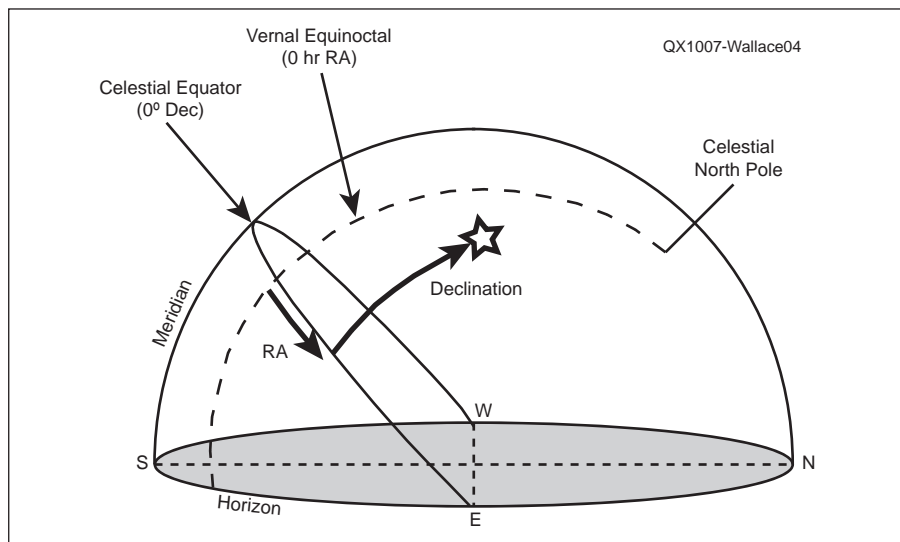


Figure 4 — Finding the right ascension and declination for an object. (Graphic used by permission from Dr. Jim McDonald.)

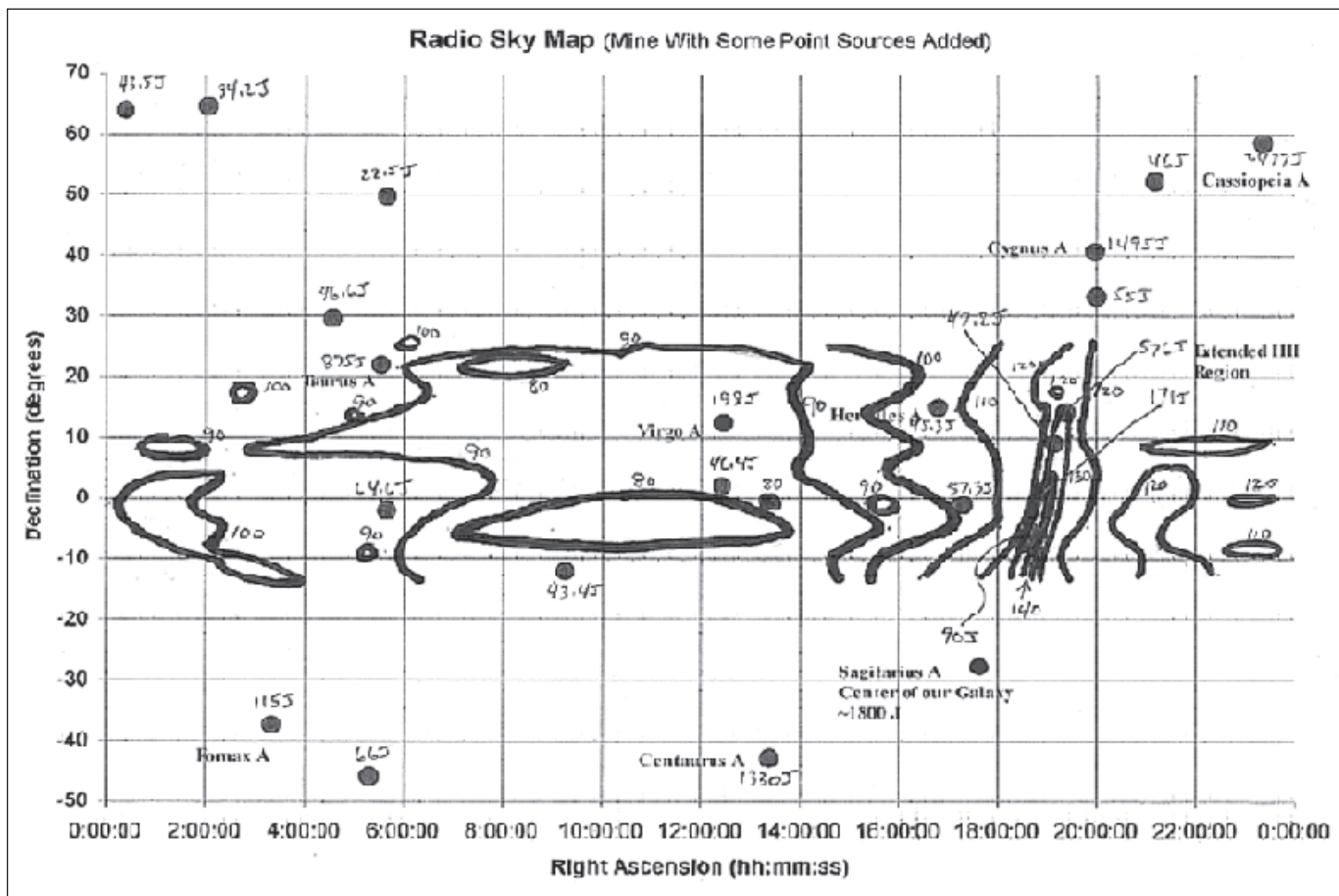


Figure 5 — This radio sky map was created from data I collected.

would correspond to the Celestial Equator. The longitude lines on a celestial sphere are called Right Ascension. Right Ascension is measured on the Celestial Equator in an easterly direction. Instead of measuring in degrees, though, it is measured in hours, minutes, and seconds. A full rotation corresponds to 24 hours, roughly the time it takes for the sphere to rotate once around. Each hour of right ascension is about 15° on the celestial sphere. The Right Ascension of 0 hours occurs on the Vernal Equinox.

Declination corresponds to latitude and is measured in degrees above or below the Celestial Equator. An object above the Celestial Equator has a positive declination; an object below the Celestial Equator has a negative declination. Since this coordinate system is relative to fixed objects in the Celestial Sphere, the Right Ascension and Declination don't change and can be shared with anyone on Earth. See Figure 4.

Radio Examples

I've included a map that I made from my observations (see Figure 5), plotted as voltages out of 255, with some point sources from charts with their flux in Janskys. (A Jansky is a measure of flux density equal to 10^{-26} watts per square meter per hertz). Try the following examples:

- 1) You find a large peak at 05:33:00 RA, +21:59:00 Dec — What object is this?
- 2) You find a small peak at 16:49:00 RA, +15:02:00 Dec — What object is this?
- 3) You find a large peak at 12:29:00 RA, +12:31:00 Dec — What object is this?

Answers to Radio Examples:

- 1) Taurus A
- 2) Hercules A
- 3) Virgo A

Equipment Needed

In Figure 6, you can see the generalized block diagram of my final radio telescope. Starting at the antenna, which was a 10 foot parabolic dish antenna, I ran a 15 foot length of the best low-loss cable I could buy (at the time this was RG-6, 50 Ω — a very thick cable) with N connectors to a temperature controlled cooler with the receiver front end devices inside. This cooler had a PID thermoelectric circuit accurate to at least 1°F with two huge power resistors for any heating needed. All the components before the DC amp were housed in the cooler. See Figure 7 for a view inside the cooler. The DC amp was housed in a foam box and had offset controls as well, and fed the A/D converter to the laptop computer running the Skypipe software (Jim Sky's site is www.radiosky.com/) housed in a plastic bin to protect it from rain. You can see the entire system in Figure 1.

Data Analysis

After collecting data for 10 years, I had enough charts (12 of each altitude) to create charts of each altitude from 25° to 75° in 5° increments. I averaged the charts and created the Microsoft *Excel* graph of all 11 altitudes shown in Figure 8. (The large peak is the Milky Way galaxy.) I next took the data and used *Mathematica* to create a 3-D graph of the data and thus my final picture. Ten years to get one picture!

Sources for Total Power Radio Telescopes and Additional Information:

- SARA website:
www.radio-astronomy.org/
 Jim Sky's Radio Sky website:
www.radiosky.com/
 Jeff Lichtman's radio astronomy supply website:
www.radioastronomysupplies.com/

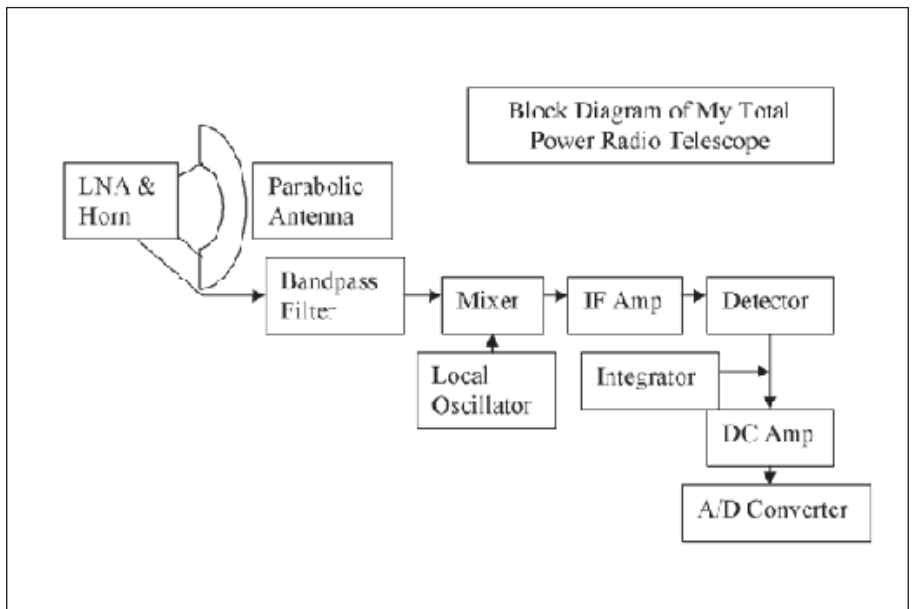


Figure 6 — Here is a block diagram of my total power radio telescope.

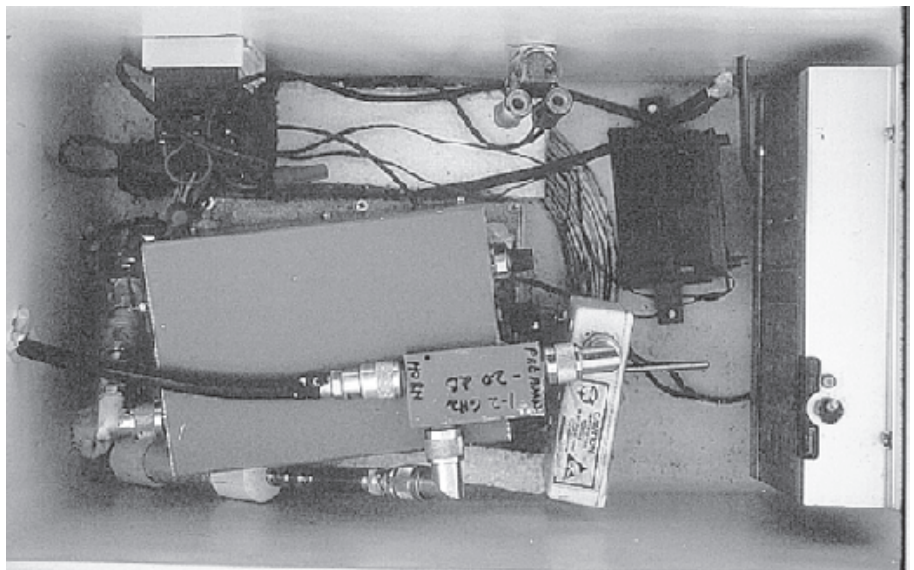


Figure 7 — This photo is a view inside the cooler, showing the front end components.

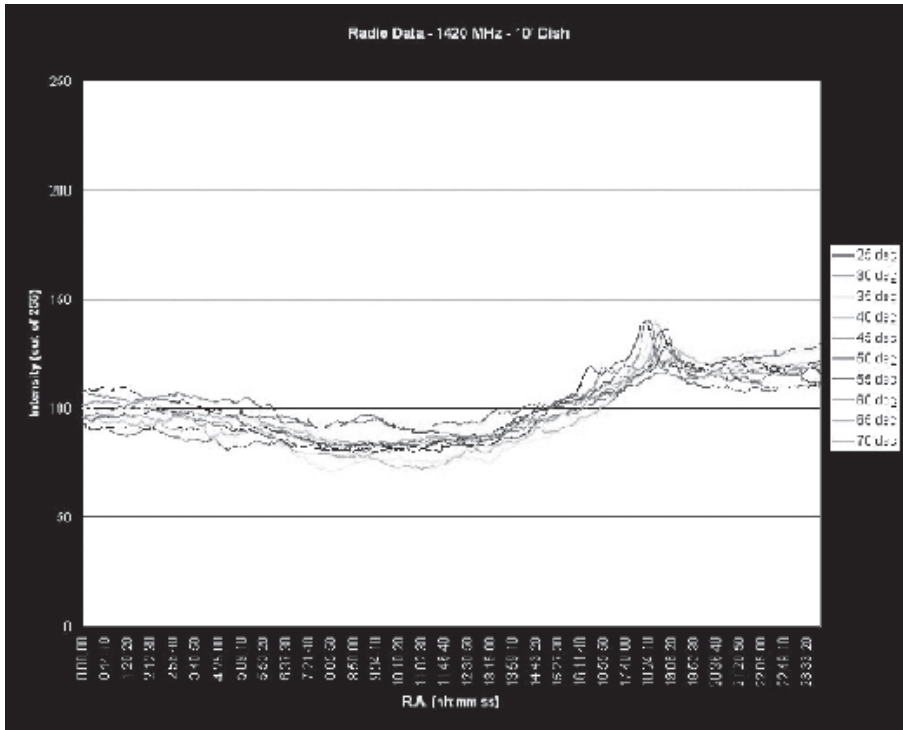


Figure 8 — This Microsoft Excel graph uses data I collected over 10 years of measurements.

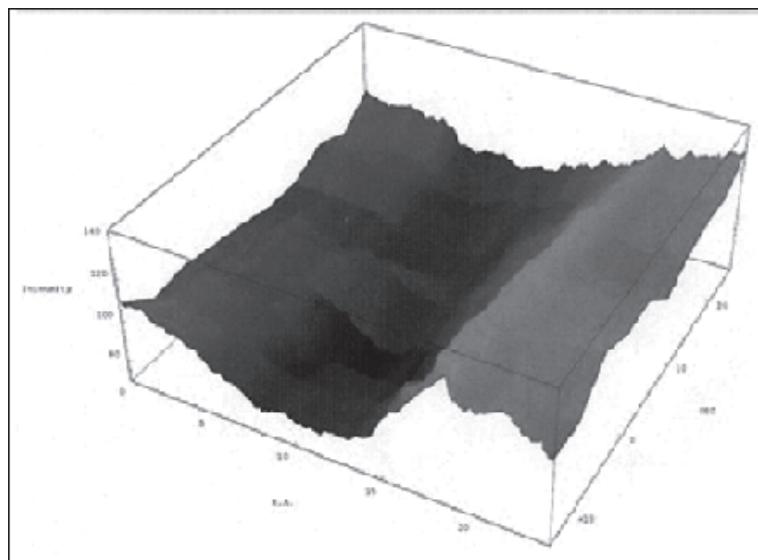


Figure 9 — I used the Mathematica program to create this 3-D graphic map of the sky.

Jon Wallace has been a high school science teacher in Meriden, Connecticut for over 28 years. He is past president of the Connecticut Association of Physics Teachers and was an instructor in Wesleyan University's Project ASTRO program. He has managed the Naugatuck Valley Community College observatory and run many astronomy classes and training sessions throughout Connecticut. Jon has had an interest in 'non-visual' astronomy for over twenty-five years and has built or purchased various receivers as well as building over 30 demonstration devices for class use and public displays.

Jon is currently on the Board of the Society

of Amateur Radio Astronomers (SARA) and developed teaching materials for SARA and the National Radio Astronomy Observatory (NRAO) for use with their Itty-Bitty radio Telescope (IBT) educational project. Other interests include collecting meteorites, raising arthropods ("bugs") and insectivorous plants. Jon has a BS in Geology from the University of Connecticut; a Master's Degree in Environmental Education from Southern Connecticut State University and a Certificate of Advanced Study (Sixth Year) in Science from Wesleyan University. He has been a member of ARRL for many years but is not a licensed Amateur Radio operator.



from
MILLIWATTS to KILOWATTS
More Watts per Dollar

Taylor TUBES

Quality Transmitting & Audio Tubes

- COMMUNICATIONS
- BROADCAST
- INDUSTRY
- AMATEUR

Immediate Shipment from Stock

3CPX800A7	3CX15000A7	4CX5000A	813
3CPX5000A7	3CX20000A7	4CX7500A	833A
3CW20000A7	4CX250B	4CX10000A	833C
3CX100A5	4CX250BC	4CX10000D	845
3CX400A7	4CX250BT	4CX15000A	866-SS
3CX400U7	4CX250FG	4X150A	872A-SS
3CX800A7	4CX250R	YC-130	5867A
3CX1200A7	4CX350A	YU-106	5868
3CX1200D7	4CX350F	YU-108	6146B
3CX1200Z7	4CX400A	YU-148	7092
3CX1500A7	4CX800A	YU-157	3-500ZG
3CX2500A3	4CX1000A	572B	4-400A
3CX2500F3	4CX1500A	807	M328/TH328
3CX3000A7	4CX1500B	810	M338/TH338
3CX6000A7	4CX3000A	811A	M347/TH347
3CX10000A7	4CX3500A	812A	M382

— TOO MANY TO LIST ALL —

ORDERS ONLY:
800-RF-PARTS • 800-737-2787

Se Habla Español • We Export

TECH HELP / ORDER / INFO: 760-744-0700

FAX: 760-744-1943 or 888-744-1943

An Address to Remember:
www.rfparts.com

E-mail:
rfp@rfparts.com

RF PARTS COMPANY

Book Review:

Noise Temperature Theory and Applications for Deep Space Communications Antenna Systems

Noise Temperature Theory and Applications for Deep Space Communications Antenna Systems, by Tom Y. Otoshi, Norwood, MA. Artech House, 2008, 292 pages, \$135.

ISBN 978-1-59693-377-4

As an amateur who has been playing with microwaves for the past 50 years, I am always looking for information that will help me build a better rig, or explain how things work. Tom Otoshi has written a book that brings a lot of antenna and noise material together. Although the title seems to indicate a narrow subject range, this book has wide application to anyone engaged in microwave communications. If you are expecting an introductory book on noise figures, or an antenna textbook, this is not the book for you; however, if you want to get the best possible performance from your microwave antenna, this book will tell you how to do it. It does not go into a lot of heavy mathematical analysis; just enough to provide the required background. It is a practical handbook for getting the best possible performance from your antenna.

Amateur microwave experimenters, especially those who engage in extreme

weak signal operations, such as EME (earth-moon-earth) communications, will find the material presented in *Noise Temperature Theory and Applications for Deep Space Communications Antenna Systems* invaluable. It is a true engineering book, not a deep theoretical discussion. It reminds me of the way material was presented in the old MIT Radiation Laboratory series. This book has just enough theory to let you know what is happening, and then gives designs and the measured results!

Each chapter has a lot of practical and useful information. The book is written for those engaged in getting their hands into things. Chapter 1 – Introductory Topics – quickly moves into the “real world” with a nuts-and-bolts discussion of the noise contributions of ground temperature and cosmic background. The next chapter discusses the different types of dish surfaces, including solid and perforated materials. Even the contributions of paint and water on the antenna surfaces are measured. Chapter 3 (Noise Temperature Experiments) talks about feed horn effects, improvement of the figure of merit (antenna gain divided by system temperature), and a particularly interesting discussion of measurement of Sun noise at 32 GHz.

In my opinion, the presentation in Chapter 4 (“Mismatch Error Analyses”) in itself is worth the price of the book. A question often asked is: How good does a match have to be to make an accurate noise temperature measurement? This chapter will show the reader how to make the analysis.

Chapter 5 is a discussion of some aspects of network analysis, and the final chapter provides a handy reference of formulas.

A well-designed amateur microwave rig for terrestrial communications should have its system temperature dominated by terrestrial noise. If you are involved in moonbounce (EME) or tracking spacecraft and other weak-signal reception where the background is the sky, you need *Noise Temperature Theory and Applications for Deep Space Communications Antenna Systems*.

Holding the call sign K6HIJ continuously since 1954, Dick is an ARRL member who has devoted his Amateur Radio career to building and experimenting in the microwave bands. He is a retired engineer and a registered Professional Engineer. Dick holds degrees in physics, mathematics and theology.

QEX

Upcoming Conferences

44th Annual Central States VHF Society Conference

July 22–24, 2010,
Doubletree Inn St Louis at
Westport
1973 Craighshire
St Louis, MO 63146

Presentations at Central States aren't necessarily technical — they cover the breadth of the VHF/UHF ham radio hobby. Highlights in past years have been demonstrations of Software Defined Radio and LASER Communication beyond line-of-sight. Presentations generally vary from 15 to 45 minutes and step you through the highlights of the topic at hand, with complete texts published as articles in the *Proceedings*. If you have questions about the Conference, contact Ron Ochu, KOØZ, No. 5 Cricklewood Ln, St. Peters, MO 63376; ko0z@arrl.net. There is more information about this year's conference available on the Central States VHF Society Web site at www.csvhfs.org/conference/.

The 14th International EME Conference

August 12-14, 2010
Dallas, Texas

Al Ward, W5ULA, Barry Malowanchuk, VE4M, Tony Emanuele, WA8RJF, and the North Texas Microwave Society announce the 14th International EME Conference. This is the premier EME event of the year. Whether you are a new or experienced EMEer, the conference will offer a wide range of technical, social and sightseeing activities for everyone.

The hallmark of past EME Conferences has been the excellent technical presentations, and the 14th EME Conference promises an outstanding technical program. Presentations include:

- Low Noise Amplifiers
- Tracking the Moon and other celestial bodies.
- SSPAs/Tube Power Amplifier/TWT Workshop
- Receiving with Software Defined Radios
- Big Dish EME

- Highlights of several DXpeditions
- Getting started with a small dish on 1296 MHz EME
- Feed design and construction
- EME Propagation
- Software
- Live EME demo on 1296 MHz by WA5WCP/5

Of course, no technical portion of a Conference is complete without the Technical Proceedings. If you would like to present or submit a technical article for inclusion in the Proceedings, please contact Al, Barry or Tony as soon as possible.

Several electronics vendors are signed up to showcase their wares. The vendor rooms will be open all day Saturday. If you are interested in obtaining a vendor table, contact the committee as soon as possible before the conference.

There will be a hospitality suite and registration on Wednesday evening so everyone can get acquainted. The Thursday family activities will include air conditioned bus tours in the Dallas-Ft Worth area. A Saturday night banquet at the hotel, with a special guest speaker is also planned. A short session on Sunday morning will wrap things up.

The Conference Hotel is The Westin at the Dallas-Ft Worth Airport, which offers first class conference amenities at an excellent conference price of \$89 USD per night, plus taxes. There are guest rooms booked for Wednesday night through Saturday night. Hotel registration is now available online at www.starwoodmeeting.com/StarGroupsWeb/res?id=0902108016&key=7BF3D.

Whether it will be your first EME Conference or your 14th, the committee is looking forward to seeing you in Dallas in August.

The 29th Annual ARRL and TAPR Digital Communications Conference

September 24-26, 2010
Portland, Oregon

Mark your calendar and start making plans to attend the premier technical conference of the year, the 29th Annual ARRL and TAPR Digital Communications Conference to be held September 24-26, 2010, in Portland, Oregon. The conference location is The

from
MILLIWATTS
to **KILOWATTS**[™]

More Watts per Dollar[™]



- **Wattmeters**
- **Transformers**
- **TMOS & GASFETS**
- **RF Power Transistors**
- **Doorknob Capacitors**
- **Electrolytic Capacitors**
- **Variable Capacitors**
- **RF Power Modules**
- **Tubes & Sockets**
- **HV Rectifiers**



ORDERS ONLY:

800-RF-PARTS • 800-737-2787

Se Habla Español • We Export

TECH HELP / ORDER / INFO: 760-744-0700

FAX: 760-744-1943 or 888-744-1943



An Address to Remember:
www.rfparts.com

E-mail:
rfp@rfparts.com



2010 ARRL/TAPR Digital Communications Conference

September 24-26
near Portland, Oregon

The scenic Northwest near Portland, Oregon is the host of the largest gathering of Amateur Radio digital enthusiasts in the world. This conference offers something for everyone from beginners to experts.

Make your reservations now for three days of learning and enjoyment. Go to the Digital Communications Conference site on the Web at www.tapr.org/dcc, or call Tucson Amateur Packet Radio (TAPR) at 972-671-8277.



Heathman Lodge, 7801 NE Greenwood Dr, Vancouver, WA 98662. Phone: 1-888-475-3100; www.heathmanlodge.com. The Heathman Lodge is across the Columbia River from Portland.

We recommended that you book your room prior to arriving. TAPR has reserved a block of rooms at the special DCC room rate of \$89.00 single/double. This special rate is good until September 1, 2010. After that you will pay the regular room rate. To book your room, call the hotel directly (phone numbers below) and mention the group code Tucson Amateur Packet Radio when making reservations. *Be sure to book your rooms early!*

The ARRL and TAPR Digital Communications Conference is an international forum for radio amateurs to meet, publish their work, and present new ideas and techniques. Presenters and attendees will have the opportunity to exchange ideas and learn about recent hardware and software advances, theories, experimental results, and practical applications.

Topics include, but are not limited to: Software defined radio (SDR), digital voice (D-Star, P25, WinDRM, FDMDV, G4GUO), digital satellite communications, Global Position System (GPS), precision timing, Automatic Position Reporting System (APRS), short messaging (a mode of APRS), Digital Signal Processing (DSP), HF digital modes, Internet interoperability with Amateur Radio networks, spread spectrum, IEEE 802.11 and other Part 15 license-exempt systems adaptable for Amateur Radio, using TCP/IP networking over amateur radio, mesh and peer to peer wireless networking, emergency and Homeland Defense backup digital communications, using Linux in Amateur Radio, updates on AX.25 and other wireless networking protocols.

This is a three-Day Conference (Friday, Saturday, Sunday). Technical and introductory sessions will be presented all day Friday and Saturday.

Join others at the conference for a Friday evening social get together. A Saturday evening banquet features an invited speaker and concludes with award presentations

and prize drawings.

The ever-popular Sunday Seminar focuses on a topic and provides an in-depth four-hour presentation by an expert in the field. Check the TAPR Web site for more information: www.tapr.org.

Call for Papers

Technical papers are solicited for presentation and publication in the *Digital Communications Conference Proceedings*. Annual conference proceedings are published by the ARRL. Presentation at the conference is not required for publication. Submission of papers are due by 30 July 2010 and should be submitted to:

Maty Weinberg, ARRL, 225 Main Street, Newington, CT 06111, or via the Internet to maty@arrl.org.

AMSAT Satellite Space Symposium and Annual Meeting

October 8-10, 2010
Chicago/Elk Grove Holiday Inn
Chicago, Illinois

This year we have selected the Chicago/Elk Grove Holiday Inn at 1000 Busse Road, Elk Grove, IL as the Symposium location. The hotel is near O'Hare Airport and has free hourly shuttles from the airport to the hotel.

Call for Papers

An official call for papers for the 2010 AMSAT Space Symposium and Annual Meeting has not been issued, but it is not too early to begin planning a paper. Proposals for papers, symposium presentations and poster presentations are generally welcomed on any topic of interest to the amateur satellite community. Watch the AMSAT Web site for more details: www.amsat.org/amsat-new/symposium/2010/index.php.



Reader's Page

Dear Larry,

I built a version of the vector network analyzer, VNWA 1.0, described by Dr Thomas Baier, DG8SAQ, in the Mar/Apr 2007 issue of *QEX*. Here are two photos of my results.

I used MAX 4544 ICs configured with 1 k Ω resistors in series with the op amp outputs to get the required 100 dB of isolation.

I originally had a problem with distortion caused by individual blocking capacitors on the op amp outputs, which was trying to drive the switches negative. Removing these capacitors cured the problem.

Photo 1 is a top view. At the bottom left is the parallel port buffer and analog switches.

At the top left is the return loss (SWR) bridge section. I used NE602 mixers and NE5532 op amps with the original resistor values. I could not find NE612 mixers in the Digi-Key catalog and I already had the NE5532 op amps.

The input section is at the top center. The little box connected to the input in the photo is a 10 MHz low pass filter I had on the bench.

The clock / DDS section is at the lower right. The clock section is all HCMOS and uses a 74HC74 as a mixer. I used a parallel mode 30 MHz crystal in a series circuit for the TXCO and the phase detector portion of a 74HC4046. The AD9851 ICs are on obsolete DDS-30 boards I got from George Heron, N2APV, at www.njgrp.com.

The voltage regulator is an LM7808. I mounted individual 5 V regulators on the other modules as needed.

Photo 2 shows a sweep of the 10 MHz low pass filter.

— 73, Jerry Fankhauser, WA8HTO, PO Box 557, Woodfield, OH 43793; n6329g@hotmail.com

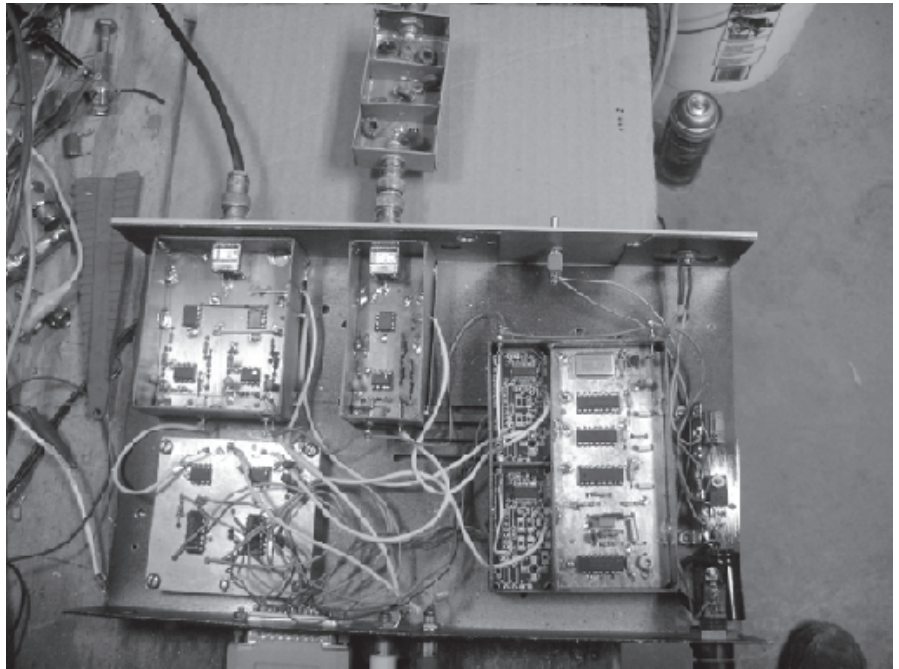


Photo 1 — Jerry Frankhauser, WA8HTO, built this version of the vector network analyzer, VNWA 1.0, designed by Dr Thomas Baier, DG8SAQ.

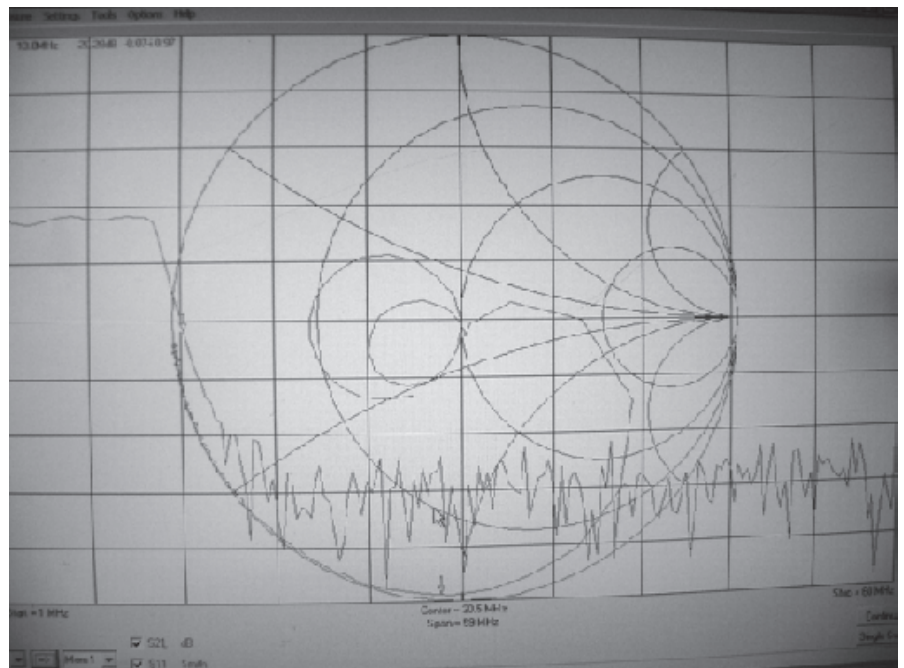


Photo 2 — This screen shot shows the VNWA 1.0 measured results of a sweep of Jerry's 10 MHz low pass filter.



Letters to the Editor

Build a Low-Cost Iambic Keyer Using Open-Source Hardware (Sep/Oct 2009)

Larry,

I read the article by Richard Chapman in the Sep/Oct, 2009 issue of *QEX* with great interest. He built a keyer using the Arduino board and writing the program in *C*.

It was interesting because, although there have been many articles about keyers in the amateur literature, none of them (to my knowledge) have used a higher level language — they are all in assembler code.

To build a similar keyer to the one in the article, however, you have to buy an Arduino board, an Atmel programmer and install an integrated development environment (IDE) such as *WinAVR* to build the code. *WinAVR* is free and the hardware isn't much but it won't leave a lot of change from a \$100 bill.

STMicroelectronics recently offered a \$7 board called their STM8S-Discovery board, which has a built-in programmer using the USB port and they also offer a free IDE for programming it in *C*. This board is available from distributors like Digikey and Mouser and is a great deal. I've been expecting someone to write an article about using this board for Amateur Radio projects (it has lots of FLASH memory and RAM space so it could be used for quite sophisticated projects).

— Regards, Jim Koehler, VE5FP, 2258 June Rd, Courtenay, BC V9J 1X9, Canada; jark@shaw.ca

Hi Jim,

Thanks for the tip about this inexpensive development board. It sounds like another good learning tool. If you have a project in mind, please share it with our readers.

— 73, Larry Wolfgang, WR1B, QEX Editor; lwolfgang@arrl.org

A Question for QEX Readers (From May/June 2010 Letters)

Dear Rod,

I am glad to see someone else experimenting with these mixers. I use the 74HC4052, but I believe the issues will be the same. There are two issues to take a look at. The first issue is that the mixer is very sensitive to harmonics. Harmonics will directly degrade IMD performance. Harmonics would also likely mix with your clock spurs in the 300 MHz to 500 MHz range that you noted. The difference frequencies may very well be near audio. This problem is often neglected or insufficiently addressed in low cost SDRs. Try adding an

RF filter ahead of the mixer to suppresses harmonics by at least 60 dB.

The second issue to look at is that the audio amplifier will react unfavorably to RF. Most low cost SDRs use a single capacitor to decouple RF from the audio amplifier. This is not enough. Try adding a passive filter between the mixer and audio amplifier. The filter should have several sections and provide good attenuation outside of your desired passband.

You may test the amplifier for sensitivity to RF by first sending a high quality audio signal to the amplifier. Make sure IM2 measures over -100 dBc. It will take a great audio oscillator to do this. I use my audio oscillator with a good LC filter. I use Linrad and my Delta44 sound card to make this measurement. Now inject some RF at various frequencies and observe the level needed to degrade IM2. It may respond to only a few millivolts.

This may give you an idea for the amount of attenuation needed. You may also evaluate the RF spectrum of the mixer output. I use a scope for this. This level may be a few hundred millivolts from only clock leakage.

Please let us know the results after you test for these two factors. I have only tested my mixer at 4 MHz. That is my intermediate frequency. The 74HC4052 is good up to about 10 MHz, but has very good dynamic range due to the higher power supply voltages used (± 5 V dc).

— 73, Jim Shaffer, WB9UWA, 1310 Hanson Dr, Normal, IL, 61761; wb9uwa@gmail.com

Crystal Ladder Filters for All (Nov/Dec 2009)

Dear Larry,

Jack Hardcastle, G3JIR and I have recently been contacted by Dave Gordon-Smith, G3UUR, who made us aware of his development of the "quasi-equiripple" (QER) modification of the popular Cohn ladder filter. This is described in the 2010 *ARRL Handbook* in Chapter 11, section 11.6.2 (Crystal Filter Design). It is a significant improvement, combining the simplicity of the Cohn topology with very low ripple values in the passband. This allows the design of filters with ripple values between 0.1 dB (6 poles) and less than 1 dB (12 poles) — impossible to achieve with a standard Cohn filter. I have therefore applied the Dishal equations to Dave's model and implemented it in the new version 2.0.3 of the Dishal program as "QER(G3UUR)." The help file has been updated with a short description and also shows a simulation picture of an 8-pole SSB filter with Cohn versus QER curves.

Dave also verified my suspicion that the popular simplified evaluation formula for his oscillator method to characterize crystals leads to slightly inaccurate results. This has also been updated, using the more accurate equations. The user has still the option of using the simplified form for compatibility reasons, however.

I would like thank Dave for this contribution to further enhance the Dishal program. I am sending you the complete updated package of Dishal 2.0.3. I hope that the current version 2026 can be replaced with this new version on the *QEX* files download Web site.

— 73, Horst Steder, DJ6EV Forstbachstrasse 13, 35625 Huetttenberg, Germany; h-g.steder@freenet.de

Hi Horst,

Thank you for sending the updated version of your filter calculation program. I have put the new files on the *QEX* files Web site so that anyone going there to look for the file from your article will download the new version. I have also placed the new file in the Jul/Aug 2010 section of the Web site for the convenience of our readers. Go to www.arrl.org/qexfiles and look for the file **11x09_Steder_Hardcastle.zip**.

— 73, Larry, WR1B

Next Issue in QEX

Phil Anderson, WØXI, describes an automatic gain control circuit that he designed for use with his ultrasonic receiver. Phil leads us through the design considerations and component choices in a way that makes the article interesting from a design/engineering viewpoint. The same circuit could find a home in direct conversion receivers and other QRP receivers or transceivers. Readers will certainly come up with many different ways to adapt Phil's AGC circuit to other applications.

Create Your Own Microprocessor Devices!

ARRL's PIC Programming For Beginners

NEW!

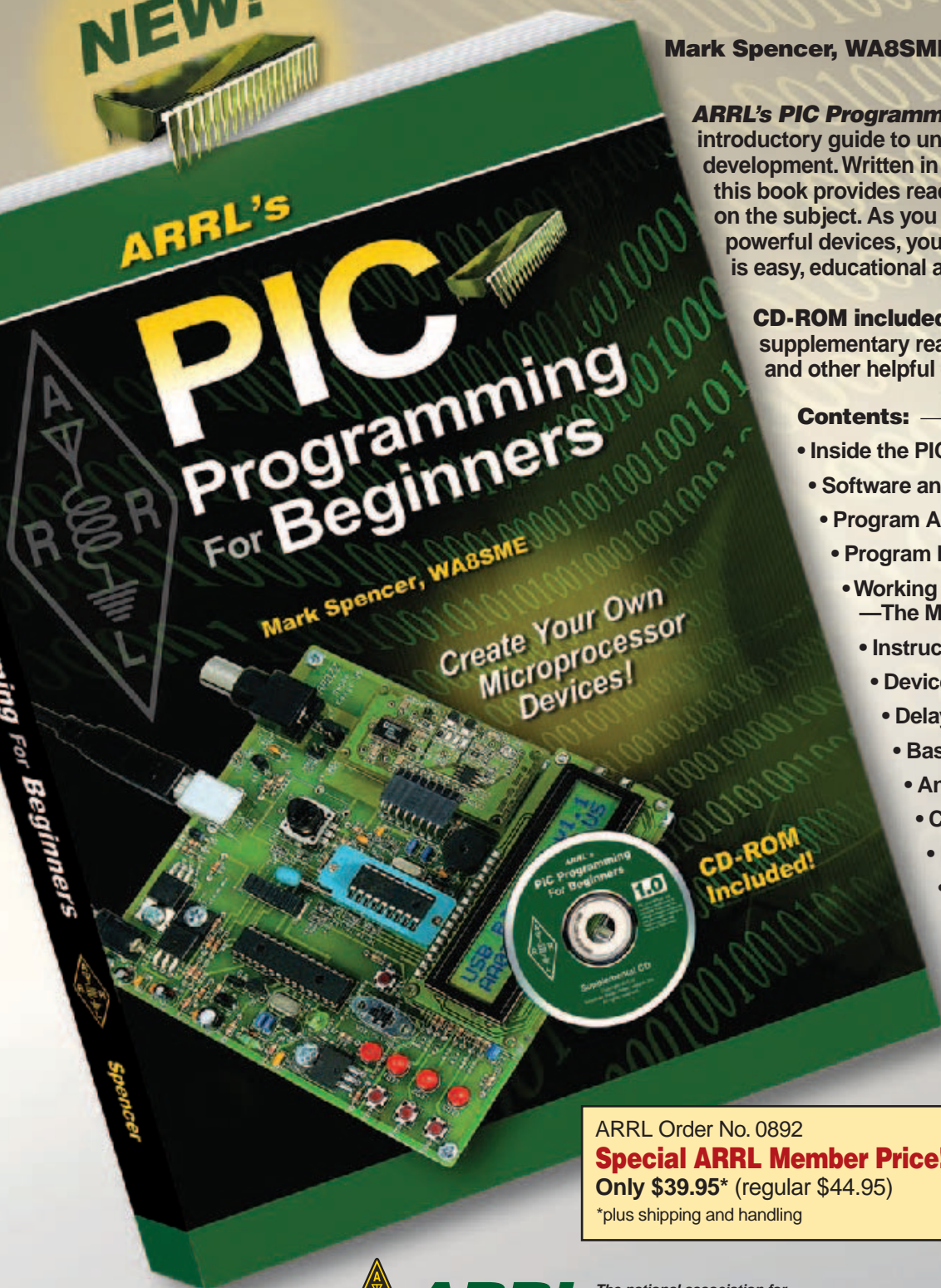
Mark Spencer, WA8SME

ARRL's *PIC Programming for Beginners* is an introductory guide to understanding PIC® design and development. Written in a building block approach, this book provides readers with a strong foundation on the subject. As you explore the potential of these powerful devices, you'll find that working with PICs is easy, educational and most importantly fun.

CD-ROM included with programming resources, supplementary reading, short video clips and other helpful data.

Contents:

- Inside the PIC16F676
- Software and Hardware Setup
- Program Architecture
- Program Development
- Working With Registers
—The Most Important Chapter
- Instruction Set Overview
- Device Setup
- Delay Subroutines
- Basic Input/Output
- Analog to Digital Converters
- Comparators
- Interrupts
- Timer 0 and
Timer 1 Resources
- Asynchronous Serial
Communications
- Serial Peripheral Interface
Communications
- Working With Data
- Putting It All Together
...and more!



ARRL Order No. 0892

Special ARRL Member Price!

Only \$39.95* (regular \$44.95)

*plus shipping and handling



ARRL The national association for
AMATEUR RADIO™

225 Main Street, Newington, CT 06111-1494 USA

SHOP DIRECT or call for a dealer near you.
ONLINE WWW.ARRL.ORG/SHOP
ORDER TOLL-FREE 888/277-5289 (US)

QEX 7/2010

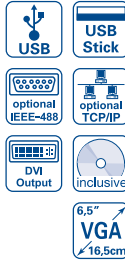
GREAT VALUE IN TEST & MEASUREMENT

Call for
educational
discount

350 MHz 2/4 CHANNEL DIGITAL OSCILLOSCOPE HMO 3522 / HMO 3524



from \$4,422



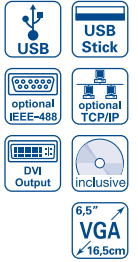
250 MHz:
HMO2524

- ✓ 4 GSa/s Real time, 50 GSa/s Random sampling, low noise flash A/D converter (reference class)
- ✓ 4 MPts memory, memory Zoom up to 100,000:1
- ✓ MSO (Mixed Signal Opt. H03508/H03516) with 8/16 logic channels
- ✓ Serial bus trigger and hardware accelerated decode, I²C, SPI, UART/RS-232 (Opt. H0010)
- ✓ 8 user definable marker for easy navigation
- ✓ Pass/Fail Test based on Masks ✓ Lowest noise fan
- ✓ Vertical sensitivity 1 mV/div., Offset control ±0.2...±20V
- ✓ 12 div. x-axis display range, 20 div. y-axis display range (VirtualScreen)
- ✓ Trigger modes: slope, video, pulsewidth, logic, delayed, event

3 GHz SPECTRUM ANALYZER HMS 3000 / HMS 3010



from \$3,581



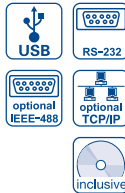
1 GHz:
HMS1000
HMS1010

- ✓ Frequency range 100 kHz...3 GHz
- ✓ Amplitude measurement range -114 dBm...+20 dBm DANL -135dBm with Preamp. Option H03011
- ✓ Tracking Generator (HMS 3010) -20 dBm/0 dBm
- ✓ Sweep time 20 ms...1000 s
- ✓ Resolution bandwidth 100 Hz...1 MHz in 1-3 steps, 200 kHz (-3 dB) additional 200 Hz, 9 kHz, 120 kHz, 1 MHz (-6 dB)
- ✓ Spectral purity <-100 dBc/Hz (@ 100 kHz)
- ✓ Video bandwidth 10 Hz...1 MHz in 1-3 steps
- ✓ Integrated AM and FM demodulator (int. speaker)
- ✓ Detectors: Auto-, min-, max-peak, sample, RMS, quasi-peak

PROGR. 2/3/4 CHANNEL HIGH-PERFORMANCE POWER SUPPLY HMP SERIES



from \$1,419

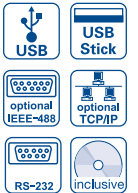


- ✓ HMP2020: 1 x 0...32V/0...10A 1 x 0...5.5V/0...5A, max. 188W
- ✓ HMP2030: 2 x 0...32V/0...5A 1 x 0...5.5V/0...5A, max. 188W
- ✓ HMP4030: 3 x 0...32V/0...10A, max. 384W
- ✓ HMP4040: 4 x 0...32V/0...10A, max. 384W
- ✓ 188/384W output power realized by intelligent power management
- ✓ Low residual ripple: < 150 μ V_{rms} due to linear post regulators
- ✓ High setting- and read-back resolution of up to 1 mV/0.1 mA
- ✓ HMP4030/HMP4040: Keypad for direct parameter entry
- ✓ Galvanically isolated, earth-free and short circuit protected output channels
- ✓ Advanced parallel- and serial operation via V/I tracking
- ✓ EasyArb function for free definable V/I characteristics
- ✓ FuseLink: individual channel combination of electronic fuses
- ✓ Free adjustable overvoltage protection (OVP) for all outputs
- ✓ All parameters clearly displayed via LCD/glowing buttons

25/50 MHz ARBITRARY FUNCTION GENERATOR HMF2525 / HMF2550



from \$1,670

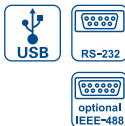


- ✓ Frequency range 10 μ Hz...25 MHz / 50 MHz
- ✓ Output voltage 5 mV_{pp}...10 V_{pp} (into 50 Ω) DC Offset \pm 5 mV...5V
- ✓ Arbitrary waveform generator: 250 MSa/s, 14 Bit, 256 kPts
- ✓ Sine, Square, Pulse, Triangle, Ramp, Arbitrary waveforms incl. standard curves (white, pink noise etc.)
- ✓ Total harmonic distortion 0.04% (f < 100 kHz)
- ✓ Burst, Sweep, Gating, external Trigger
- ✓ Rise time < 8 ns, in pulse mode 8...500 ns variable-edge-time
- ✓ Pulse mode: Frequency range 100 μ Hz...12.5 MHz / 25 MHz, pulse width 10 ns...999 s, resolution 5 ns
- ✓ Modulation modes AM, FM, PM, PWM, FSK (int. and ext.)
- ✓ 10 MHz Timebase: \pm 1 ppm TCXO, rear I/O BNC connector
- ✓ Front USB connector: save & recall of set-ups and waveforms
- ✓ 8,9 cm (3.5") TFT: crisp representation of the waveform and all parameters

LCR - BRIDGE HM8118



from \$2,011



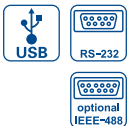
incl. HZ188

- ✓ Basic Accuracy 0.05%
- ✓ Measurement functions L, C, R, |Z|, X, |Y|, G, B, D, Q, θ , Δ , M, N
- ✓ Test frequencies 20 Hz...200 kHz
- ✓ Up to 12 measurements per second
- ✓ Parallel and Series Mode
- ✓ Binning Interface H0118 (optional) for automatic sorting of components
- ✓ Internal programmable voltage and current bias
- ✓ Transformer parameter measurement
- ✓ External capacitor bias up to 40V
- ✓ Kelvin cable and 4 wire SMD Test adapter included in delivery
- ✓ Galvanically isolated USB / RS-232 Interface, optional IEEE-488

1.2 GHz RF- SYNTHESIZER HM8134-3



from \$4,303



3 GHz:
HM8135

- ✓ Outstanding Frequency range 1 Hz...3 GHz
- ✓ Output power -135 dBm...+13 dBm
- ✓ Frequency resolution 1 Hz (accuracy 0.5 ppm)
- ✓ Input for external time base (10 MHz)
- ✓ Modulation modes: AM, FM, Pulse, ϕ , FSK, PSK
- ✓ Rapid pulse modulation: typ. 200 ns
- ✓ Internal modulator (sine, square, triangle, sawtooth) 10 Hz...200 kHz
- ✓ High spectral purity
- ✓ Standard: TCXO (temperature stability: \pm 0.5 x 10⁻⁶)
Optional: OCXO (temperature stability: \pm 1 x 10⁻⁸)
- ✓ Galvanically isolated USB / RS-232 Interface, optional IEEE-488
- ✓ 10 configuration memories including turn-on configuration

